Copyright Warning & Restrictions

The copyright law of the United States (Title 17, United States Code) governs the making of photocopies or other reproductions of copyrighted material.

Under certain conditions specified in the law, libraries and archives are authorized to furnish a photocopy or other reproduction. One of these specified conditions is that the photocopy or reproduction is not to be "used for any purpose other than private study, scholarship, or research." If a, user makes a request for, or later uses, a photocopy or reproduction for purposes in excess of "fair use" that user may be liable for copyright infringement,

This institution reserves the right to refuse to accept a copying order if, in its judgment, fulfillment of the order would involve violation of copyright law.

Please Note: The author retains the copyright while the New Jersey Institute of Technology reserves the right to distribute this thesis or dissertation

Printing note: If you do not wish to print this page, then select "Pages from: first page # to: last page #" on the print dialog screen

ABSTRACT

NOVEL MEMBRANE STRUCTURES FOR AIR AND WATER PURIFICATION

by
Smruti Ragunath

Membrane separations have undergone rapid developments in recent years. The key component in the process is the membrane itself which acts as a selective barrier regulating transport of components between the two sections. The main advantage of membrane separation process in comparison to other unit operations is its unique separation principle, ease of operation, lower energy requirement, and can be easily coupled with other downstream processes. Different membrane based applications include filtration, osmosis, dialysis, gas separation, pervaporation, membrane extraction and membrane distillation (MD). The membranes can be fabricated by a variety of processes such as phase inversion, sol-gel, track etching, stretching, interfacial polymerization, etc. Much effort has gone into developing methods for enhancing the performance of the membranes by modifying membrane surface including immobilization of nanoparticles and nano carbons.

This research work demonstrates different surface modifying techniques to enhance the membrane performance for different applications such as extraction of volatile organics (VOCs) from air, generation of pure water from sea water via membrane distillation, removal of bacterial debris and endotoxin from water via membrane distillation. The techniques adapted in this research include immobilization of carbon nanotubes (CNTs) on membrane surface to alter the solute membrane interactions; hydrophilization of membrane surface to allow partial wetting of the membrane surface,

thus enhancing the MD flux for desalination; incorporation of CNTs via phase inversion technique to form a composite CNIM layer on top of a porous support layer to enhance the membrane in MD application. For bacterial disinfection application, presence of CNTs provide anti-bacterial properties that result in effective rejection and removal of bacterial contaminants from water.

Overall the various membrane modification and membrane based separation approach results in enhanced removal of VOCs from air, higher salt rejection; better permeate flux and also as potential disinfectant for water treatment process.

NOVEL MEMBRANE STRUCTURES FOR AIR AND WATER PURIFICATION

by
Smruti Ragunath

A Dissertation
Submitted to the Faculty of
New Jersey Institute of Technology
in Partial Fulfillment of the Requirements for the Degree of
Doctor of Philosophy in Environmental Science

Department of Chemistry and Environmental Science

May 2017

.

APPROVAL PAGE

NOVEL MEMBRANE STRUCTURES FOR AIR AND WATER PURIFICATION

Smruti Ragunath

Dr. Somenath Mitra, Dissertation Advisor — Date
Distinguished Professor of Chemistry and Environmental Science, NJIT

Dr. Edgardo T Farinas, Committee Member — Date
Associate Professor and Chair of Chemistry and Environmental Science, NJIT

Dr. Tamara Gund, Committee Member — Date
Professor of Chemistry and Environmental Science, NJIT

Dr. Yong I Kim, Committee Member — Date
Assistant Professor of Chemistry and Environmental Science, NJIT

Dr. Robert B Barat, Committee Member — Date
Professor of Chemical, Biological and Pharmaceutical Engineering, NJIT

BIOGRAPHICAL SKETCH

Author: Smruti Ragunath

Degree: Doctor of Philosophy

Date: May 2017

Undergraduate and Graduate Education:

- Doctor of Philosophy in Environmental Science,
  New Jersey Institute of Technology, Newark, NJ, 2017

- Master of Science in Pharmaceutical Engineering,
  New Jersey Institute of Technology, Newark, NJ, 2010

- Bachelor of Science in Biotechnology,
  SASTRA University, Thanjavur, T.N. India, 2008

Major: Environmental Science

Publications:

Smruti Ragunath and Somenath Mitra, "Removal of endotoxin via membrane distillation", in preparation.

Smruti Ragunath, Sagar Roy, and Somenath Mitra, "Carbon nanotube immobilized membrane with controlled nanotube incorporation via phase inversion polymerization for desalination via membrane distillation", submitted to *Desalination*, 2017 (under review).

Sagar Roy, Smruti Ragunath and Somenath Mitra, "Enhanced pure water recovery in membrane distillation by implementing heating stages between a series of membrane modules", submitted to *Separation and Purification Technology*, 2016 (under review).

Smruti Ragunath, Sagar Roy and Somenath Mitra, "Selective hydrophilization of permeate surface to enhance flux in membrane distillation", in *Separation and Purification Technology*, 170(2016) 427-433.

Smruti Ragunath and Somenath Mitra, "Carbon nanotube immobilized composite Hollow fiber membranes for extraction of volatile organics from air", in *Journal of Physical Chemistry C,* 119(2015) 13231-13237.

Chutarat Saridara, Chaudhrey Mustansar Hussain, Smruti Ragunath and Somenath Mitra, "Enhanced preconcentration of selected chlorofluorocarbons on multiwalled carbon nanotubes with polar functionalities", in *Journal of Separation Science,* 38 (2015) 426-432.

Chutarat Saridara, Smruti Ragunath, Yong Pu and Somenath Mitra, "Methane preconcentration in a microtrap using multiwalled carbon nanotubes as sorbents", in *Journal of Analytical Chimica Acta,* 677(2010) 50-54.

Presentations:

Smruti Ragunath, Sagar Roy and Somenath Mitra, "Novel membranes for sea water desalination via membrane distillation", presented at 253rd ACS National Meeting, San Francisco, CA, April 2017

Smruti Ragunath, Sagar Roy, and Somenath Mitra, "Modification of permeate surface by hydrophilization to enhance flux in membrane distillation for desalination", presented at 253rd ACS National Meeting, San Francisco, CA, April 2017.

Somenath Mitra, Smruti Ragunath and Sagar Roy, "Carbon nanotube enabled water treatment", presented at 253rd ACS National Meeting, San Francisco, CA, April 2017.

Smruti Ragunath, Sagar Roy and Somenath Mitra, "Selective hydrophilization of the permeate surface to enhance flux in membrane distillation", presented at 101st NJWEA Annual Meeting held at Atlantic City, NJ, May 2016.

Smruti Ragunath and Somenath Mitra, "Carbon nanotube immobilized composite membrane (CNIM): A novel membrane for removal of VOCs from air", presented at XIth Annual Graduate Research Day, Newark, NJ, October 2015.

Smruti Ragunath and Somenath Mitra, "Carbon nanotube immobilized composite membrane (CNIM): A novel membrane for removal of VOCs from air", presented at 250th ACS National Meeting, Boston, MA, Aug 2015.

Smruti Ragunath, Sagar Roy and Somenath Mitra," CNT immobilized membrane (CNIM): Novel membranes for generation of pure water from sea or brackish Water via membrane distillation", presented at 250th ACS National Meeting, Boston, MA, Aug 2015.

Smruti Ragunath, Sagar Roy and Somenath Mitra, "Novel membranes for generation of pure water from sea or brackish water via membrane distillation", presented at 100th NJWEA Annual Meeting held at Atlantic City, NJ, May 2015.

Smruti Ragunath and Somenath Mitra, "Carbon nanotube immobilized composite membrane (CNIM): A novel membrane for removal of VOCs from air", presented at Dana Knox Research Showcase, Newark, NJ, April 2015.

Smruti Ragunath and Somenath Mitra, "Extraction of volatile organics using carbon nanotube immobilized composite membranes", presented at Annual EAS Conference, Somerset, NJ, November 2014.

Smruti Ragunath, Madhuleena Bhadra, Sagar Roy and Somenath Mitra, "Carbon nanotube enhanced membrane distillation: A new generation membranes for sea or brackish water desalination", presented at Xth Annual Graduate Research Day, Newark, NJ, October 2014.

Smruti Ragunath and Somenath Mitra, "Development of instrumentation for real-time monitoring of greenhouse gases", presented at 247th ACS National Meeting, Dallas, TX, April 2014.

Smruti Ragunath and Somenath Mitra, "Development of instrumentation for real-time monitoring of greenhouse gases", presented at 244th ACS National Meeting, Philadelphia, PA, Aug 2012.

Smruti Ragunath and Somenath Mitra, "Development of instrumentation for real-time monitoring of greenhouse gases", presented at Annual EAS Conference, Somerset, NJ, Nov 2010.

Smruti Ragunath, Anjali Mitra, Ornthida Sae-Khow and Somenath Mitra, "Microwave demulsification of biocolloids", Presented at ACS 239th National Meeting, San Francisco, CA, March 2010.

Smruti Ragunath, Chutarat Saridara, Somenath Mitra, "Instrumentation for real-time monitoring of greenhouse gases", to be presented at Dana Knox Research Showcase, Newark, NJ, April 14th 2010.

This thesis is dedicated

To my beloved gurus' Sri Sri Ravi Shankar and Mrs. Mangalam Sethuraman for their continued blessings and grace without which this wouldn't have been possible.

To my late grandfather, Mr. Srinivasan Subramanian for his blind faith that I would hold a doctorate degree one day.

To my advisor, Dr. Somenath Mitra for believing in my potential and giving me an opportunity to bring my dreams come true.

To my parents, Mr. and Mrs. Ragunath; my husband Mr. Narayanan Seetharaman for their endless sacrifice, support, motivation and for patiently bearing my emotional tantrums.

To my lovely daughter Srishti Narayanan, a true blessing in my life who had been very supportive and understanding all through these years, spending years away from us so I can complete this degree.

ACKNOWLEDGMENT

I would like to express my sincere gratitude to my advisor, Dr. Somenath Mitra for providing valuable guidance, support and opportunity to pursue research under his supervision during the course of my Doctoral Program. Special thanks to Dr. Edgardo T Farinas, Dr. Tamara Gund, Dr. Yong. I. Kim and Dr. Robert. B. Barat for their support as the committee member.

I would like to express my gratitude for Dr. Ziavras. G. Sotirios, Ms. Clarisa González- Lenahan, and Mr. Jeffrey Grundy, as well as the staff of Graduate Studies Office and the Office of International Students and Faculty for helping me during the course of my study at NJIT. I thank the New Jersey Water Resource Research Institute (NJWRRI), Phase II SBIR grant from US Department of energy, National Science Foundation, Electric Power Research Institute(EPRI) for their financial support. I appreciate all the help provided to me by the Department of Chemistry and Environmental Science. Special thanks to department staff Ms. Sylvana Brito, Ms. Genti Price, Dr. Chaudhery Mustansar Hussain, Mr. Yogesh Grandhi and late Ms. Gayle Katz for making my period of study more comfortable.

Additionally, I would like to express my sincere gratitude to Dr. Sagar Roy for his constant guidance during the course of the work. I would like to thank my other colleagues namely Dr. Ornthida Sae-Khow, Dr. Chintal Desai, Dr. Megha Thakkar, Dr. Zhiqian Wang, Dr. Zheqiong Wu, Dr. Madhuleena Bhadra, Kun Chen, Worawit Intrchom, Samar Azizighannad, Xianyang Meng, Madihah Saud Humoud, Kabir Mitra, and Joydeep Chakraborty for their support and encouragement for their constant support and encouragement. My sincere gratitude for Dr. Chutarat Saridara for her motivation

since my acquaintance from master thesis phase. I would like to thank my friends Dr. Priyaradhi Santhanam, Lakxmi Gurumurthy, Ram Gurumurthy, Chandramouleswaran Ravichandran, Kannan Narasimhan, Supriya Ravichandran, Varsha Ramesh, Anusha Rajan, Barathi Chandrasekar, Seema Yadav, Venkat Velegala, Abhinay Madduri, Deepthi Wukkalam, Harish Damadoran and those from Art of Living family Amrapalee Panchala, Vrushali Pachpande, Abheetha Narayanan, Neha Jain, Shubra Bhatnagar, Amit Haryani for their constant motivation and encouragement.

Finally, I would like to thank my family members Mrs. Savi Vijay my sister in-law and brother in-law Mr. Vijay Shrinivas, my parent in-laws Mr. and Mrs. Seetharaman, my parents Mr. and Mrs. Ragunath, sister Mrs. Dheepika Arunkumar, my uncle and aunt Mr. Gopinath and Mrs. Saraswathy Gopinath and all my family members who had been instrumental in my achievement by their support, patience and encouragement through my life.

LIST OF TABLES

LIST OF FIGURES

LIST OF FIGURES
(continued)

LIST OF FIGURES
(continued)

Figure **Page**

TABLE OF CONTENTS

TABLE OF CONTENTS
(continued)

TABLE OF CONTENTS
(continued)

TABLE OF CONTENTS
(continued)

Chapter **Page**

TABLE OF CONTENTS
(continued)

TABLE OF CONTENTS
(continued)

Chapter **Page**

CHAPTER 1

INTRODUCTION

1.1 Background

Membranes have been used in many industrial scale separations, such as, gas purification, water treatment, desalination, filtration, dialysis, dehumidification, osmosis, reverse osmosis, and electro dialysis (Baker, 2000). They have also been used to achieve a variety of analytical scale separations that include extraction, concentration and cleanup. Being semi permeable, they primarily function as a barrier that allows the selective transport of a solute. In analytical applications, this allows the enrichment of the species of interest and their removal from the sample matrix. The movement of the analyte of interest may be driven by a chemical, pressure or an electrical potential gradient(Patnaik, 2010).

In recent years, membrane techniques have advanced numerous analytical techniques by facilitating separations without the mixing of two phases, thus eliminating problems such as emulsion formation and high solvent usage. These techniques can also allow the simultaneous extraction and enrichment of analyte, and typically facilitate trace level analysis while consuming small amounts of solvents. Membrane extraction has been applied to a wide range of analyte including biological molecules(Davarani et al., 2012), metals(Pálmarsdóttir et al., 1997,Ndungù et al., 1998) and organic pollutants(Berhanu et al., 2006). They have also been successfully used in diverse environmental media that include air and water, and at the same time are becoming popular in biomedical applications with matrices such as, urine, blood and blood plasma to analyze drugs and their metabolites(Halvorsen et al., 2001,Andersen et al., 2003). Such media are complex and usually require tedious and multiple sample preparation steps. Additionally, micro

scale sample volumes, particularly in liquid membranes lead to high enrichment in order of thousands(Chimuka et al., 2004) and detection limits in the range of sub ppb levels. As a result, techniques such as membrane-based micro extraction often referred to as liquid phase micro extraction (LPME) are seen as an alternative to solid-phase extraction (SPE), solid-phase micro extraction (SPME) or traditional liquid-liquid extraction (LLE). It is also worth mentioning that they have also been micro fabricated in MEMS devices.

Applications of membrane extraction are quite diverse, and encompass different types of membranes, module designs as well as the variation in extraction chemistry(Hylton et al., 2007). Though it is conceivable that they can be collectively used to achieve any sample preparation, the key to their success lies in achieving high selectivity and flux at the same time; two parameters that often tend to be divergent. Consequently, there is tremendous interest in developing newer membranes to suit diverse applications.

In an effort to develop the next generation membrane with high permeability and selectivity, much effort has gone into the design of both membrane materials and architecture(Kathios et al., 1994) . Of particular recent interests have been in the use of nanomaterials and nanostructures which have successfully engineered pore size, surface area as well as physical and chemical properties such as sorbent characteristics and interactions with solutes(Hussain et al., 2012). A variety of nanomaterials including carbon nanotubes (CNTs), zeolites, and gold have been implemented in membrane structures.

1.2 Principles of Membrane Separation

A membrane is a selective barrier through which different gases, vapors and liquids permeate at varying rates. The membrane facilitates the contacting of two phases at the membrane interface. Molecules move through membranes by the process of diffusion and are driven by a concentration (ΔC), pressure (ΔP) or electrical potential (ΔE) gradient. This is demonstrated in Figure 1.1. The interesting aspect of this technique is that both the donor and acceptor can flow continuously leading to the development of automated, real-time monitoring techniques.

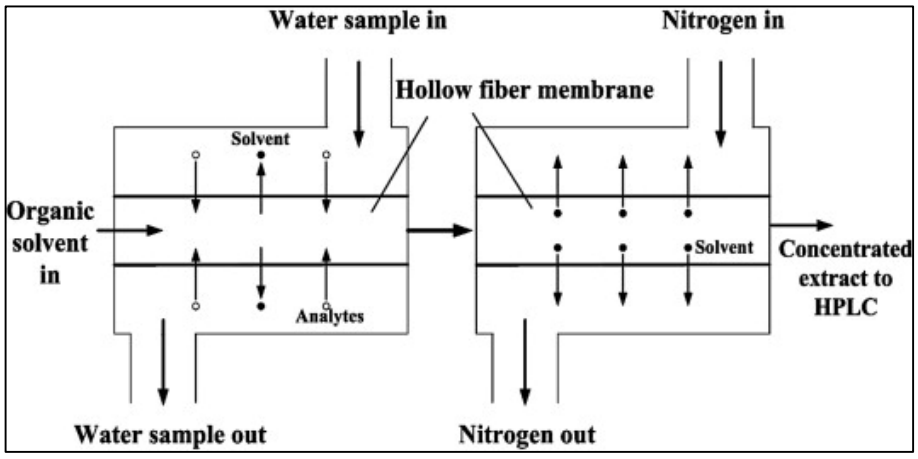

Figure 1.1 Total analytical system by interfacing membrane extraction to pervaporated concentration.
Source:(Wang et al., 2005)

This diffusion-based transport can be expressed by Fick's first law of diffusion:

$$J = -D\,\frac{dc}{dx} \tag{1.1}$$

where J is the flux (g/cm^{2}s), D is the diffusion coefficient (cm^{2}s), and dc/dx is the concentration gradient. It is important to note that the diffusion coefficient is a function of concentration. Thus, theoretical predictions in analytical applications are a difficult task, where concentration varies by orders of magnitude. The enrichment factor (EF) and extraction efficiency (EE) are the two major parameters used to evaluate the effectiveness of a particular extraction. The EF may be defined as the ratio of analyte concentration in the extract to that in the initial donor:

$$EF = \frac{C_s}{C_w} \tag{1.2}$$

where, C_s is the analyte concentration in the final extract and C_w is the analyte concentration in the original sample.

The EE refers to the fraction of analyte that is extracted into the acceptor such that:

$$EE = \frac{n_s}{n_w} = \frac{C_s V_s}{C_w V_w} = EF\,\frac{V_s}{V_w} \tag{1.3}$$

where, n_s and n_w are the analyte mass in the final extract and in the original water sample, V_s and V_w are the volume of the concentrated extract and the original water sample respectively.

1.3 Membranes

1.3.1 Nanostructured Membranes

As already mentioned, the two important membrane characteristics are their flux and selectivity. These are controlled by chemical and physical characteristics, morphology as well the presence of and absence of pores. A broad classification for membranes is that between the porous and nonporous. This essentially refers to the presence or absence of pores in the membrane. The former has openings through which select molecules pass. Movement through these membranes can also be by size exclusion and is used in applications such as nanofiltration and dialysis. Separation can also be accomplished by hydrophobicity, for example a hydrophobic porous membrane does not allow water to permeate. During extraction, two liquid phases meet at the pores, and during pervaporation the analyte vaporize at these sites. Non-porous membranes are solid (pore-free) structures and the molecules must move through them via diffusion, and therefore the partitioning of the analyte is critical.

The membrane may also have diverse structures. For instance, homogenous (isotropic) membranes are uniform throughout while asymmetric (anisotropic) and composite thin-films are not. Isotropic membranes include micro porous, nonporous dense and electrically charged membranes. Separation in micro porous membranes (pore size between 10^{1}-10^{4}nm) is a function of particle and pore size distribution, and are used for processes such as microfiltration. In nonporous dense membranes, transport is via diffusion and separation is influenced by partition coefficient as well as diffusivity of components in

the membrane. These types of membranes are commonly used for extraction, reverse osmosis and pervaporation. Anisotropic membranes refer to those in which the material, the porosity and pore size vary throughout the structure and include thin-film composites and Loeb-Sourirajan membranes(Baker, 2000). The composite membrane usually consists of different polymers where the surface layer determines selectivity, while the porous layer serves as a support.

Homogenous solid membranes such as silicone tend to provide lower fluxes but higher selectivity. On the other hand, the porous membranes provide higher flux but lower selectivity. Composite membranes are a compromise. The porous part provides for a high flux, while the solid layer on top provides selectivity. For example, a one-micron silicone layer on top of a polypropylene composite provides high VOCs flux while preventing large amounts of water from permeating through. For thin-film composites, the thin surface layer represents a small percentage of the overall membrane but is responsible for much of the membrane's selectivity. Scanning electron microscope (SEM) images of porous and composite membranes are shown Figure 1.2.

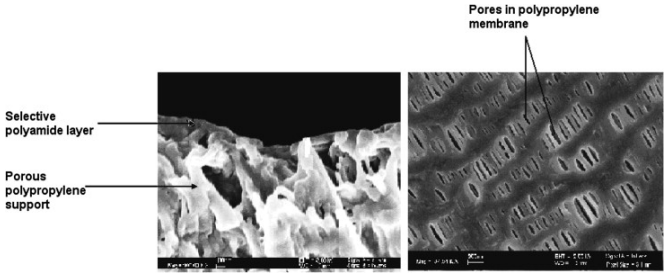

Figure 1.2 SEM of thin-film composite (polyamide surface layer supported by polypropylene) and microporous polypropylene.
Source:(Loeb et al., 1962)

An assessment of permeability and selectivity has shown asymptotic limitations on the separation capability of pure polymeric membranes. Efforts at improving these have looked at the development of novel materials as well as the modification of their structure and morphology. Recent interest has been focused on developing strategies for incorporation of nanomaterials such as carbon nanotubes, zeolites, carbon black, gold in membrane matrix or surface for the generation of nanostructured membranes with higher flux and selectivity.

The rate of mass transport through the membrane, Q, is controlled by the diffusion of solute can be estimated under steady-state conditions by use of the following equation:

$$Q = BAD(\Delta P)C_w/b \tag{1.4}$$

where, A is the surface area of the membrane, D is the diffusion coefficient in the membrane material, ΔP is the vapor pressure (or concentration) gradient, b is the thickness of the membrane, B is a geometric factor defined by the porosity of the membrane and C_w is the inlet concentration. The presence of nanomaterials can affect several of these parameters; B and D are altered by the presence of the nanoparticles, while the partition coefficient is affected by the physical/chemical properties of the nanomaterials while their high surface area can facilitate greater flux. Therefore, an important consideration associated with the incorporation of nanomaterials in the membranes are their chemical properties, size distribution, agglomeration, interaction with the membrane matrix, effect on porosity, surface area and morphology. Additionally, such nanomaterials can be

effective sorbents. Together these can enhance the selective partitioning as well as the permeation of the solute of interest.

A common approach to the fabrication of nanostructured membrane involves adding the filler material to a polymer solution followed by film casting or spinning and is referred to as the mixed matrix membrane (MMM). Good polymer-filler adhesion and uniform dispersion allows the formation of uniform membranes of submicron thickness. Such membranes possess some unique properties that benefit from the polymer as well as the nanofillers. Due to their small sizes, the nanoparticles can be implemented within micron or submicron thick films to serve as high flux barriers. For example, in fabrication of a polymeric layer tightly packed with nanomaterials like zeolite or CNTs form a dense mixed matrix region. Incorporation of nanocarbons within polymeric membranes have been studied to increase permeate flux in extraction and pervaporation processes(Sholl et al., 2006,Hinds et al., 2004). Dense arrays of aligned MWNTs can potentially be used for solute transport though the tube pores(Hinds, et al., 2004). These exceptionally high transport rates as demonstrated by the CNTs was attributed to the specific pore size of the nanotubes, molecular smoothness of the surface and hydrophobicity and has been proposed as means for desalination(Gethard et al., 2011) via membrane distillation. Additionally, ability to tailor surface properties by chemical and biochemical functionalization of a specific nanomaterials is an attractive route for membrane development. Similarly, they can be incorporated in porous structures where they alter the shape, size selective nature and allow molecular sieving(Arora et al., 2007).

Nanostructured membranes (Figure 1.3) are beginning to find applications in various fields such as gas separation(Sanip et al., 2011,Kim et al., 2007), extraction(Hylton et al., 2008), pervaporation(Peng et al., 2007), and reverse osmosis(Lee, 2011). Some recent developments and updated reports in nanostructured membranes are presented here.

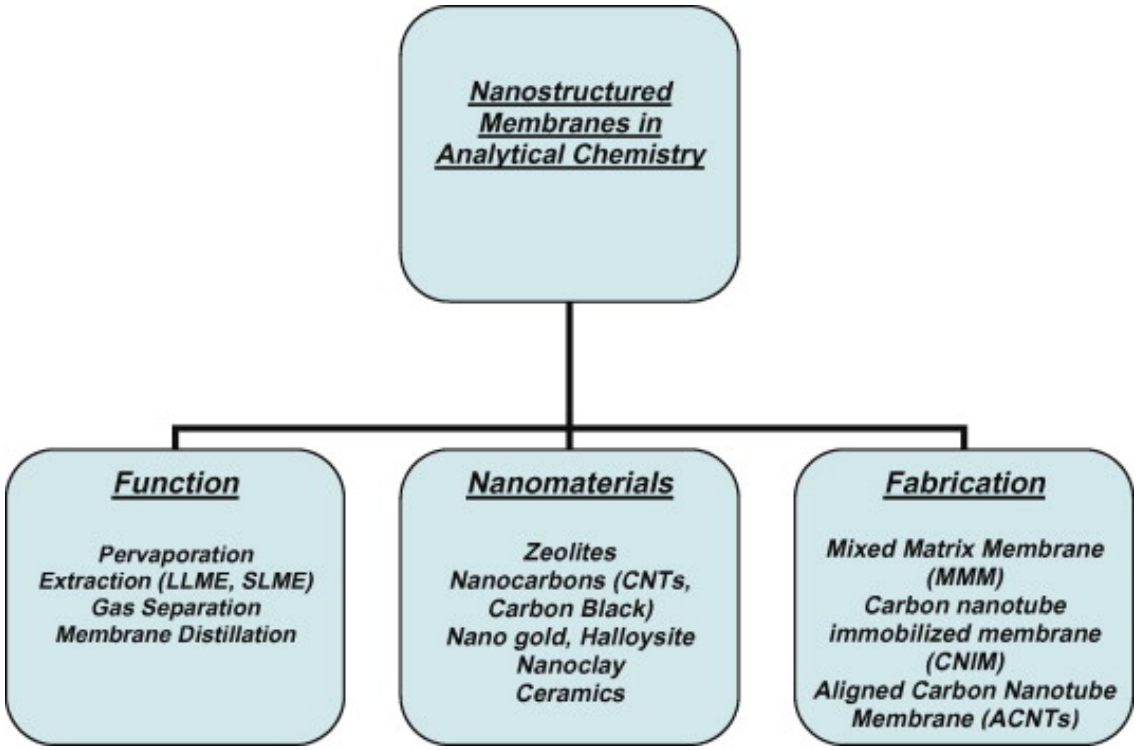

Figure 1.3 Nanostructured membranes.
Source:(Sanip, et al., 2011,Hylton et al., 2008)

1.3.2 Carbon Nanotube Membrane

Since their discovery in 1991, CNTs have received much attention. Carbon nanotubes (CNTs), which are essentially graphene sheets rolled into tubes as single-walled (SWNT) or multiple-walled (MWNT) structures, can be interesting materials for membrane systems. There has been much interest in these materials because of their excellent thermal, electrical and structural properties. In addition, their favorable adsorption properties have fostered their use as sorbent materials in many analytical and extraction processes(Huang et al., 2012,Fang et al., 2006). They are found to be excellent sorbents for volatile and semivolatle organics(Hussain et al., 2008) as well as small molecules such as methane(Saridara et al., 2010), water vapors(Ellison et al., 2005) and other gases(Fujiwara et al., 2001). Consequently, they have found applications in chromatography as well as air and water sampling. They have also been used as effective media in SPE(Bhadra et al., 2012) and SPME(Hussain et al., 2011). In membranes, they can increase the selective partitioning and permeation of the solutes of interest.

In typical CNT membrane-based liquid extraction, when the two phases contact at the pores, the interactions can take place via rapid solute exchange on the CNTs, thus increasing the effective rate of mass transfer and flux. The high aspect ratio of the CNTs dramatically increases the active surface area as well which contribute to flux enhancement. Fabrication of CNT membranes are discussed in the following section.

1.3.2.1 Carbon Nanotube Nanocomposite Membrane. Initial attempts at incorporating CNTs in membranes involved the formation of CNT-nanocomposite by solution casting. Peng and coworkers(Peng et al., 2007) fabricated membranes with chitosan functionalized MWNTs. Surface decoration/wrapping of carbon nanotubes with chitosan biopolymer led to dissolution and dispersion in PVA solution. The mixture was subsequently mechanically stirred, ultrasonically agitated and cast onto a glass plate. The pristine nanocomposite was dried to form 80 μm thick membrane. The membrane was used in pervaporation of benzene/cyclohexane (50/50, w/w) mixture.

1.3.2.2 Aligned Carbon Nanotube Membrane (ACNTs). Although great deal of practical and fundamental studies has been reported on CNT- Mixed Matrix Membrane (MMM), related researches in this area did not receive much attention until Hinds et. al.(Hinds, et al., 2004) reported aligned carbon nanotubes (ACNTs) membrane using CVD on quartz substrate across a polystyrene film**.** The quartz substrate (2cm x 2cm) with aligned multiwalled CNTs was coated drop wise with 50% (by weight) of polystyrene (PS). Excess polymer was removed by spin coating at 3000 rpm for 1 minute. Following that, neat toluene was poured dropwise onto the sample and allowed to set for 1 minute to further dissolve excess polymer covering the tops of CNTs and spin coated for 1 minute at 3000 rpm. Finally, the sample was dried in a vacuum oven at 70ºC for 4-5 days under 25-inch Hg pressure to fabricate the aligned CNT/PS composite film which was removed from quartz substrate by HF solution (1:2 by volume). Additionally, plasma oxidation was

performed to remove excess polymer as well as open CNT tips. The resulting free standing composite films as formed, with the CNT alignment intact from top to bottom were accessible to the outer molecule both sides of the formed membrane. Figure 1.4 illustrates the fabrication of cross sectional schematic of aligned CNT (ACNTs) membrane fabrication steps.

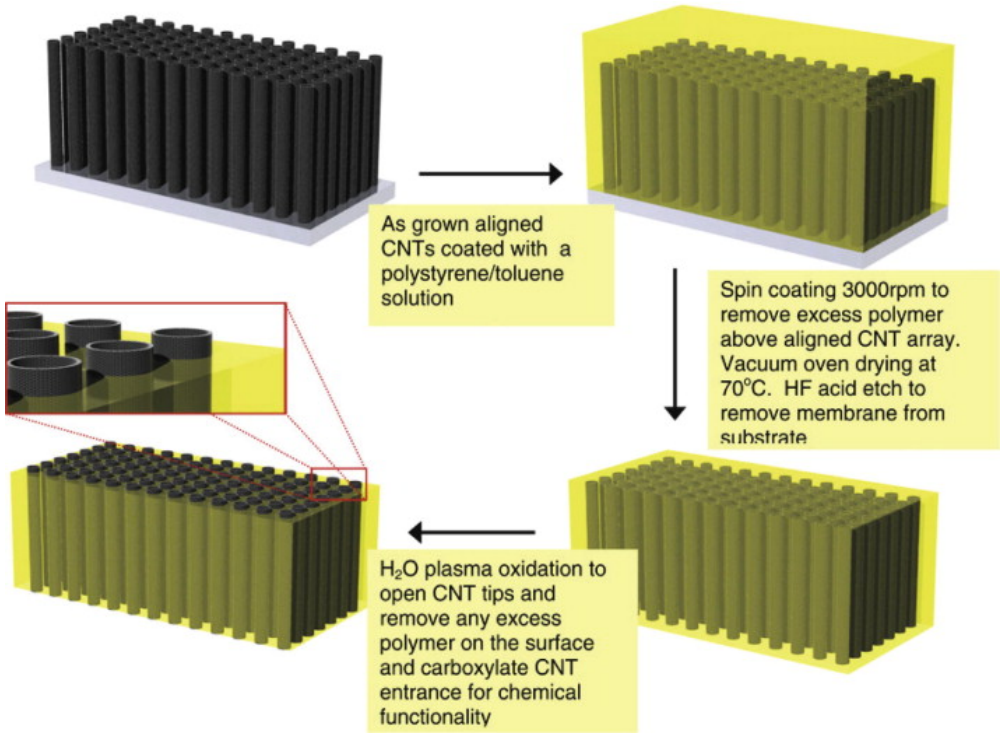

Figure 1.4 Aligned carbon-nanotube (CNT) membrane fabrication steps.
Source:(Bhadra et al., 2013)

1.3.2.3 Carbon Nanotube Immobilized Membrane (CNIM). Mitra et al.(Sae-Khow et al., 2009) immobilized Carbon Nanotubes within the pores of membranes leading to the development of unique membrane structure referred to as the CNIM. This was achieved by

immobilizing CNT using dispersion in a polymer solution. The dispersion was injected into the lumen of a conventional hollow fiber under pressure. This served as the immobilization step, and the polymer served as the glue that held the CNTs in place. Such membranes were robust, thermally stable and possessed high selectivity. The goal here was to immobilize CNTs without covering its active surface with the polymer, or having a thick polymeric layer over it. This is advantageous as well as challenging. However, accomplishing this is highly desirable so that their surface is free to interact directly with the solute. The membrane produced from this method has been used for liquid-liquid extractions, membrane distillation and pervaporation(Sae-Khow, et al., 2009,Sae-Khow et al., 2010,Sae-Khow et al., 2010,Gethard et al., 2011,Gethard et al., 2011). Typical membrane produced by this process is shown in Figure 1.5 (a –b). Additionally, Figure 1.5 (c – d) shows the typical SEM image of CNIM membrane in comparison to the unmodified polypropylene membrane.

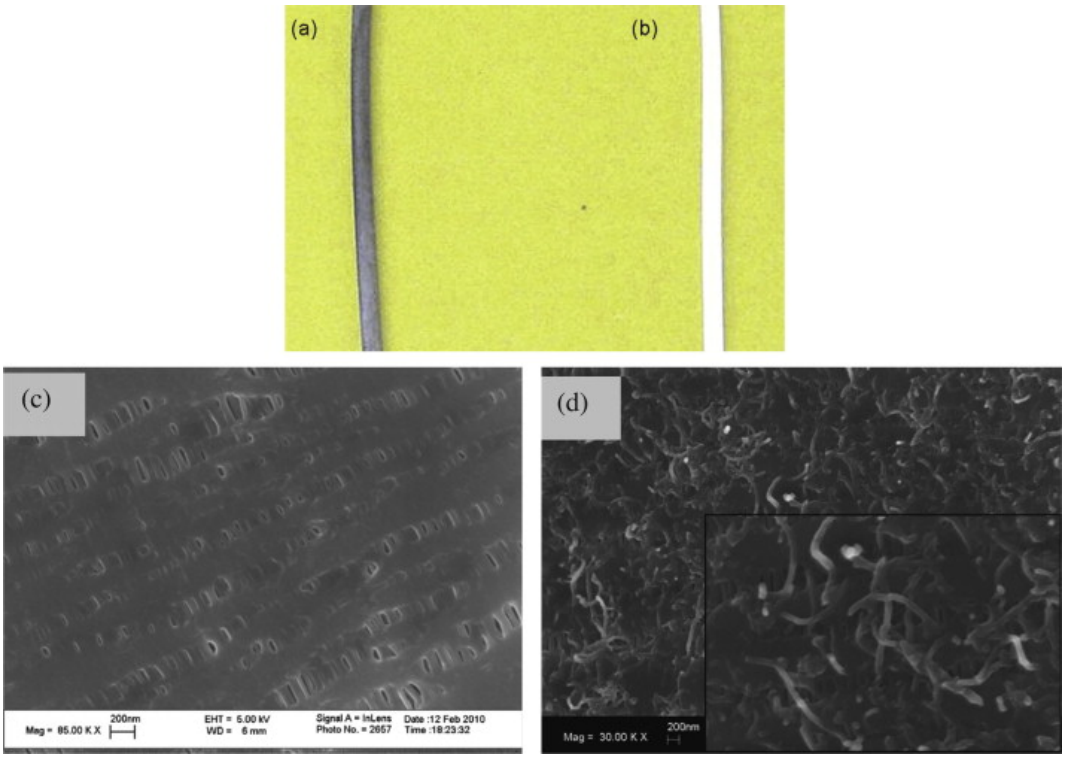

Figure 1.5 (a) Photograph of carbon-nanotube immobilized membrane (CNIM); (b) photograph of pure polypropylene; (c) SEM image of unmodified polypropylene membrane; and, (d) CNIM.
Source:(Sae-Khow, et al., 2009)

1.3.3 Application of Nano Structured Membrane

The nanostructured membranes are relatively new developments and even newer when it comes to analytical chemistry. Some applications that show a great deal of promise are presented here. In the analytical field, the largest application has been with the incorporation of CNTs. This is an attractive because the CNTs are excellent sorbents that can enhance partition coefficients, increase the selectivity and result in enhanced enrichment and extraction efficiency. Functionalization of CNTs can also be used to alter selectivity because it alters solute solvent interactions.

1.2.3.1 Carbon Nanotube Membranes in Pervaporation. The outstanding sorbent characteristic of CNTs has led to the exploration in pervaporation. Pervaporation performance of the resulting MWNTs incorporated polyvinyl alcohol PVA-MMM) was carried out by Choi et al.(Choi et al., 2007) where an increase in flux and a decrease in the selectivity was reported with the increase in MWNTs content. These were attributed to two key factors: the crystallinity of membrane and the molecular transport through the nanotubes. Higher amount of MWNTs created strong interaction with PVA and therefore prevented the packing of molecules to form crystal, resulting in a decrease in the crystallinity of the PVA matrix. Peng et al.(Peng, et al., 2007) studied the pervaporation properties of CNT-PVA membranes for the separation of benzene/cyclohexane mixtures. The CNTs were dispersed with cyclodextrin by grinding during the formation of MMM in order to reduce the aggregation and improve the compatibility of CNTs in the polymer

matrix. The resulting MMMs exhibited the highest benzene permeation flux of 61.0 gm^{-2} h^{-2} with separation factors of 41.2 for the mixture with weight percent of 1:1. Upon the comparison of pervaporation properties with the PVA and cyclodextrin dispersed PVA membranes, the MMMs prepared through the incorporation of CNTs demonstrated enhanced mechanical strength properties and pervaporation properties. Mondal and Hu(Mondal et al., 2008) have reported the adverse effects of the presence of high MWNT content in pervaporation process. Functionalized MWNTs were incorporated into segmented polyurethane (SPU) to study the water vapor transport properties. In such MMM system, MWNTs were found to influence both crystalline and amorphous regions of SPU matrix by imparting stiffness to the polymer matrix, particularly when added in excess.

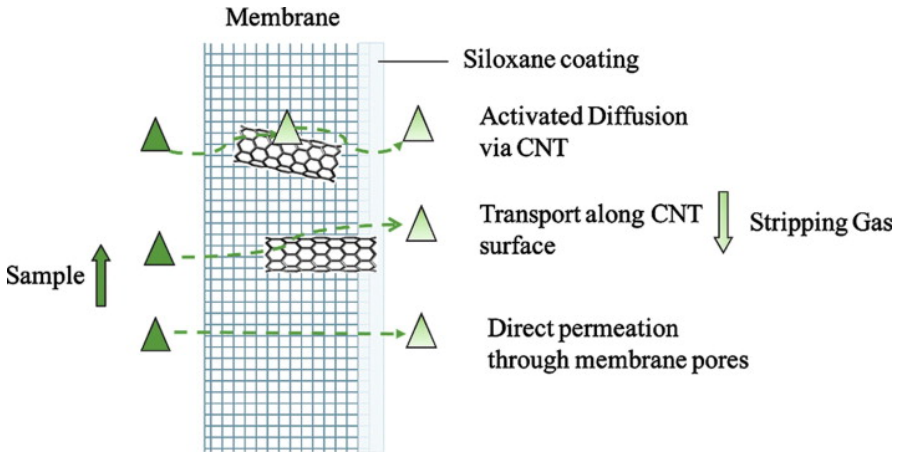

Figure 1.6 Mechanism of pervaporation in carbon-nanotube immobilized membrane (CNIM).
Source: (Sae-Khow, et al., 2010)

Sae - Khow and Mitra(Sae-Khow, et al., 2010) reported the development of novel CNIM using a composite membrane for the pervaporative removal of organics from an aqueous matrix. The CNIM demonstrated several advantages including enhancement in organic removal and mass transfer by 108 and 95% respectively and also enhanced recovery at low concentrations, lower temperatures, and higher flow rates. The nanotubes provided additional pathways for enhanced solute transport, affecting both the partitioning and diffusion through the membrane as shown in detailed mechanism depicted as Figure 1.6.

1.3.3.2 Carbon Nanotube Membrane in Membrane Extractions. The sorbent characteristics of the CNT membrane have been exploited in membrane extraction as well. Eshaghi et al.(Es'haghi et al., 2010) demonstrated a three-phase supported liquid membrane consisting of an aqueous (donor phase), organic solvent/nano sorbent (membrane) and aqueous (acceptor phase) system operated in direct immersion sampling mode. The MWNTs dispersed in the organic solvent were held in the pores of a porous membrane supported by capillary forces and sonication. Their proposed method allowed the very effective and enriched recuperation of an acidic analyte into one single extract. The method showed good linearity in the range of 0.0001-50 micro g/L, reproducibility and detection limits in the pico gram/L with enrichment as high as 2100.

Hylton et al. (Hylton, et al., 2008) used CNIM to carry out three-phase supported liquid micro extraction (μ-SLME) as well as liquid-liquid extraction (μ-LLME). The

immobilization was carried out such that the CNT surface was accessible to adsorption/desorption. Several organic compounds including haloacetic acids and non-polar organics were studied using a hollow fiber CNIM. The incorporation of MWNTs improved the extraction efficiency by as much as 144%. Sae Khow et al.(Sae-Khow, et al., 2009) reported the effect of both polar and non-polar compounds as analyte and reported that the enrichment factor enhancement by 30-113% using CNIM. O.Sae Khow and Mitra(Sae-Khow, et al., 2010) also demonstrated the simulateneous extraction and concentration on CNIM, where the CNTs enhanced both these phenomenon (Figure 1.7) leading to superior performance in terms of higher enrichment factors and extraction efficiency. The CNTs immobilized in the pores of a polypropylene hollow fiber, led to nearly 250% enrichment enhancement over the unmodified parent membranes. The detections limits for polycyclic aromatic compounds were between 0.042 and 0.25 μg/L. This flow through system was designed for on-line extraction in automated analysis.

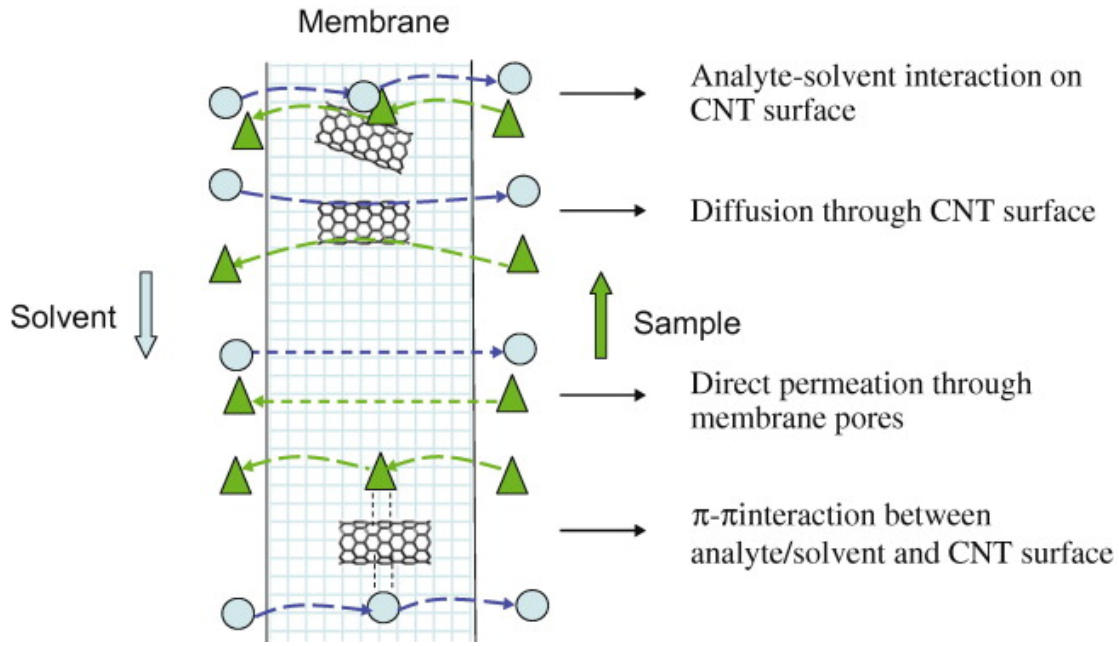

Figure 1.7 Carbon-nanotube (CNT)-assisted extraction and enrichment. Triangles represent the analyte molecules and the circles represent the solvent molecules
Source: (Sae-Khow, et al., 2010).

More recently, Bhadra et al.(Bhadra et al., 2012) demonstrated for the first time that Carbon Nanotubes could be immobilized on the surface of solid polymeric membranes, which can also lead to enhanced extraction of polar and non-polar organics. A polar membrane was used on which nonpolar CNTs were immobilized. This CNIM combination showed dramatic enhancement of enrichment factor by 92% and solvent retention by as much as 29%.

1.3.3.3 Carbon Nanotube Membranes in Membrane Distillation. A novel analytical method that also used carbon naotube based membranes is membrane

distillation (MD). Mitra et. al.(Gethard, et al., 2011,Gethard, et al., 2011) recently reported this real-time, online concentration technique, where the aqueous matrix is removed from the sample to enhance analyte enrichment. Therefore, MD is a universal method that cn be used for a wide range of compounds, and is unlike conventional membrane extractions that rely on the permeation of the analyte into an extractant phase. An alternate to thermal distillation, here a heated aqueous solution (or polar solvent such as ethanol) is passed through the lumen of a hydrophobic hollow fiber, which prevents the transport of the liquid phase across the membrane. However, the solution is partially converted to vapor (60-90^{o}C) and MD relies on the net flux of this vapor from the warm to the cool side of the membrane. The driving force for the vapor transport is determined by the vapor pressure difference across the membrane, which depends upon the temperature difference.

MD provides a complimentary approach to conventional membrane extraction which relies on the selective permeation of the analyte, and is often a challenge because selective membranes for diverse analytes are not always available. MD with CNIM (Figure 1.8(a)) has shown great promise because the CNTs were instrumental in increasing water vapor as well as solvent flux . The mechanism of MD with CNTs is shown in Figure 1.8(b) for removing polar solvents for concentrating pharmaceutical compounds. Comparison between MD performance with and without CNTs is shown in Figure 1.8(c). Enrichment using CNIM(Gethard, et al., 2011) doubled compared to membranes without CNTs, while the methanol flux and mass transfer coefficients

increased by 61% and 519%, respectively. Additionally, the carbon nanotube enhanced MD process showed excellent precision (RSD of 3–5%), and the detection limits for pharmaceutical compounds were in the range of 0.001 to 0.009 mg L^{-1}.Overall, it was postulated that the CNTs served as sorbent sites thereby providing additional pathways for enhanced solvent vapor transport, thus enhancing preconcentration.

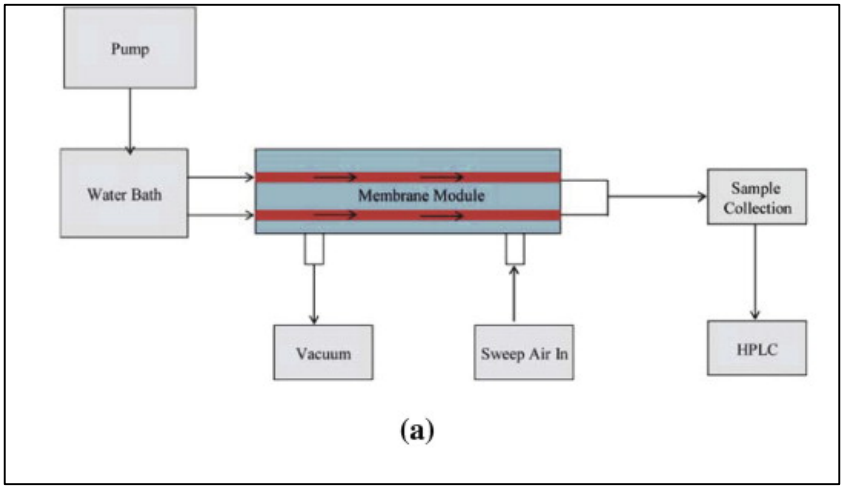

(a)

(b)

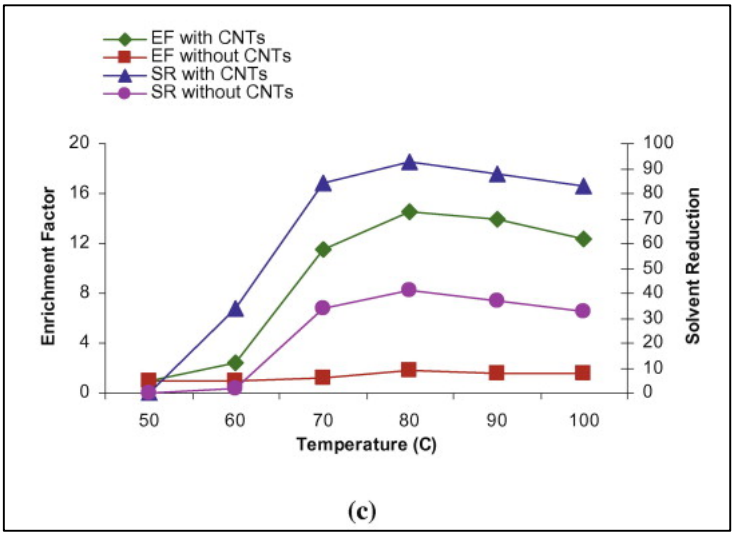

(c)

Figure 1.8 (a) Membrane distillation (MD) as an on-line preconcentration technique; (b) membrane device; (c) MD performance on unmodified membrane and carbon-nanotube immobilized membrane (CNIM)
Source: (Gethard, et al., 2011).

1.4 Objectives

The objective of this research is to develop nanostructured membranes for air and water treatment applications. Different surface modification techniques were adapted to modify the surface properties of membranes to enhance membrane flux for various membrane based applications such as membrane extraction of VOCs from air, membrane distillation for desalination and removal of bacterial debris. This work is presented in four parts.

1.4.1 Removal of VOCs from Air

Membrane extraction of volatile organics from air was evaluated as a real-time VOC removal technique where VOCs from are removed from air stream and simultaneously analyzed using a gas chromatograph. This technique was aimed to explore a possibility of more greener approach for VOC removal/extraction from polluted or effluent air stream. It was demonstrated that CNT immobilized membrane performed better in comparison to unmodified membrane.

1.4.2 Permeate Surface Modification for Desalination

Oxidation of permeate surface was performed to introduce polar groups on membrane surface to allow partial wetting of permeate surface that would facilitate rapid condensation of diffused vapors. This results in better flux in membrane distillation process for desalination.

1.4.3 CNIM for Desalination

Carbon nanotube immobilized membranes (CNIM) are fabricated via phase inversion technique using a controlled approach for carbon nanotube (CNT) incorporation which provides additional pathways for water vapor diffusion. Surface morphology differed for membranes fabricated with varying PVDF concentrations which altered the CNT distribution and its interaction with water vapor.

1.4.4 Removal of Endotoxin via Membrane Distillation

Generating endotoxin free water is a challenge in the health care industry where the maximum allowable endotoxin level for sterile water for injection are set between 0.25 and 0.5 EU/mL. Conventional approach to generating endotoxin free water comprise of a combination of thermal distillation and reverse osmosis. In this approach, we use direct contact membrane distillation technique for removal of endotoxins from water.

CHAPTER 2

CARBON NANOTUBE IMMOBILIZED COMPOSITE HOLLOW FIBER MEMBRANES FOR EXTRACTION OF VOLATILE ORGANICS FROM AIR

2.1 Introduction

Volatile organic compounds (VOCs) have numerous industrial applications and have been a source of air pollution for decades(Król et al., 2010,Król et al., 2010). Conventional, control technologies for VOCs include thermal incineration, catalytic combustion, photocatalysis, adsorption, and air stripping. Each technology has its own merits and limitations, and the applicability is situation-dependent on factors such as background matrix as well as concentration. Some of these processes are energy intensive, expensive for dilute streams, and may also lead to the formation of secondary pollutants(Dewulf et al., 1999,Khan et al., 2000,Ruddy et al., 1993). Some are multistep processes, for example adsorption requires not only expensive sorbents but also regeneration(Barro et al., 2009,Harper, 2000,Urashima et al., 2000,Ghoshal et al., 2002,Ras et al., 2009). Membrane separation can be an effective VOCs control alternative in which the organics are not exposed to high temperatures, there is no requirement of additional chemicals, the process can have small instrument footprint, and the compounds can be recovered(Kimmerle et al., 1988,W. Baker et al., 1987,Sohn et al., 2000,Paul et al., 1988,Baker et al., 1994). Other advantages of membrane methods are low energy requirements, high selectivity, and the ability to handle high levels of moisture. These methods can be cost-effective with the

development of novel membranes that provide higher performance in terms of flux and selectivity.

Membrane separation has undergone rapid developments in recent years with diverse applications in air and water treatment such as desalination, dialysis, ultrafiltration, gas separation, dehumidification, electro dialysis, and pervaporation(Baker, 2000,Ho et al., 1992). Membrane separation can provide high selectivity and enrichment factors which can be used for capturing VOCs from dilute air stream(Badjagbo et al., 2007,Panek et al., 2009,Ketola et al., 2002). Various porous, non-porous as well as composite polymeric membranes made from polymers such as polyimide, polyethylene, polypropylene, polytetrafluoroethylene, polyvinylidene fluoride, polyvinyl chloride, polydimethylsiloxane have been used for separating VOCs from air as well as water(Noble et al., 1995). Recent efforts for enhancing selectivity and permeability have led to the development of thin film composite membranes(Koops et al., 1993,Smitha et al., 2004) and mixed matrix membranes consisting of interpenetrating polymeric materials with solid fillers(Jiang et al., 2007,Kittur et al., 2005). The fillers often comprise of nanomaterials that can enhance membrane performance.

The unique sorbent properties of CNTs have been utilized in different membrane separations where they offer several alternative mechanisms of solute transport(Hylton, et al., 2008,Hussain et al., 2008). Theoretical studies have shown that the permeation rate of certain liquids and gases through CNTs surpass that expected from classical diffusion models (Hinds, et al., 2004,Hummer et al., 2001) which has been attributed to the smooth

CNT surface, frictionless rapid transport, molecular ordering (Noy et al., 2007) and increase in diffusivity(Holt et al., 2006,Chen et al., 2006).

Recently, we have reported the development of novel polymeric membranes by immobilizing CNTs on the membrane surface(Sae-Khow, et al., 2010,Gethard, et al., 2011,Sae-Khow et al., 2010). Referred to as carbon nanotube immobilized membrane (CNIM), where the CNTs serve as a nano-sorbents or mediator for solute transport(Gethard, et al., 2011,Sae-Khow et al., 2010,Gethard et al., 2010,Gethard et al., 2012). The objective of this research is to study the extraction of VOCs from air streams using CNIM. This would have applications in air purification as well as concentrating the VOCs.

2.2 Experiment

2.2.1 Chemicals, Materials and Membrane Modules

Analytical grade toluene, dichloromethane, ethanol and acetone used in the experiments and were obtained from Sigma Chemicals (St. Louis, MO). High purity N2 (Air Gas, NJ) and deionized water (Barnstead 5023, Dubuque, Iowa) was used in all experiments. The raw multiwalled CNTs were purchased from Cheap Tubes Inc., Brattleboro, VT. The CNTs were further purified in our laboratory(Chen et al., 2008,Chen et al., 2007). The average diameters of the CNTs were ~30 nm and the length was as long as 15 μm.

The base membrane used was a 0.260 mm OD and 0.206 mm ID hollow fiber composite membrane (Applied Membrane Technology, Minnetonka, MN) with 1-μm thick

homogenous siloxane as the active layer deposited on microporous polypropylene as the support. The membrane module was constructed using ten 30-cm long hollow fibers in a 0.318 cm OD stainless steel casement. The membranes were held in the casing using 'T' connectors (Component and Controls, NJ) and sealed at both ends using fast setting epoxy (Loctite epoxy, Henkel Corporation, CT). This prevented the mixing of the two counter current streams. The effective surface area of the module was calculated 19.4 cm^2.

2.2.2 Fabrication of CNT Immobilized Membrane

Effective dispersal of CNTs and immobilization on the membrane surfaces were essential for CNIM fabrication. Ten mg of CNTs was dispersed in acetone and sonicated for 3 hr. while 0.2 mg polyvinylidenedifluoride (PVDF) was dissolved in acetone and mixed with the CNTs dispersion. The mixture was then sonicated for another 30 min. CNIM composite membrane was fabricated by coating the siloxane layer with CNT mixture. The PVDF served as a binder that held the CNTs in place. Later, the membrane was washed with acetone to remove the excess PVDF. The original hollow fiber membrane was sonicated with PVDF solution without the CNTs and to serve as a control.

2.2.3 Experimental Procedure

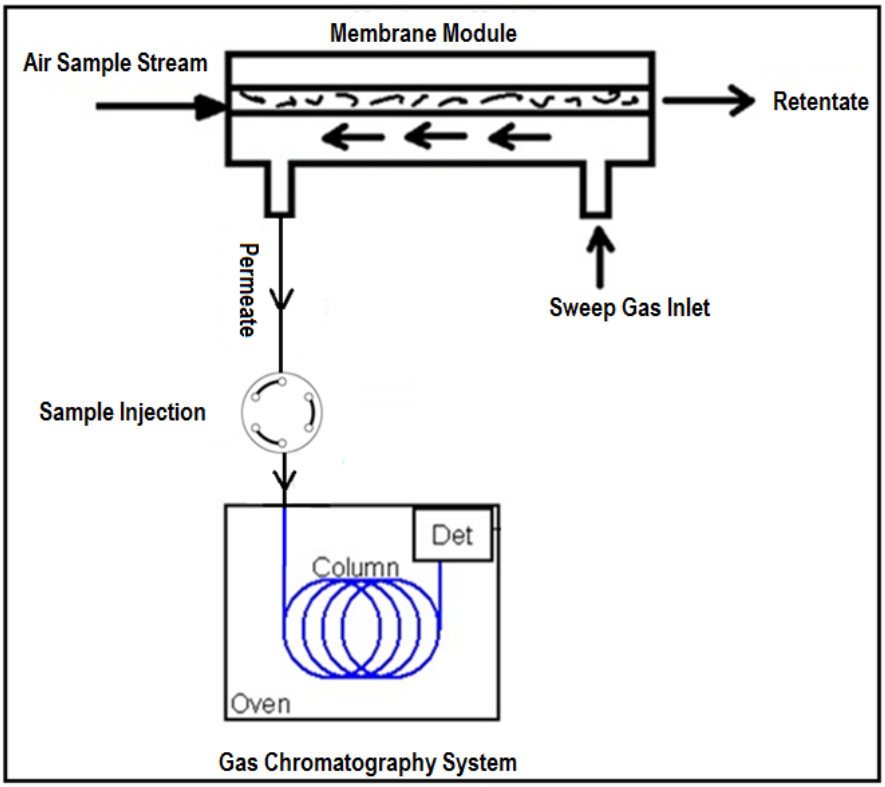

Figure 2.1 Schematic diagram of membrane separation system.

The schematic diagram for the experimental system used for VOCs removal is shown in Figure 2.1. Air stream containing VOCs was flown into the hollow fiber membrane module. The feed was mixed with a dry air stream to deliver pre-specified concentrations of VOCs. The feed flow rates were varied between 2 to 10 mL/min and the VOCs concentrations was maintained between 20 to 200 ppm. A countercurrent gas flow was used on the permeate side to transport the permeated VOCs from the membrane to a

6-port injection valve (Valco Instruments Co.Inc., TX) and injected at regular intervals into a Gas Chromatograph (GC).

Sample analysis was carried out using a portable SRI 8610 GC (SRI Instruments, CA) equipped with a flame ionization detector. A 0.53 mm ID, 30m long, 3.0 μm thick open tubular capillary column (Rxi-624 Sil MS, Restek Corporation, USA) was used for separation. A Peak simple version 3.72 for Windows platform (SRI Instruments, CA) was used for data acquisition and analysis.

2.2.4 Membrane Characterization

Characterization of both unmodified composite membrane and the CNIM were carried out using scanning electron microscopy (SEM) (Leo 1530 VP, Carl Zeiss SMT AG Company, Oberkochen, Germany). The membranes were cut into 0.5 cm long pieces and coated with carbon film before SEM analysis. Thermogravimetric analysis (TGA) was used to investigate the thermal stability of the membrane. TGA was carried out using a Perkin-Elmer Pyris 7 TGA system at a heating rate of 10° C/ min in air.

2.3. Results and Discussion

2.3.1 Membrane Characterization

The SEM images of the CNIM and unmodified membranes are shown in Figure 2.2. The outer surface of the unmodified membrane was a dense homogenous siloxane layer which is shown in Figure 2.2 (a). The CNTs were coated on the siloxane layer. It is clear from Figure 2.2 (b) that the CNTs were uniformly distributed on the membrane surface.

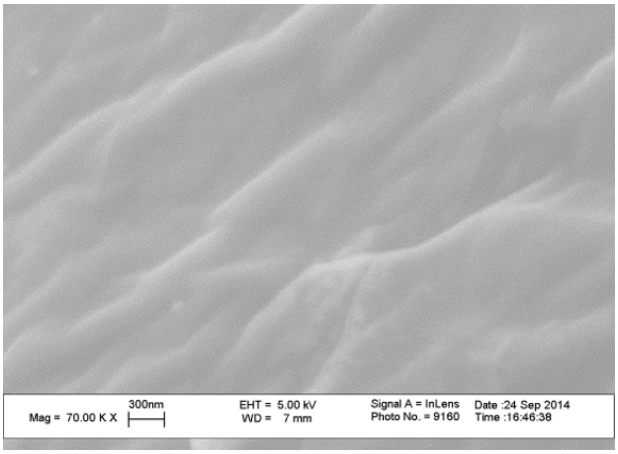

(a)

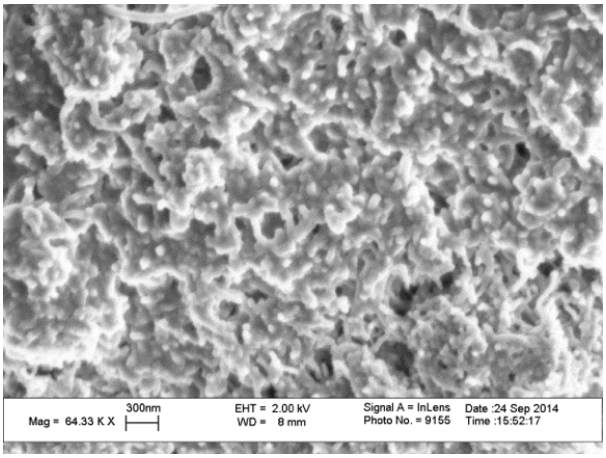

(b)

Figure 2.2 SEM images of (a) unmodified membrane (b) CNIM membrane.

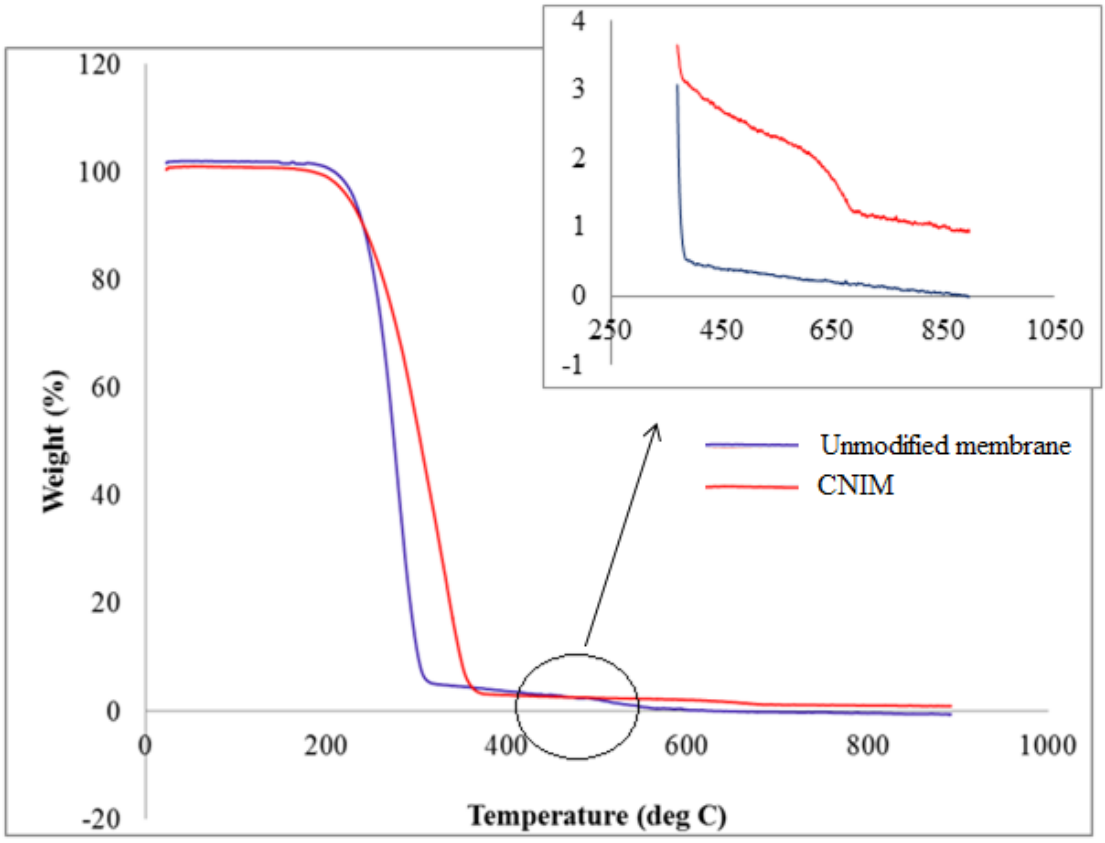

Figure 2.3 TGA for CNIM and unmodified membrane

Figure 2.3 shows the thermogravimetric analysis of the membranes. The addition of CNTs to the membrane surface somewhat enhanced the thermal stability of the membranes. It is seen from the figure that the unmodified membrane degraded in the range of 212ºC – 315ºC while CNIM degradation started at the same temperature, it was a little slower and continued to nearly 373ºC. On basis of the TGA analysis, the CNT content of the membrane was estimated to be 0.1 wt. %.

2.3.2 Extraction of VOCs from Air

The rate of transport of the analytes through the membrane or flux can be expressed by Fick's law of diffusion,

$$J = \frac{P(p_i - p_o)}{l} \tag{2.1}$$

where J (gm-mol/m2.sec) is the flux, P is the permeability (gm-mol.m/m2.sec.Pa), $p_i$and p_o are the partial pressure of the VOCs at the inlet and permeate sides of the membrane, and l is the membrane thickness. Permeability is dependent on thermodynamics and kinetics of membrane/solute interactions and can be expressed as a product of solubility (S) (or partition coefficient) in the membrane and diffusivity (D). Since CNTs are excellent sorbents as well as molecular transporters, together these properties can increase both selectivity and permeability. During membrane extraction, interactions can take place via rapid solute exchange on the CNTs thus increasing the effective rate of mass transfer and flux. The high aspect ratio of CNTs can also dramatically increase the active surface area, which may contribute to enhanced flux.

Extraction efficiency (EE) of VOCs for the membrane was determined as follows:

$$Extraction\ Efficiency\ (\%) = \frac{Co * Vo}{Ci * Vi}\ x\ 100 \tag{2.2}$$

where Co, Ci are concentration of solute in the permeate and feed side, $Vo\ and\ \mathrm{Vi}$ are the volume of permeate and feed streams respectively. Performance of CNIM was determined based on the overall flux and extraction efficiency.

2.3.2.1 Effect of Feed Temperature on VOCs Removal. Figure 2.4 (a) and (b) demonstrate the effect of feed temperature on VOCs removal and its enhancement in CNIM. It is clear from the figure that all of the VOCs exhibited an increment in flux with increase in temperature. Dichloromethane showed highest flux among the ones studied here, followed by toluene and ethanol. However, at higher temperature the ethanol flux was found to be higher than toluene. This may be due to the higher diffusion rate of low molecular weight ethanol at elevated temperature. It was observed from Figure 2. 4 (b) that the enhancement in CNIM decreased with increase in temperature. This is because the effects of enhanced partition coefficient and faster desorption in the presence of CNTs was less pronounced at higher temperatures.

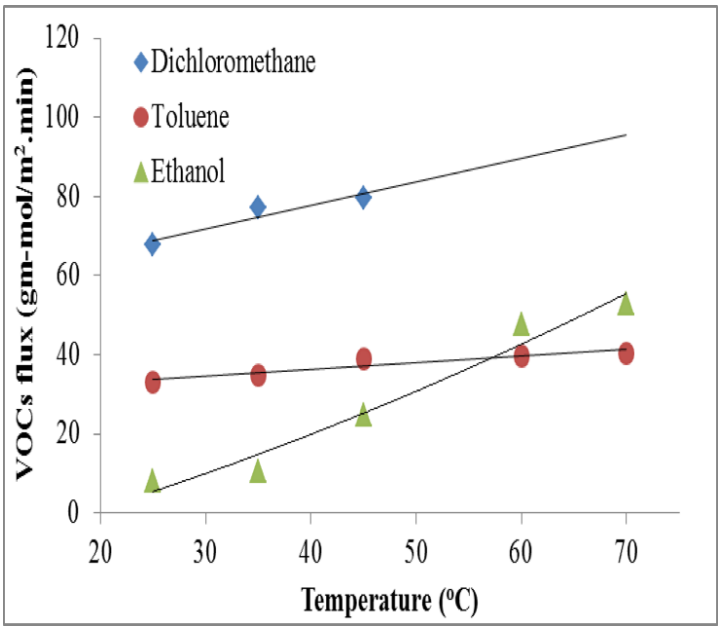

(a)

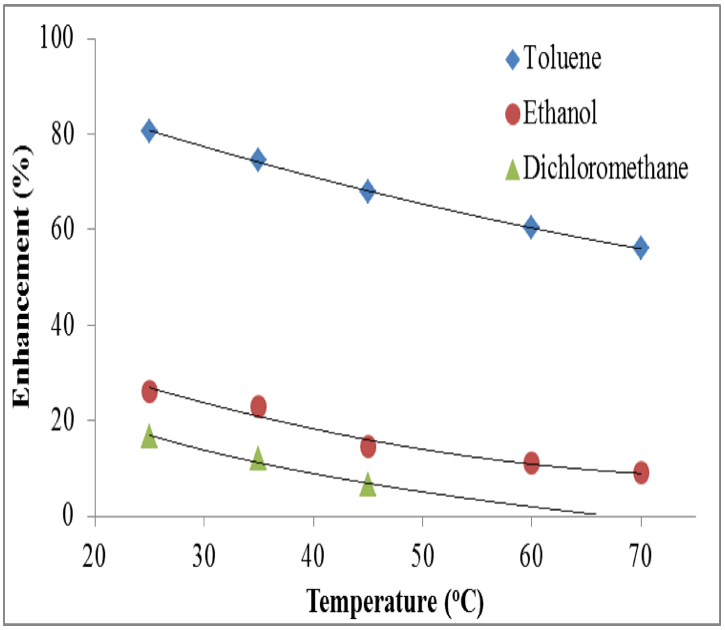

(b)

Figure 2.4 Effect of temperature on (a) VOCs flux, and (b) enhancement (%) with CNT

2.3.2.2. Effect of Feed Flow Rate on VOCs Removal. Figures 5 (a) and (b) show the VOCs removal and its enhancement in CNIM as a function of feed flow rate. The feed flow rate was varied from 2 to 10 mL/min at 25°C while the permeate stripping gas flow rate was maintained constant at 5 mL/min. It was observed from Figure 2.5(a) that the VOC flux increased with the increase in feed flow rate. This may be attributed to the fact that the increase in feed flow rate led to reduction in boundary layer formation on the membrane surface. The increase in enhancement was observed at higher flow rate indicating better mass transfer in the presence of CNTs (as shown in Figure 2.5(b)). The enhancement for toluene was found to be as high as 92% which were followed by ethanol (44%) and dichloromethane (20%). It is evident from the results that CNIM showed the highest enhancement for toluene which was nonpolar and was somewhat similar to the aromatic structure of CNTs and is known to interact with the latter by Π - Π interactions.

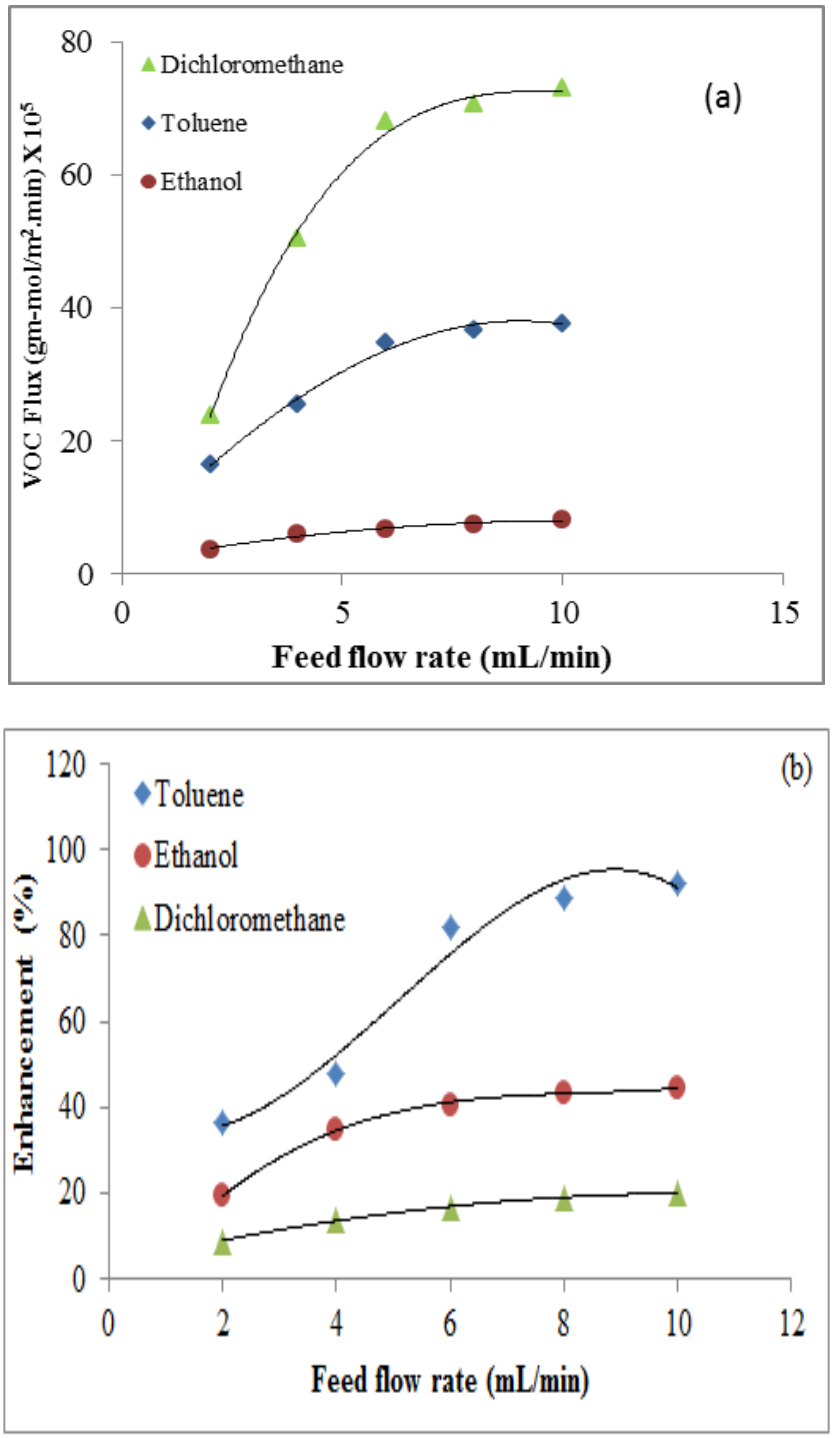

Figure 2.5 Effect of feed flow rate on (a) VOC flux and (b) enhancement with CNIM.

2.3.2.3. Extraction Efficiency as a Function of Temperature. Figure 2.6 (a) shows extraction efficiency of the different VOCs as a function of temperature in the range of 25-70°C. The increase in temperature increased extraction efficiency for all VOCs. However, the rate of increment is not very high as the diffusion coefficient increases with temperature, but the partition coefficient shows the opposite trend.

Figure 2.6 (b) exhibits the enhancement in extraction efficiency with CNIM in comparison with unmodified membrane. It was observed from the figure that the enhancement obtained with CNIM membranes were much higher at lower temperatures and decreases with increase in temperature. This was attributed to the fact that at lower temperature with relatively low diffusion coefficient of VOCs, the CNTs had a more pronounced effect in enhancing the partition coefficient and VOCs transport. The maximum enhancement for toluene was obtained 80% followed by ethanol and dichloromethane which were 26% and 17%, respectively. The highest enhancement for toluene compare to other VOCs attributed to its non-polar nature and structural symmetry with CNTs. The attainment of higher extraction efficiency at lower temperature allowed lower temperature operation with CNIM that generates less carbon foot print for the overall extraction process.

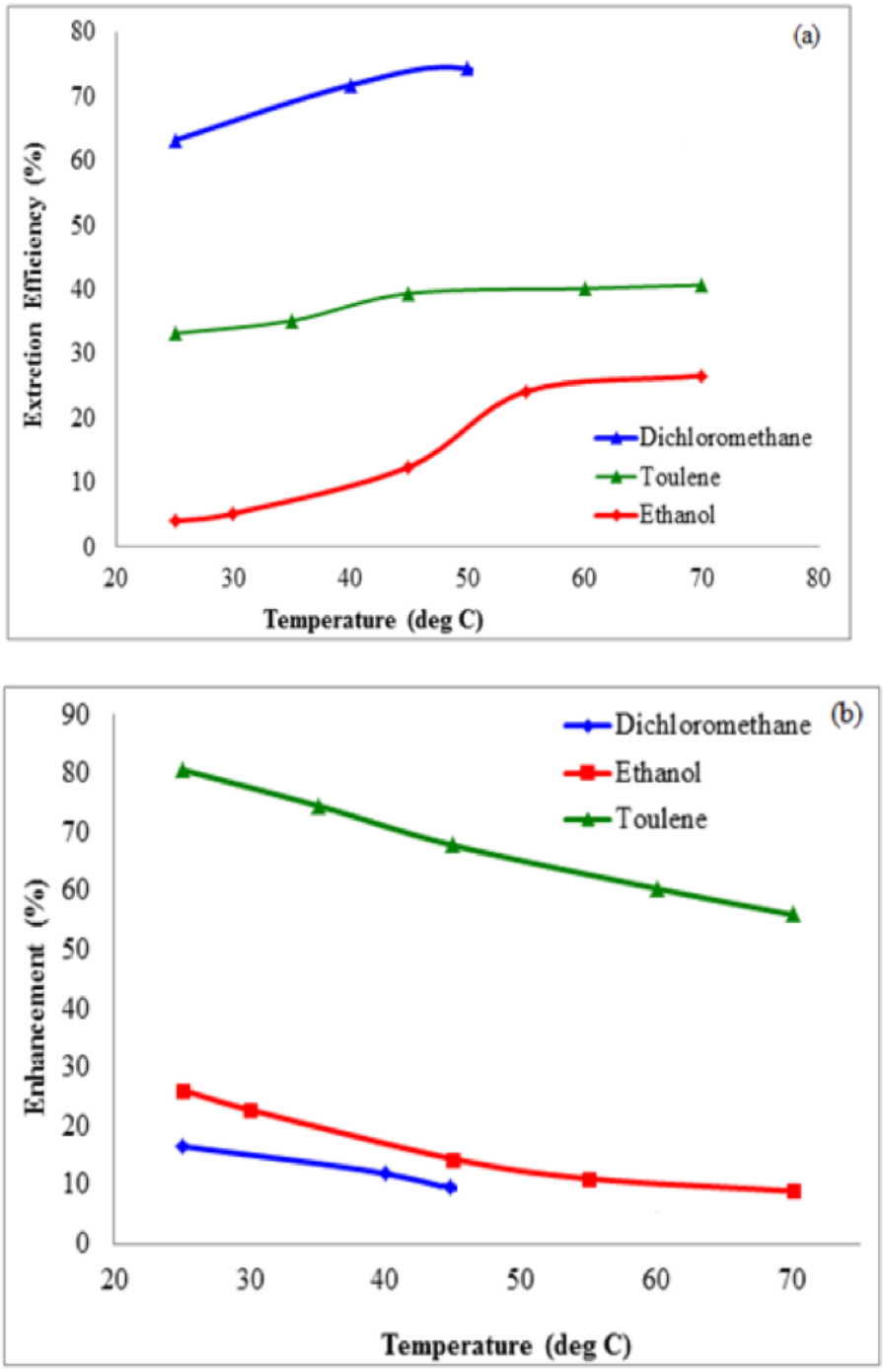

Figure 2.6 Effect of temperature on (a) extraction efficiency, and (b) enhancement with CNIM.

2.3.2.4. Extraction efficiency as a function of concentration. Figure 2.7 shows the extraction efficiency of CNIM and unmodified membrane in the concentration range of 25–200 ppm for toluene at constant temperature (25°C) and feed flow rate (6mL/min). The extraction efficiencies for both membranes increased with decrease in concentration. For example, with 200 ppm of toluene, CNIM showed an enhancement in extraction efficiency as high as 57%. At 50 ppm, the CNIM showed an extraction efficiency of 22% while the unmodified membrane reached the same efficiency at four times that concentration. Higher enhancement in the CNIM opens up the possibility of extracting VOCs from low concentration streams.

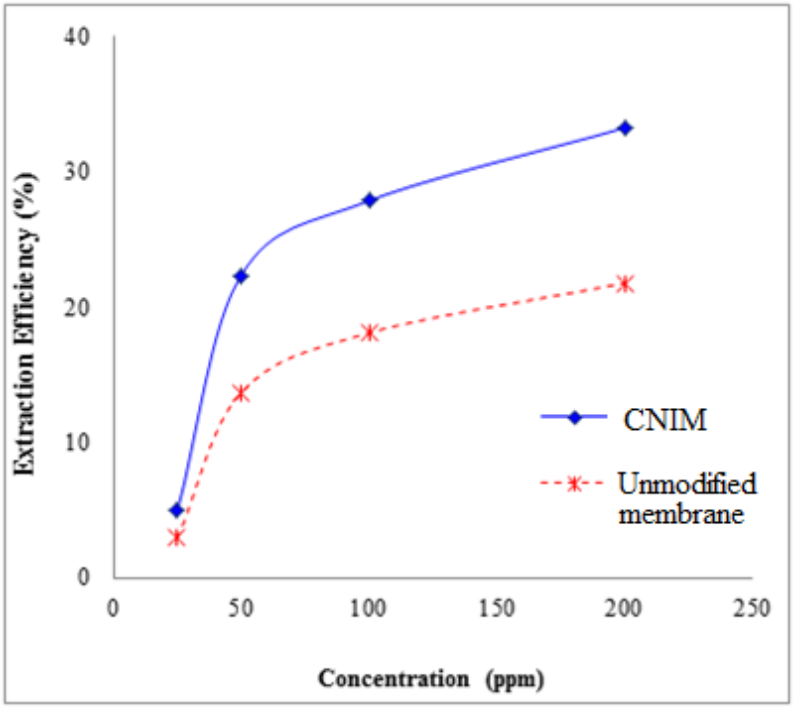

Figure 2.7 Extraction efficiency of toluene as a function of feed concentration.

2.3.3 Mass - transfer Coefficient

Vapor permeation through the membrane is known to follow a solution-diffusion model which involves sorption of the VOCs onto the membrane followed by diffusion through the polymer matrix and finally desorption into the permeate side. The overall mass-transfer coefficient is calculated as follows, assuming concentration of the permeate side to be zero(Vane et al., 1999),

$$k = \frac{J_{voc}}{C_{voc}} \tag{2.3}$$

where C_{voc} is the feed concentration of individual VOC.

Table 2.1 Mass Transfer Coefficient of Different VOCs for Varying Flow Rate at 25ºC

Flow rate (mL/min)	Dichloromethane		Toluene		Ethanol	
	k (m/s)	Enhancement (%)	k (m/s)	Enhancement (%)	k (m/s)	Enhancement (%)
2	1.68E-06	8.69	1.26E-06	36.59	1.54E-07	29.36
4	3.58E-06	13.57	1.96E-06	47.92	2.33E-07	34.79
6	4.80E-06	16.60	2.52E-06	80.65	2.63E-07	40.54
8	5.19E-06	19.05	3.17E-06	88.91	2.81E-07	43.46
10	5.56E-06	22.68	3.84E-06	92.22	3.16E-07	44.25

Table 2.2 Mass Transfer Coefficient of Different VOCs for Varying Temperature at 6 mL/min Flow Rate

Temp (^{o}C)	Dichloromethane		Toluene		Ethanol	
	k (m/s)	Enhancement (%)	k (m/s)	Enhancement (%)	k (m/s)	Enhancement (%)
25	4.80E-06	16.60	2.52E-06	80.65	2.63E-07	40.54
35	5.45E-06	11.92	2.67E-06	74.54	3.96E-07	22.79
45	5.64E-06	6.40	2.99E-06	67.78	9.48E-07	14.44
60	-	-	3.05E-06	60.43	1.84E-06	11.08
70	-	-	3.11E-06	56.98	2.02E-06	8.95

Tables 2.1 and 2.2 represent the mass-transfer coefficients obtained at different flow rates and at different temperatures, respectively. The overall mass transfer is usually controlled by diffusion through the boundary layer at low flow rates. With increase in flow rate, turbulence increases which reduces the boundary layer at the membrane interface. It was observed that as flow rate increased from 2 to 10 mL/min, overall mass transfer coefficient with CNIM increased 231, 205 and 105% for dichloromethane, toluene, and ethanol, respectively. The mass transfer coefficient in CNIM was also enhanced with flow rate. Similarly, increase in temperature led to higher diffusion coefficient and lower boundary layer resistance, thereby increasing the overall mass transfer coefficient. However, the increment in mass transfer coefficient with increase in temperature was not very significant for toluene and dichloromethane because the partition coefficients tend to

be lower at elevated temperature. The effect of CNTs also reduced as the temperature increased.

2.3.4 Proposed Mechanism

The mechanism underlying enhanced mass transport is shown in Figure. 8. The CNTs are known to be excellent sorbents for VOCs and served as active sorption sites to enhance the partition coefficient. They also show rapid adsorption and desorption properties which enhances mass transfer coefficient. Immobilization of CNTs into the selective siloxane layer altered the VOCs-polymer interactions, which is one of the major physicochemical factors affecting the selectivity and diffusivity of the membrane. The CNTs also provide an alternative route for faster mass transfer via its frictionless smooth surfaces.

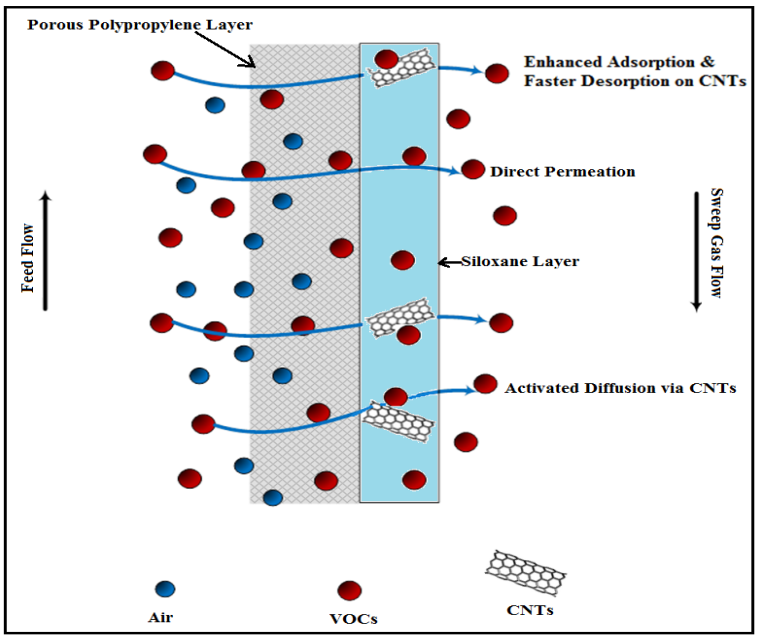

Figure 2.8 Mechanism of membrane separation process.

2.4 Conclusions

Membrane extraction of volatile organics from air is demonstrated using CNIM. Presence of CNTs showed significant enhancement in membrane performances in terms of extraction efficiency and flux. Overall, enhancement for both temperature and flowrate variation was observed for all volatile organics under study. CNIM membrane exhibited about 80% enhancement at 25 ºC and nearly 92% enhancement at 10mL flowrate for toluene. Thus, CNIM exhibited improved performance at lower temperatures and at higher flow rate, which implies that the presence of CNTs leads to higher permeation and faster mass transfer rate.

CHAPTER 3

CARBON NANOTUBE IMMOBILIZED MEMBRANE BY PHASE INVERSION FOR DESALINATION VIA MEMBRANE DISTILLATION

3.1 Introduction

Rapid climate changes and other factors have increased the demand for fresh water and consequently the need for desalination technologies for pure water generation(Service, 2006). Relatively lower energy requirements, cost and smaller foot prints make membrane based techniques like reverse osmosis (RO), forward osmosis (FO) and membrane desalination (MD) attractive desalination approaches (Shannon et al., 2008,Wade, 2001). MD is a membrane based thermal evaporative process which operates at relatively low temperatures, can provide high salt rejection and handle high salt concentrations (Alkhudhiri et al., 2012,Lawson et al., 1997,Lei et al., 2005). MD has the potential to generate pure water using low grade heat such as waste heat from power plants and solar power(Banat et al., 2002,Ding et al., 2005,Koschikowski et al., 2003,Dow et al., 2017). The major challenge facing MD is cost reduction to make it commercially viable. Consequently, a major consideration in MD is the membrane itself because it determines both flux and selectivity. Hence fabrication of membranes that can provide enhanced performances is of great interest (Alklaibi et al., 2005).

Conventional MD membranes include those made of polypropylene (PP), polyvinylidene difluoride (PVDF), polytetrafluoroethylene (PTFE) where techniques such as graft and plasma polymerization have been used to modify surface characteristics (Kong

et al., 1992,Ulbricht, 2006). A variety of more complex membranes with hydrophobic and hydrophilic surface coatings, or hydrophobic layer sandwiched between two hydrophilic layers have been reported (Khayet et al., 2003,Qtaishat et al., 2009,Khayet et al., 2003). Recent developments have reported fabrication of MD membranes with zeolite, clay nanoparticles, modification with porous alumina and nano carbon like carbon nanotubes and graphene (Das et al., 2014,Kim et al., 2010,Zhou et al., 2008,Musico et al., 2014,Ragunath et al., 2016,Bhadra et al., 2016). This includes, self-supporting CNT-Bucky paper membrane prepared by interfacial polymerization and vertically aligned CNT membranes for reverse osmosis (RO) process have been reported(Dumée et al., 2010,Dumée et al., 2011,Drioli et al., 2015).

We have reported the development of carbon nanotube immobilized membrane (CNIM) with different functionalized forms where the CNTs have been incorporated into the membrane with the help of polymer to serve as an immobilizing agent (Bhadra, et al., 2016,Bhadra et al., 2013,Roy et al., 2014). These techniques have been extended to other nano-carbons such as graphene and nano-diamond as well (Bhadra et al., 2014). CNTs incorporated on the membrane surface act as nano-sorbent and provide additional pathways for solute transport. These novel membranes have demonstrated superior performances in diverse applications such as solvent extraction, pervaporation (Hylton, et al., 2008,Sae-Khow, et al., 2010,Sae-Khow, et al., 2010), desalination (Bhadra, et al., 2013,Roy, et al., 2014), volatile organic extraction from air, micro extraction(Sae-Khow, et al., 2010,Ragunath et al., 2015), concentration of pharmaceutical waste (Gethard, et al., 2012),

and dehumidification (Roy et al., 2013). While these membranes have shown excellent performance, there is no way to control the surface morphology.

In an effort to develop the next generation of CNIM, it is important to explore other methods of CNT incorporation where the surface morphology and CNT distribution can be controlled. Phase inversion is a well-known membrane fabrication technique for preparing porous membranes where a polymeric layer can be incorporated via solvent evaporation, precipitation from vapour phase, thermal precipitation, immersion precipitation and dry-wet phase inversion(Ulbricht, 2006,van de Witte et al., 1996). A selective layer can also be created using solvent/non-solvent evaporation approach where a polymer is uniformly dispersed in a solvent/non-solvent mixture and casted on a support. Upon evaporation, the solvent creates a continuous polymeric phase while the non-solvent part creates the voids resulting in a porous layer[36-38]. The objective of this research was to synthesize CNIM using solvent/non-solvent type phase inversion where the surface morphology and consequently membrane performance can be varied.

3.2 Experiment

3.2.1 Materials

Hydrophobic polypropylene (PP) membranes with nominal pore size of 0.45 μm were purchased from Sterlitech Corp., (WA, USA). Multiwall carbon nanotubes (MWNT) were purchased from Cheap Tubes Inc., (Brattleboro, VT, USA). Other chemicals which

includes polyvinylidene fluoride (PVDF), acetone and methanol were purchased from Sigma Aldrich (PA, USA).

3.2.2 Membrane Fabrication

Surface modification of polypropylene membrane was carried out by creating a porous selective layer on the surface of the support membrane via solvent/non-solvent evaporation type phase inversion approach(Zhao et al., 2008,Qian et al., 2008,Van de Witte et al., 1996). Here we used a volatile solvent (acetone) with desirable dispersibility for both polymer and CNTs. Methanol was used as the non-solvent to facilitate pore formation as it had comparatively lower vapour pressure and was immiscible with the PVDF-CNT mixture. Uniform dispersion of casting solution was prepared with pre-weighed amount of PVDF and CNT in acetone followed by the addition of methanol. PVDF-CNT mixture was cast on polypropylene substrate using a casting knife. The cast membrane was allowed to dry at 60°C in a vacuum oven. After initial trial and error, the acetone to methanol volume ratio was optimized to be 80:20 for fabrication of membranes with different polymer loading. Membranes were cast with well dispersed solution containing varying amount of PVDF from 0.001 – 0.03 wt.% while the CNT concentration was fixed at 0.01% based on preliminary trial error experiments.

3.2.3 Membrane Characterization

Surface morphology of the membranes was characterized using scanning electron microscope (SEM) (Leo 1530 VP, Carl Zeiss SMT AG Company, Oberkochen, Germany). The membrane samples were cut to 0.5 cm long pieces and carbon coated for SEM imaging. The elemental composition of the membranes was analysed using energy dispersive x-ray spectroscopy (EDX). The surface topography and roughness of the membranes was determined using atomic force microscopy (Park NX10 AFM, Park Systems, USA) under ambient conditions. Measurements were obtained in non-contact mode (Park SmartScan^{TM}) using silicon-nitride cantilever containing silicon probe with resonant frequency of 50kHz, tip radius 2-5 nm for a scan area of 5μm and average surface results has been reported. Furthermore, thermal gravimetric analysis (TGA) to study the thermal stability of modified and unmodified membranes using PerkinElmer Pyris 7 TGA system at isothermal heating rate of 10°C/min in air.

The effective surface porosity over the effective pore length was measured by gas permeation tests previously reported in other similar studies (Wang et al., 1999). The total molar flux per unit trans membrane pressure difference across the porous PP membrane can be described as

$$\frac{J_w}{\Delta p} = \frac{2}{3}\left(\frac{8RT}{\pi M}\right)^{0.5}\frac{1}{RT}\frac{r\varepsilon}{L_p} + \frac{\bar{p}}{8\mu RT}\frac{r^2\varepsilon}{L_p} \tag{3.1}$$

where ε is surface porosity, r is mean pore radius of the membrane, μ is gas viscosity, R is gas constant, $\overline{p}$ is the average feed and permeate pressure, M is molecular weight of gas, L_p is effective pore length and T is temperature (k). The first term of the equation represents the Knudsen flow and the second term the Poiseuille flow. The gas permeation flux per unit of driving force ($\frac{J_w}{\Delta p}$) can be calculated as,

$$\frac{J_w}{\Delta p} = \frac{N_{t,w}}{A} \tag{3.2}$$

where, $N_{t,w}$ is total molar gas permeation rate (mol s^{-1}), Δp is the trans membrane pressure difference across the membrane area A. The total gas permeation rate through the membrane at difference pressure was measured using a bubble flow meter. By plotting nitrogen flux ($\frac{J_w}{\Delta p}$) as a function of mean pressure $\overline{p}$, the effective surface porosity over pore length was calculated from the slope (S_0) and intercept (I_0) as follows:

$$r = \frac{16}{3}\left(\frac{S_0}{I_0}\right)\left(\frac{8RT}{\pi M}\right)^{0.5}\mu \tag{3.3}$$

$$\frac{\varepsilon}{L_p} = \frac{8\mu RTS_0}{r^2} \tag{3.4}$$

The overall membrane porosity was calculated from the ratio of the pore volume to the total volume of the membrane. The membrane pore volume was determined by measuring the increment on the membrane mass before and after being fully impregnated with butanol. The porosity of the membrane was calculated as follows(Edwie et al., 2012),

$$\varepsilon = \frac{V_p}{V_m} \tag{3.5}$$

where V_p and V_m are the pore volume and total volume of the membrane respectively and average results for both unmodified and the best performing membrane has been reported.

Surface hydrophobicity of the membrane was estimated by contact angle measurements. Water droplets (measured volume of about 2μL) were dropped on membrane surface using Hamilton micro-syringe (0 – 10 μL) on both modified and unmodified membranes. Droplet position was recorded using a stage mounted video camera. Minimum of five reading were recorded and average contact angle measurements are reported.

3.2.4 Experimental Setup

The schematic membrane distillation experimental setup is shown in Figure 3.1 Typical setup consisted of PTFE membrane cell having an effective membrane area

of 14.5 cm^2, Viton O-rings, PTFE tubing, PFA and PTFE connectors, feed and permeate flow pump. Constant temperature heating water bath (Neslab Water Bath Model GP 200, NESLAB Instruments, Inc., Newington, NH, USA) was used to maintain constant feed temperature and a low temperature bench top chiller unit (Polyscience LS5, Cole-Parmer, USA) was used to maintain the permeate temperature between 15-20 °C. Feed and permeate solutions were circulated in a cross flow mode. Both feed and permeate flow passing through the membrane modules were recycled from their respective reservoirs using peristaltic pumps (Cole-Parmer, USA). The inlet and outlet membrane temperatures were monitored using temperatures control probes (Four-channel Data Logging Thermometer, RS-232, Cole-Parmer, USA).

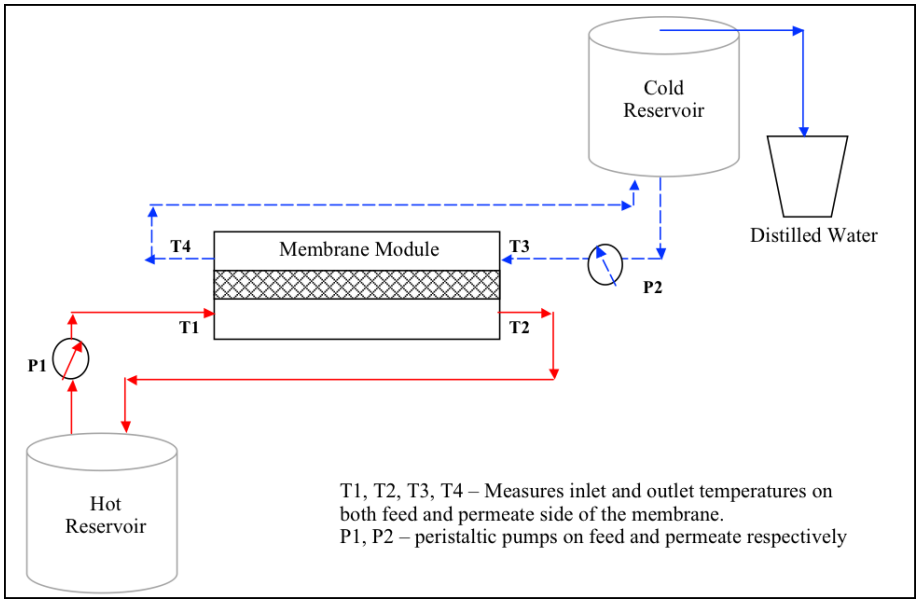

Figure 3.1 Schematic diagram of the experimental setup.

3.3 Results and Discussion

3.3.1 Membrane Characterization

Table 3.1 presents the different membranes that were fabricated, their characteristics and surface PVDF composition estimated from EDX analysis. The atomic weight percent of fluorine on the membrane surface that was estimated from EDX analysis was as high as 23.9% for 0.03 wt.% polymer loading. A corresponding increase in contact angle was observed indicating a rise in hydrophobicity of the membrane surface. Surface characterization by SEM, EDX and AFM analysis are shown in Figure 2(a-c). The figure presents the membrane characterization of unmodified (M0), and modified membranes with 0.001 (M1), 0.01 (M4) and 0.03 (M6) wt.% PVDF respectively.

Formation of uniform layer of CNIM by phase inversion are seen from the SEM images. However, distribution of CNTs on the surface varied with PVDF concentration. For instance, the selective layer formed in M1 was a continuous porous CNT layer due to minimal presence of polymer content. Whereas at` higher polymer loading a decrease in pore size was observed in both SEM and AFM images presented in Figure 3.2 – 3.4. EDX mapping images of both unmodified membrane and modified membrane confirmed the increase in surface fluorine concentration for membranes which are identified as red and green for carbon and fluorine respectively. Surface roughness(R_a) measured from AFM analysis for the modified membranes increased from 75.1 to 156 and finally to 177nm for membranes M1, M4 and M6 respectively. Surface characterization of other membranes are not presented for brevity

Table 3.1 Summary of Different Phase Inversion Membrane Fabrication and Characterization.

Membrane	Amount of PVDF in solution (wt.%)	EDX –Analysis (% of Fluorine atom)	Amount of PVDF on membrane surface (wt.%)	Contact Angle Measurement
M0	0	0	0	93º
M1	0.001	0.9	1.5	100º
M2	0.003	1.6	2.7	102º
M3	0.004	2.6	4.3	104º
M4	0.01	7.7	12.8	110º
M5	0.02	13.8	23.0	111º
M6	0.03	23.9	39.8	116º

.

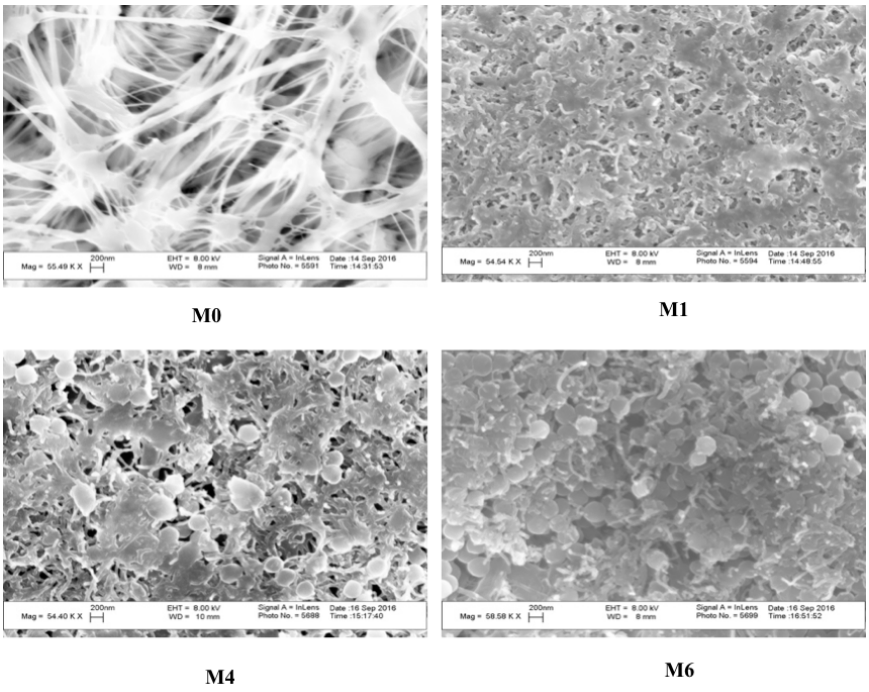

Figure 3.2 SEM characterization of modified membranes M0, M1, M4, M6.

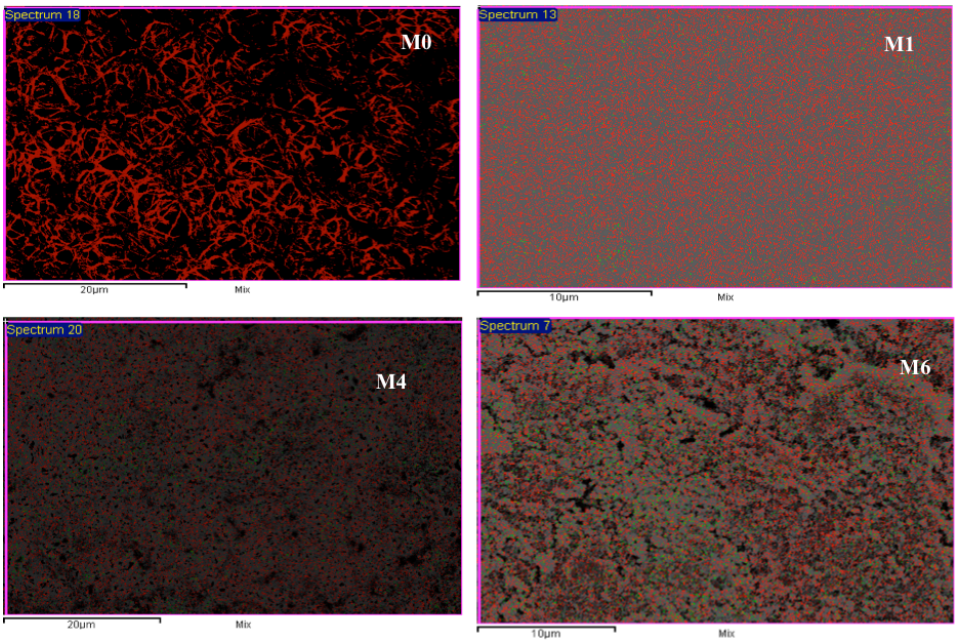

Figure 3.3 SEM - EDX characterization of modified membranes M0, M1, M4, M6.

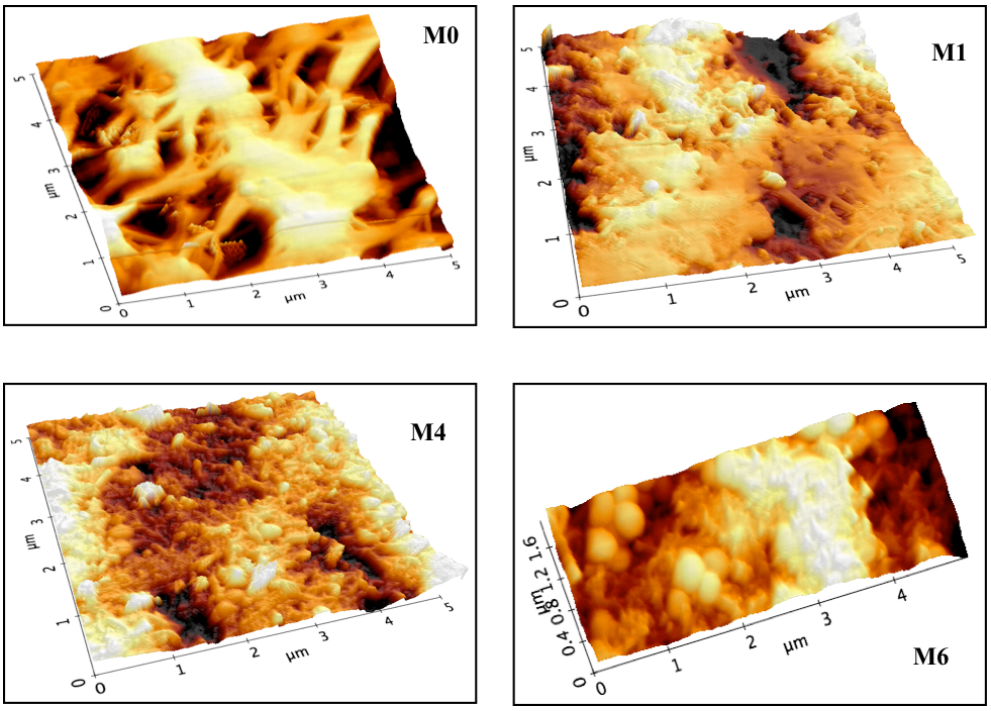

Figure 3.4 AFM characterization of modified membranes M0, M1, M4, M6.

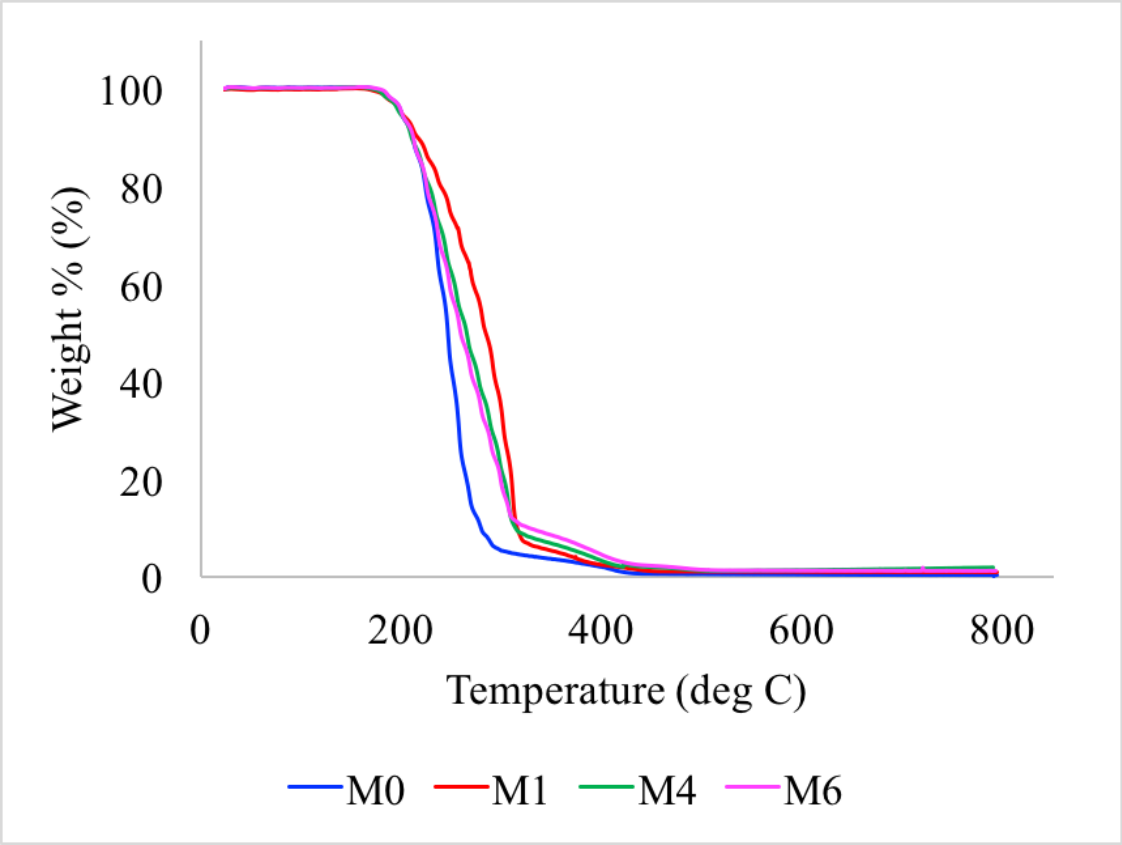

Figure 3.5 Thermal gravimetric analysis of unmodified and modified membranes.

The TGA analysis is presented in Figure 3.5. which shows that the modified membranes were quite stable in comparison to unmodified membranes. The modified membranes degraded in range of 185 – 324 ° C for M1, 185 – 322 ° C for M4, and 180 – 314 ° C for M6, respectively. Whereas the unmodified membrane degradation took place between 168° to 297°C leading to complete degradation at 418 °C. This implies, the modification process enhanced overall thermal stability of the membranes. The CNT concentration in the membranes were estimated to be around 1.1 (± 0.02) wt.%.

The average pore size of unmodified membrane was calculated to be 0.40 μm with 80.0 % porosity and ratio of porosity over pore length ($\frac{\varepsilon}{L_p}$) was 2.15 x 10^7. The pore size for modified membranes ranged between 0.39 – 0.37 μm, with porosity of 80.0 – 77.8 % and ratio of porosity over pore length was calculated to be between 2.25 – 2.55 x 10^7. As expected the modification process altered the membrane morphology, however the change in pore size and porosity were minimal.

3.3.2 DCMD Performance of CNIM Fabricated by Phase Inversion

Performance of the CNIMs was compared with that of the original membrane by determining the flux at different flow rates, temperatures and salt concentrations. The MD experiments were performed for a duration of 3 hours upon attaining equilibrium, the flux was monitored every 30 minutes and averaged. All experiments were repeated three times and the relative standard deviation for the experiments was estimated to be within 1%. The water vapour flux, J_w, across the membrane can be expressed as:

$$J_w = \frac{W_p}{t \,.\, A} \tag{3.6}$$

where, w_p is the total mass of permeate, t is the permeate collection time and A is the membrane surface area. Also, J_w can be denoted as:

$$J_w = k(P_f - P_p) \quad (3.7)$$

where, k is the mass transfer coefficient, P_f and P_P is the water vapour concentration in feed and permeate side(Schofield et al., 1987,Qtaishat et al., 2008,Phattaranawik et al., 2001).

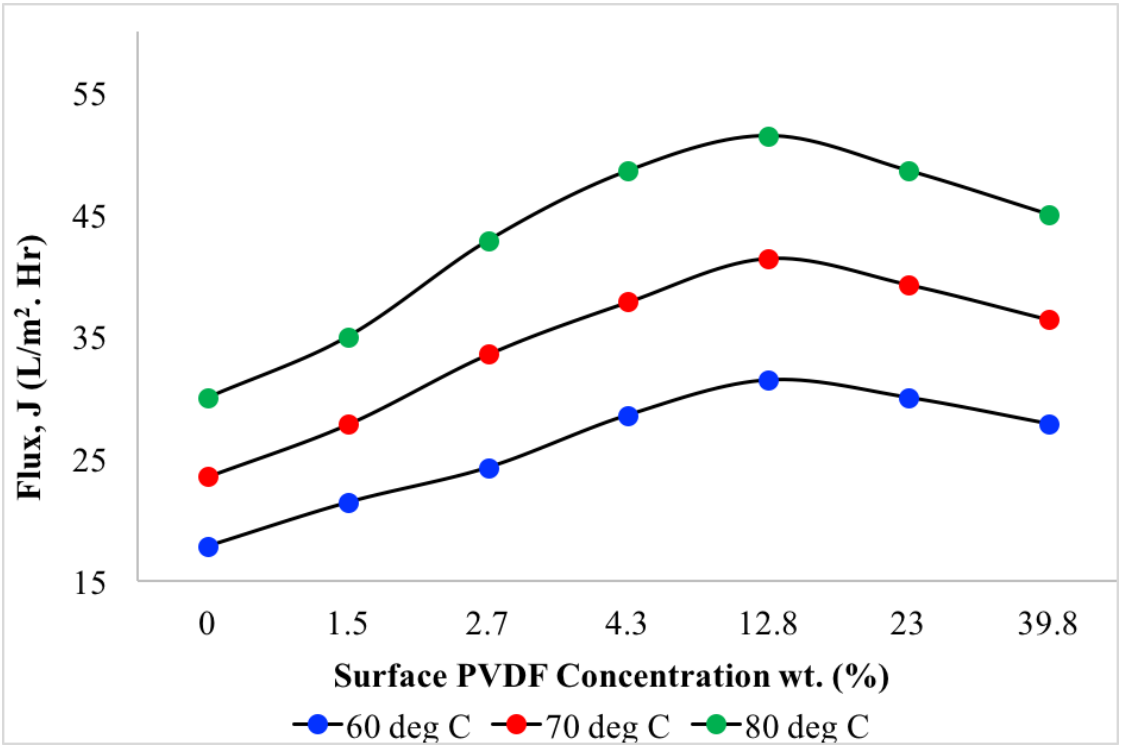

Figure 3.6 MD performance for different phase inversion membranes as a function of temperature.

MD performance for CNIM fabricated via phase-inversion with varying PVDF content as a function of temperature is presented in Figure 3.6. Operating temperatures were varied from 60 – 80 °C, at constant feed and permeate flow rates

of 150 mL/min. MD flux increased with increasing temperature for different membranes, due to increased vapour pressure gradient(Mengual et al., 2004). From figure 4(a), flux for CNIM membrane with 0.01 wt.% PVDF content increased from 31.4 l/m^2 h at 60°C to 51.4 l/m^2 h at 80°C. Alternately, unmodified membrane exhibited relatively lower flux ranging between 17.9 – 30.0 l/m^2 h in the same temperature range. Further increase of PVDF content to 0.03 wt.% reduced the permeate flux to 27.9 l/ m^2 h at 60°C and 45.0 l/m^2 h. at 80°C. The initial increase in permeate flux was attributed to enhanced adsorption and rapid desorption provided by the unique surface properties of CNTs(Gethard et al., 2011). However further increase in PVDF concentration reduced the surface CNT: PVDF ratio which altered the membrane morphology and availability of active sites for water vapour diffusion, thus reducing overall permeate flux.

Enhancement for water vapour flux attained by phase inversion membrane over unmodified membrane was calculated as follows,

$$Enhancement = \frac{J_{CNIM-PI} - J_{unmodified}}{J_{unmodified}} \times 100 \quad (3.8)$$

where $J_{CNIM-PI}$ was flux by phase inversion membrane (l/ m^2 h) and $J_{unmodified}$ was the flux from the unmodified membrane.

Figure 3.7 presents the enhancement attained as a function of temperature for membranes M1, M4, and M6. Enhancement decreased with increasing temperatures

for all the membranes presented. For instance, enhancement reduced from 76% at lower feed temperature to 71.4% at maximum operating temperature of 80°C. This was because, higher temperature results in higher vapour pressure gradient resulting in higher water vapour diffusion and enhancement with CNIM layer was less pronounced(Gethard, et al., 2011). Maximum enhancement was obtained for membrane M4 with 0.01 wt.% PVDF concentration. The enhancement attained where higher for membrane M4 (76.0%), followed by M6 (56.0%) and M1(20.0%) for a feed temperature of 60°C. From the results, it is evident that membrane M4 exhibited superior performance in comparison to other membranes in consideration. Reduced performance by M6 was due to reduced availability of diffusion sites by masking CNTs between the PVDF layer which is evident from SEM images presented in Figure 3.2.

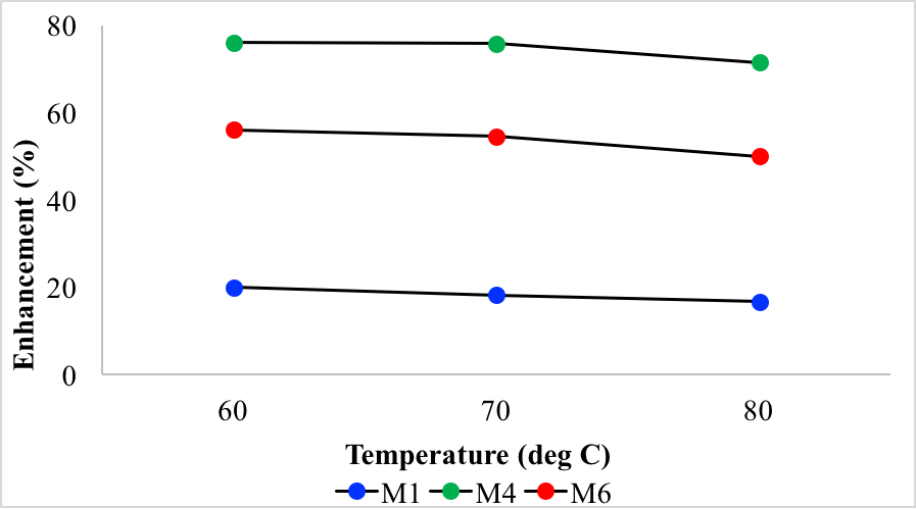

Figure 3.7 Enhancement attained as a function of temperature for different phase inversion membranes.

Figure 3.8 shows the MD flux attained as a function of varying feed flowrate for membranes M0, M1, M4 and M6. The flow rates were varied between 100 to 200 mL/min at a constant temperature of 70°C and permeate flow of 150 mL/min. Increase in water vapour flux was observed with increase in flow rates for all membranes under study. For instance, flux increased from 35.7 to 50.0 l/m^2.h for 0.01 wt.% PVDF concentration, whereas in the unmodified membrane the flux increased from 23.6 to 30.7 l/m^2. h. The increase in permeate flux with increased flow rate could be attributed to reduced boundary layer effect along the membrane interface as an effect of increased turbulence at higher flow velocities. Additionally, higher flowrates reduced the contact time of the feed with the membrane surface which led to higher average bulk temperatures, resulting in higher driving force for MD(Gryta, 2002). Enhancement attained were higher for membrane M4 (62.8%), followed by M6 (51.1%) and M1(16.3%) for feed flow of 200mL/min at 70°C.

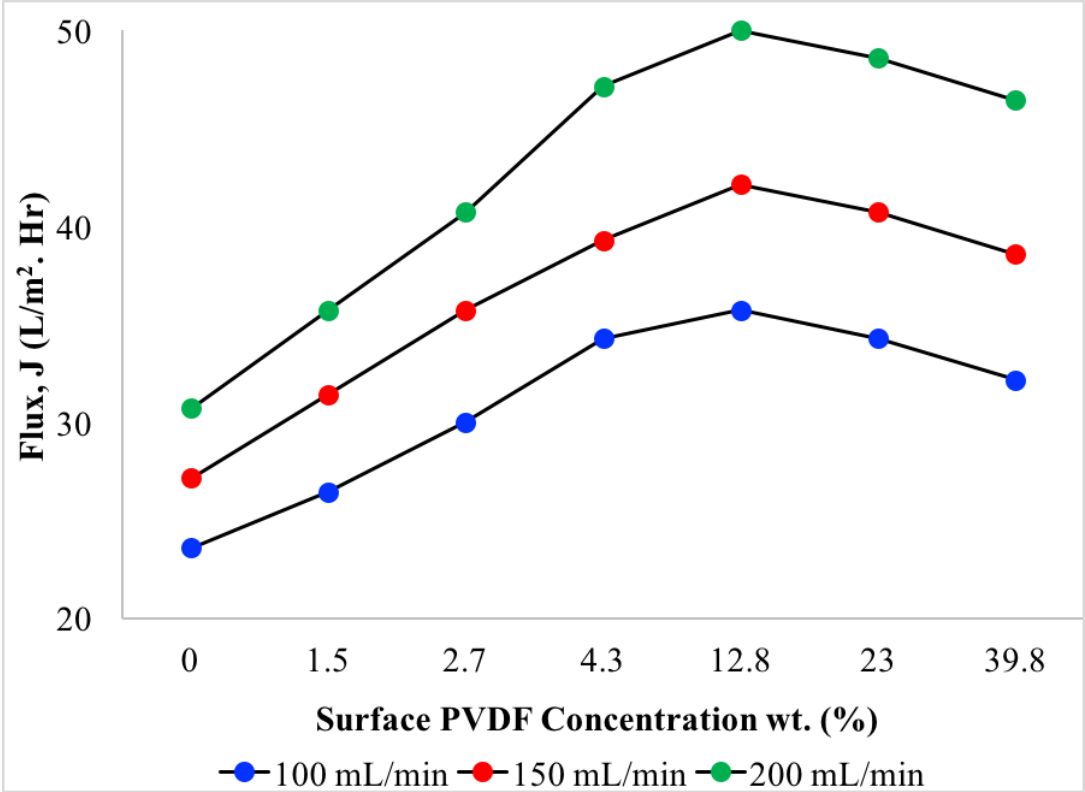

Figure 3.8 MD Performance for different phase inversion membranes as a function of feed flowrate.

Figure 3.9 presents the effect of feed concentration on DCMD flux at a constant flow rate of 150 mL/min and feed temperature of 60°C. Higher salt concentration is known to reduce mass transport across the membrane interface. As expected, overall water vapour flux decreased for all membranes with increase in feed concentration(Cath et al., 2004,Martínez-Díez et al., 2001,Wirth et al., 2002,Schofield et al., 1990). For the modified membrane, the flux decreased from 33.8 l/m^2 h for pure water to 30.8 l/m^2 h for feed concentration of 35000 ppm, and

that of unmodified membrane decreased from 19.2 to 15.4 l/m^{2}h. The reduction in flux for unmodified membrane was 25.0 % compared to 9.7 % for phase inversion membrane. Permeate conductivity measured for both membranes showed no significant leakage with increase in feed concentration and the conductivity measured after each experiment was between 1 and 3 µS, which is equivalent to distilled water.

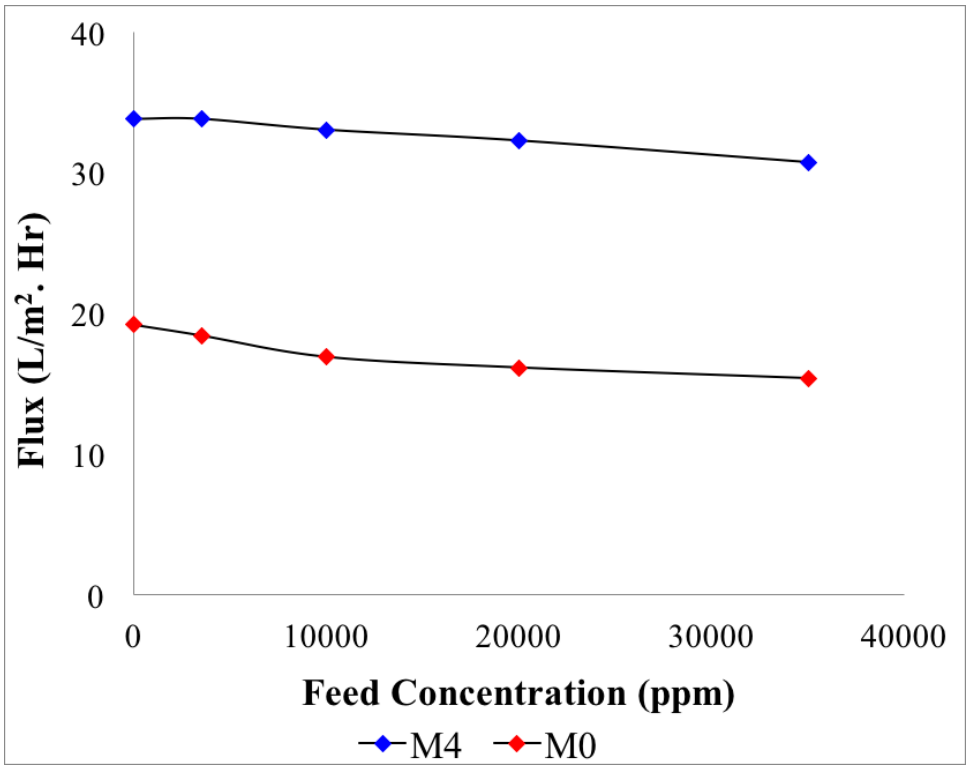

Figure 3.9 MD Performance for different phase inversion membranes as a function of feed concentration.

3.3.3. Study of Mass Transfer Co-efficient

The rate of mass transfer across the membrane is given as:

$$\kappa = \frac{Jw}{(P_f - P_p)} \tag{3.9}$$

where Jw is the water vapor flux of the system, κ is the mass transfer coefficient, P_f and P_p are partial vapor pressure of average feed and permeate temperatures. The mass transfer coefficients calculated were found to be significantly higher for CNIM with phase inversion as compared to the unmodified membrane.

Table 3.2 Effect of Feed Concentration on Mass Transfer Co-efficient at Constant Temperature and Flow Rate

Flow rate: 150mL/min; Temperature: 60 °C	Mass-transfer Coefficient, κ (kg/m2.sec.Pa) x 10^{-07}	
Feed Concentration	M4	M0
0	5.84	3.16
3500	5.44	3.11
10000	5.33	2.70
20000	5.09	2.78
35000	4.69	2.40

Table 3.2 summarizes the effect of varying feed concentration on mass transfer coefficient. Both membranes showed decrease in mass transfer coefficients with increase in feed salt concentration due to reduced vapour pressure at higher salt concentrations. Overall mass transfer coefficients decreased from 5.84 x 10^{-07} to 4.69 x 10^{-07} for CNIM membrane, and 3.16 x 10^{-07} to 2.40 x 10^{-07} for unmodified membrane. The overall mass transfer co-efficient reduced by 31.6% for unmodified membrane, whereas the reduction was only 16.8% for modified membranes. The enhanced performance by phase inversion membranes are similar to what has been reported before(Bhadra, et al., 2013,Ragunath, et al., 2015,Gethard, et al., 2011). The CNTs provided selective sorption of water vapour while repelling liquid brine. This enhances overall water vapour transport(Dumée et al., 2013). What phase inversion provides was a way of controlling the amount of PVDF and CNTs on the surface which could alter hydrophobicity, pore size and thus water vapour permeation.

3.4 Conclusion

We demonstrate phase-inversion as an effective method for modifying surface properties of CNIM. Membranes with varying surface PVDF concentrations where the CNT concentration remained fixed were studied for DCMD. The selective PVDF-CNT layer on the feed side of the membrane surface led to enhanced flux at lower temperature, thus making the overall process more energy efficient. Optimum polymer content provided maximum flux and enhancement over an unmodified

membrane reached as high as 76%. Higher polymer concentrations reduced the membrane performance. Overall, the phase inversion approach provides an effective way to incorporate CNTs on membrane surfaces for different applications, and this can be extended to other nanomaterials as well.

CHAPTER 4

SELECTIVE HYDROPHILIZATION OF PERMEATE SURFACE TO ENHANCE FLUX IN MEMBRANE DISTILLATION

4.1 Introduction

Desalination of sea and brackish water is commercially carried out by methods such as multi stage flash distillation (MSF), multiple effect desalination (MED), and reverse osmosis (RO). These techniques have their limitations such as high energy consumption and equipment cost (Banat, et al., 2002,Wade, 2001). At this point, there is a need to develop cost effective low temperature processes that can utilize industrial waste heat and solar energy to desalinate water.

Recent studies (Goh et al.) show that membrane distillation (MD) as a promising alternative that involves the transport of vapors through a micro porous, hydrophobic membranes (Ding, et al., 2005,Koschikowski, et al., 2003). The driving force is provided by the vapor pressure gradient across the membrane (Lawson, et al., 1997,Lei et al., 2005). The advantage of MD is that it can be operated at relatively lower temperatures, does not require large vapor space as in MSF, is less prone to fouling than RO, can generate high purity water and can handle water with high salt concentrations. All of these advantages make it attractive for the production of high purity water where low quality industrial heat is available in the form of boiler blow downs, flue gasses, or low pressure steam (Calabrò et al., 1991,El-Bourawi et al., 2006,Calabro et al., 1994). MD has also been used with

thermally sensitive food and pharmaceutical products (Cassano et al., 2015). Various modes of MD have been developed where the condensing medium varies from cold distillate to a sweep gas or vacuum (Lawson, et al., 1997).

MD is carried out using hydrophobic micro porous membranes to facilitate selective water vapor transport. Different membranes in flat-sheet or hollow fiber forms, made of polytetrafluoroethylene (PTFE), polypropylene (PP), and polyvinylidene-di-fluoride (PVDF) have been used in MD (Fujii et al., 1992,Kesting, 1985). Several techniques such as phase inversion and stretching of dense films have been used to make MD membranes, and hydrophilic membranes have been surface treated to enhance hydrophobicity (Kim et al., 2016). Composite membranes consisting sandwiched hydrophobic/hydrophilic layers has also been reported (Kong, et al., 1992,Lloyd et al., 1991,Lloyd et al., 1990,Kim et al., 1991,McGuire et al., 1993,Wu et al., 1992,Lim et al., 1991).

Despite various advantages, the potential of MD is yet to be fully realized. MD performance can be negatively affected by increased heat loss, mass transfer resistance, trapped air within membrane pores, pore wetting and temperature polarization (Martínez et al., 2007,Martínez-Díez et al., 1999). Much effort has gone into developing methods for enhancing the performance of the membranes by modifying membrane surface including immobilization of nanoparticles and nano carbons (Vatanpour et al., 2014,Bet-moushoul et al., 2016,Bonyadi et al., 2007,Cho et al., 2011,Prince et al., 2012). An important consideration is the fast removal of water vapors in the permeate side of the membrane to

increase the concentration gradient for mass transfer. This is applicable for all types of MD [6]. As the water vapor comes through, it needs to be rapidly condensed and removed. While the feed side of the membrane needs to be highly hydrophobic to prevent pore wetting, it is feasible to have a more hydrophilic permeate surface so that it would have higher affinity to the water vapor, and consequently facilitate its rapid removal. The objective of this research is to enhance MD flux by selective hydrophilization of the permeate side of the membrane. A more specific objective is to study this phenomenon in direct contact membrane distillation (DCMD) where pure water is used to collect the permeated water vapors.

4.2 Experimental

4.2.1 Materials and Methods

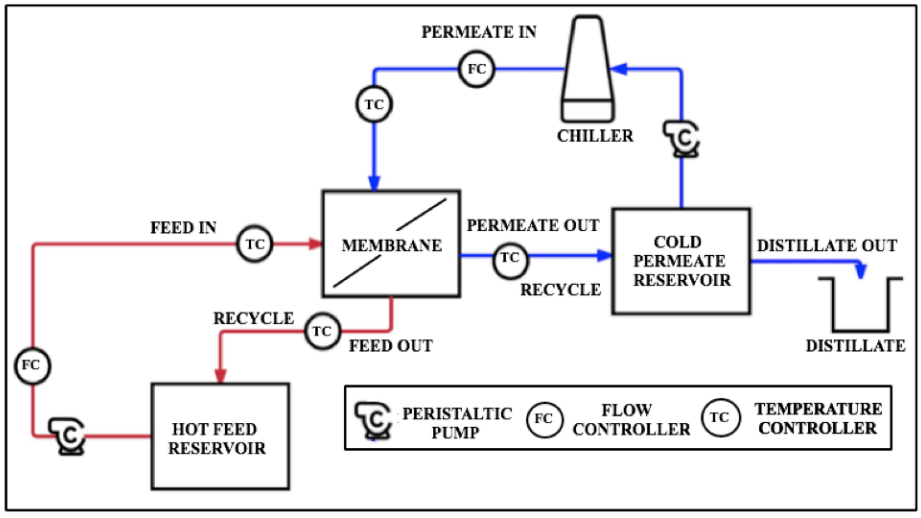

Figure 4.1 Experimental setup for direct contact membrane distillation using hydrophilized membrane.

MD experiments were carried out in the DCMD mode (Bhadra et al.). The schematic diagram of the experimental setup is shown in Figure 4.1. Typical setup consists of a PTFE membrane cell having an effective membrane area of 14.5 cm^2. The membrane holder had Viton O-rings, PTFE tubing, PFA and PTFE connectors, as well as pumps for feed and permeate flow. The system has been described before (Roy, et al., 2014). Constant temperature water bath (Neslab Waterbath Model GP 200, NESLAB Instruments, Inc, Newington, NH, USA) was used to maintain steady feed temperature and a bench top chiller (Polyscience LS5, Cole-Parmer, USA) was used to maintain the permeate temperature around 15-20°C. Feed and permeate solutions were contacted in the membrane module in a counter current flow. Both the feed and permeate were recycled from their respective reservoirs using Master Flex Easy Load peristaltic pumps (Cole-Parmer, USA). The inlet and outlet membrane temperatures were monitored using temperature sensors (Four-channel Data Logging Thermometer, RS-232, Cole-Parmer, USA). Hydrophobic PTFE membrane of 0.2 μm pore size and 130 μm overall thickness with polypropylene support was obtained from Advantec (Toyo Roshi Kaish, Ltd, Japan).

4.2.2 Membrane Hydrophilization

The membrane under study was a highly hydrophobic Teflon membrane with polypropylene support. Surface modification via chemical treatment of the polypropylene

backing was carried out to enhance the hydrophilicity of the permeate side. The process was initiated with treatment with chromic acid solution which was prepared by mixing potassium dichromate ($K_2Cr_2O_7$), sulfuric acid and water in a ratio of 1:20:30 (Roy, et al., 2013). After preliminary wetting in acetone, the membrane was treated with the chromic acid solution for 1 min in an oven maintained at 60^o C. The membrane was then washed with distilled water.

The hydrophilization was characterized by measuring the contact angle of water droplet on membrane surface, Fourier transform infrared (FTIR) spectroscopy (Magna IR System 560, Nicolet Instrument Corporation, Wisconsin, USA) and Scanning Electron Microscope with Energy Dispersive X-ray (SEM-EDX) Spectroscopy (Leo 1530 VP, Carl Zeiss SMT AG Company, Oberkochen, Germany). All characterization was performed three times and average was reported. Performance of the hydrophilized membrane was compared with that of the unmodified membrane by determining the flux at different flow rates, temperature and salt concentration. After attaining equilibrium, the MD experiments were performed for a duration of 3 hours, the flux was monitored every 30 minutes. All experiments were repeated three times and the relative standard deviation for the experiments was estimated to be within 1%.

4.2.3 Gas Permeation Test

The effective surface porosity over the effective pore length was measured by gas permeation tests reported in the literature (Wang, et al., 1999). The total molar flux per unit trans membrane pressure difference across the porous PTFE membrane can be described as

$$\frac{J_w}{\Delta p} = \frac{2}{3}\left(\frac{8RT}{\pi M}\right)^{0.5}\frac{1}{RT}\frac{r\varepsilon}{L_p} + \frac{\bar{p}}{8\mu RT}\frac{r^2\varepsilon}{L_p} \tag{4.1}$$

where ε is surface porosity, r is mean pore radius of the membrane, μ is gas viscosity, R is gas constant, $\bar{p}$ is the average feed and permeate pressure, M is molecular weight of gas, L_p is effective pore length and T is temperature (k). The first term of the equation represents the Knudsen flow and the second term the Poiseuille flow. The gas permeation flux per unit of driving force ($\frac{J_w}{\Delta p}$) can be calculated as,

$$\frac{J_w}{\Delta p} = \frac{N_{t,w}}{A} \tag{4.2}$$

where, $N_{t,w}$ is total molar gas permeation rate (mol s^{-1}), Δp is the trans membrane pressure difference across the membrane area A. The total gas permeation rate through the membrane at difference pressure was measured using a bubble flow meter. By plotting

nitrogen flux ($\frac{J_w}{\Delta p}$) as a function of mean pressure $\bar{p}$, the effective surface porosity over pore length was calculated from the slope(S_0) and intercept (I_0) as follows:

$$r = \frac{16}{3}\left(\frac{S_0}{I_0}\right)\left(\frac{8RT}{\pi M}\right)^{0.5}\mu \tag{4.3}$$

$$\frac{\varepsilon}{L_p} = \frac{8\mu RTS_0}{r^2} \tag{4.4}$$

4.3 Result and Discussion

4.3.1 Membrane Characterization

Effective porosity over pore length of the membrane was calculated form Eq. (4.4) and was calculated to be 2.1 × 10^{-5} m^{-1} for unmodified membrane. The value obtained for hydrophilized membrane had no significant change compared to the unmodified membrane, confirming the modification process did not alter membrane porosity.

The membrane was characterized using Scanning Electron Microscopy (SEM) along with Energy Dispersive X-ray (EDX) Spectroscopy (Xu et al., 2009,Tylkowski et al., 2015,De los Rios et al., 2007). Figure 4.2 (a) shows the SEM image of the membrane permeate side while Figures 4.2 (b) and (c) show EDX images of the permeate side before and after hydrophilization. The EDX analysis of permeate side of the membrane showed an increase in oxygen content from 1.5 to 7% after hydrophilization.

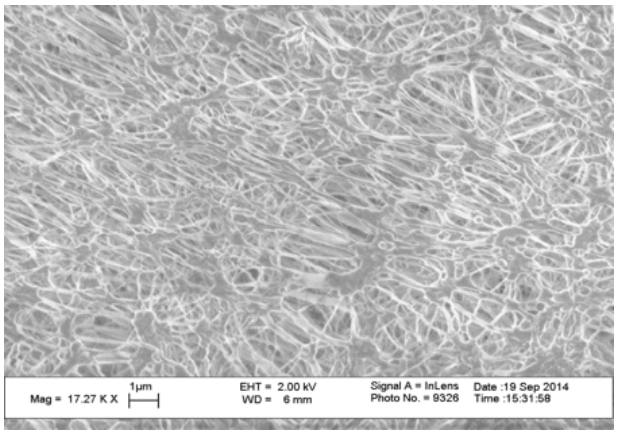

(a)

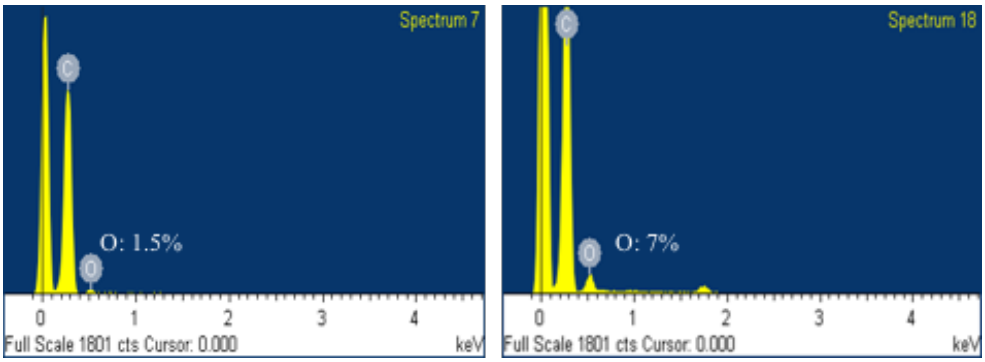

(b) (c)

Figure 4.2 SEM image and EDX analysis: (a) SEM of the permeate side of membrane, (b) EDX of unmodified permeate side and (c) EDX of hydrophilized membrane.

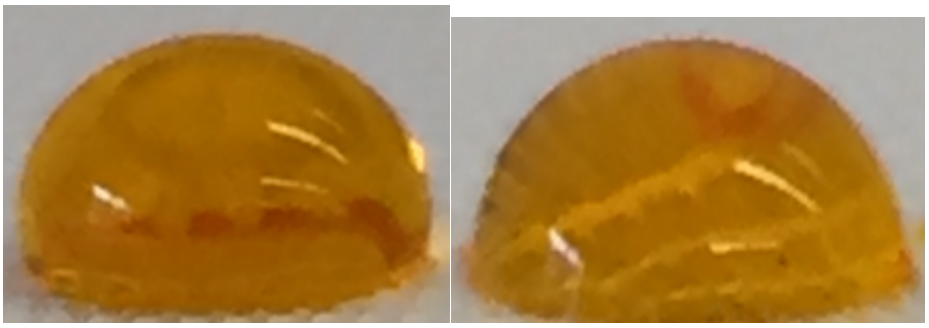

(a) (b)

Figure 4.3 Water contact angle measurement for (a) Hydrophilized membrane, (b) Unmodified membrane.

The hydrophilicity of the modified membrane was also studied by contact angle measurements. A low contact angle on the permeate side can lead to the pore wetting of the membrane by increased surface energy (Dumée, et al., 2013). After hydrophilization, the contact angle was found to decrease from 94º±2 to 73º±2. Lowering contact angle via partial hydrophilization in the permeate side of the membrane was expected to have positive effect on the membrane performance. The photographs of the contact angle measurements performed at the permeate side of both the hydrophilized and unmodified membrane are shown in Figure 4.3 (a) and (b).

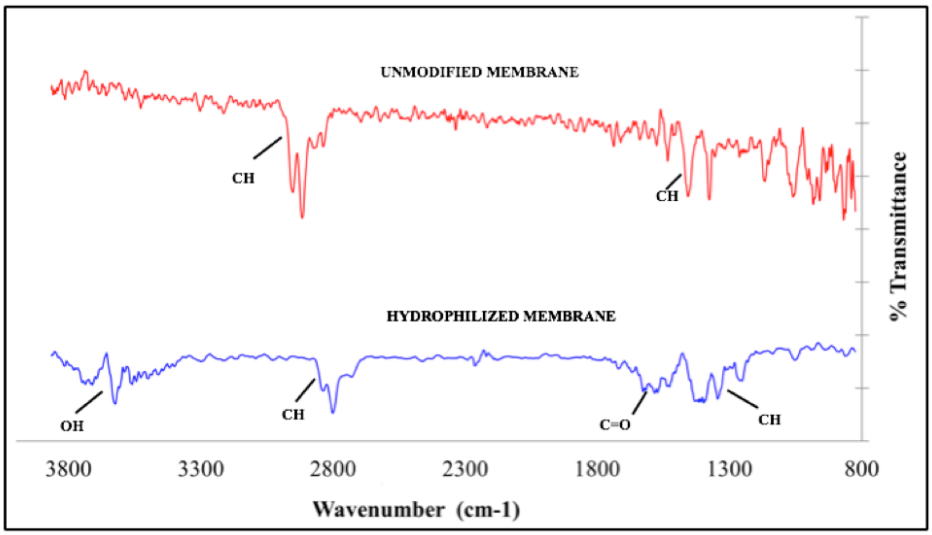

Figure 4.4 FTIR spectra of unmodified and hydrophilized membrane.

Chemical hydrophilization on the permeate side introduced polar functionalities such as carbonyl and hydroxyl groups on the surface, which were confirmed using FTIR analysis. Figure 4.4 shows the presence of strong C-H stretch at 2800–3000 cm^{-1} and C-H bending around 1350 – 1480 cm^{-1} which were attributed to polypropylene backbone. The

presence hydroxyl stretch between 3200–3600 cm^{-1} and at 3500–3700 cm^{-1} were observed after hydrophilization along with the carbonyl stretch between 1670 – 1820 cm^{-1}. There was also slight shift in the C-H to 2820 – 2850 cm^{-1}.

4.3.2 Effect of Hydrophilization on Membrane Performance

The overall permeate flux was calculated as follows:

$$J = \frac{w_p}{t.A} \tag{4.5}$$

where w_p is the total mass of the permeate, t is the permeate collection time and A is the membrane surface area. The performance of the membranes was studied as a function temperature, flow rate and salt concentration.

As seen in Figure 4.5 (a), the water vapor flux increased with temperature in both of the membranes. This was attributed to the exponential increase in vapor pressure with temperature (Mengual, et al., 2004,Criscuoli et al., 2013). It was seen that the hydrophilized membranes exhibited higher water vapor flux compared to the unmodified membrane. Maximum water vapor flux of 61.4 L/m^2.hr was attained at 80°C feed temperature at a permeate flow of 200 mL/min for the hydrophilized membrane. The effect of hydrophilization of the permeate side was quite dramatic with an enhancement as high as 52% at 60° C. Figure 4.5 (b) presents a plot of vapor pressure gradient as a function of temperature gradient at a constant feed flow rate. As expected an increase in vapor pressure

difference was observed when the temperature gradient was raised. This was true for both membranes.

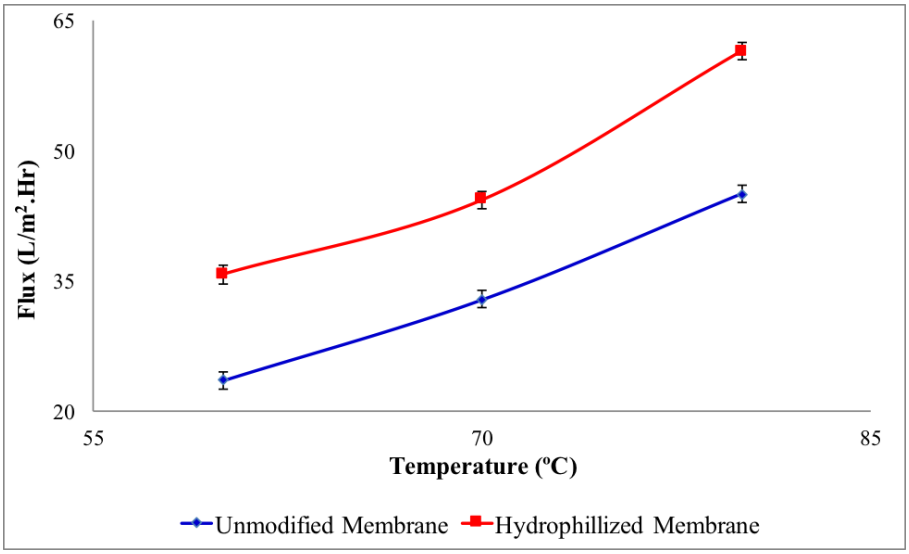

(a)

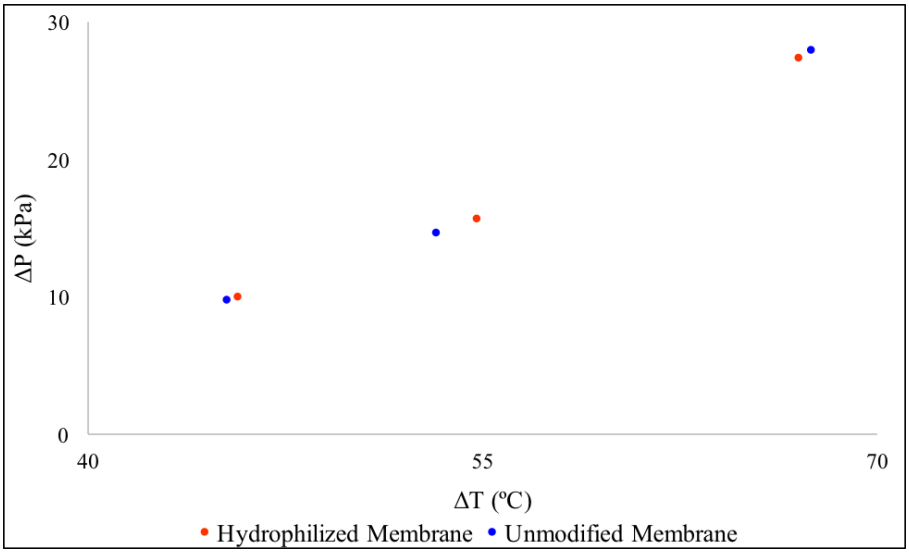

(b)

Figure 4.5 (a) Effect of temperature on water vapor flux at a feed flow rate of 200 mL/min; (b) Plot of temperature gradient versus vapor pressure gradient.

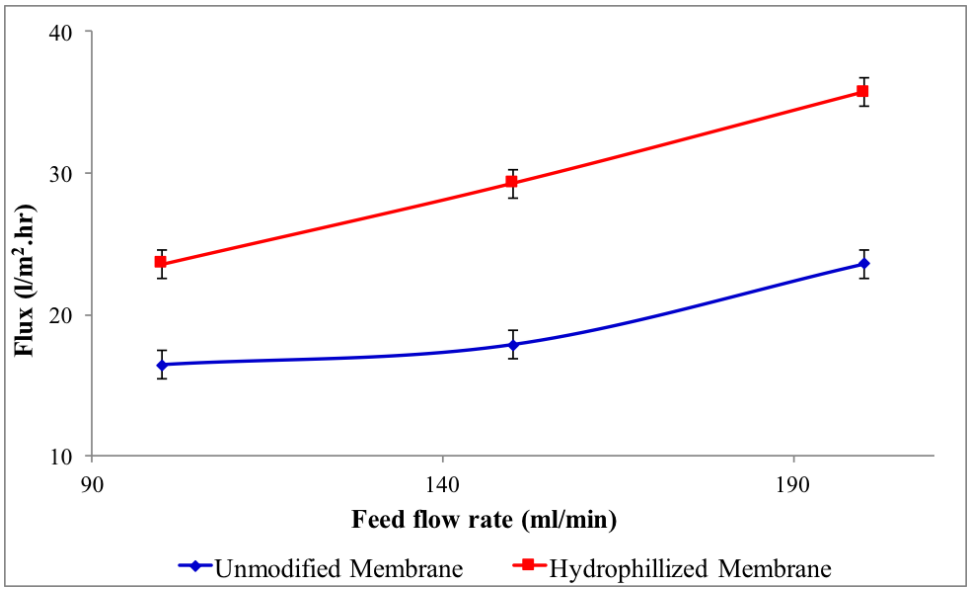

(a)

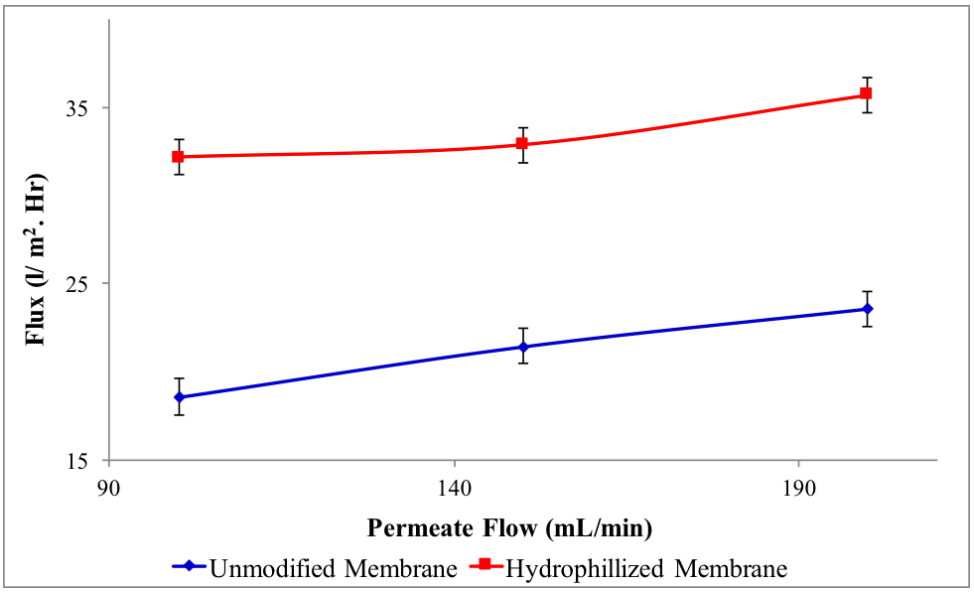

(b)

Figure 4.6 (a) Effect of feed flow rate variation on water vapor flux at feed temperature of 60º C; (b) Effect of permeate flow rate variation on water vapor flux at operating temperature of 60º C.

Figure 4.6 (a) shows the effect of varying feed flow rate at 60° C at a constant permeate flow rate of 200 mL/min, while Figure 4.5 (b) shows the effect of varying permeate flow rate at the same temperature but at constant feed flow rate of 200 mL/min. Higher flux were observed in both cases. Nearly 73% enhancement was attained at 100 mL/min and 60°C for hydrophilized membrane at constant feed flow rates. The increase in permeate flux with flow rate was attributed to increased turbulence and reduced boundary layer effect at elevated flow rates. Additionally, higher flow rate led to lower residence time resulting in higher outlet temperature as well as higher average bulk temperature which lead to an increased the driving force for MD (Gryta, 2002).

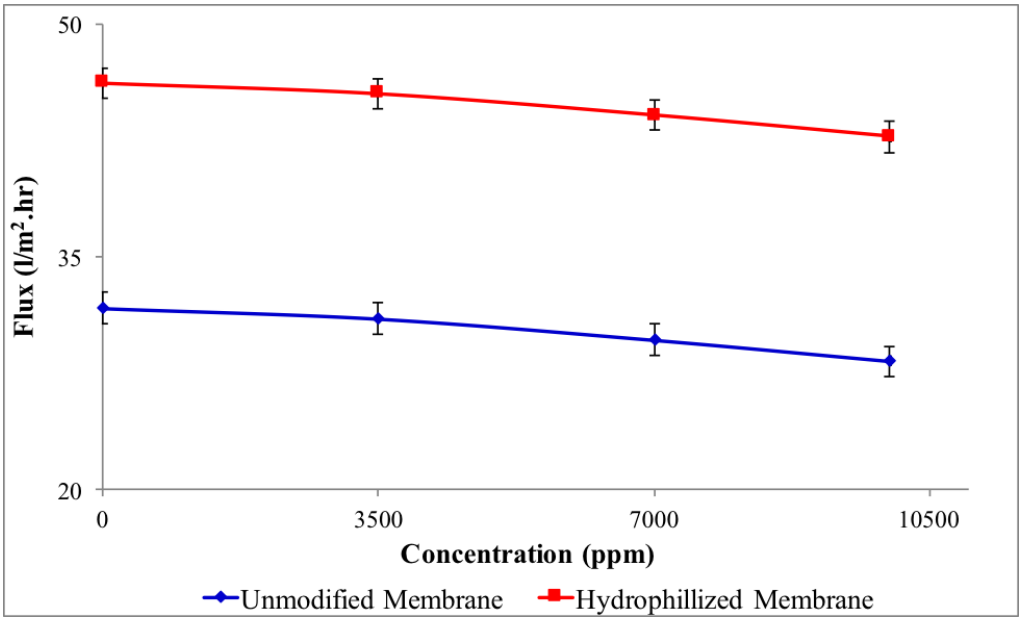

Figure 4.7 Effect of varying feed concentration on water vapor flux at a feed flow rate of 200mL/min and operating temperature of 70º C.

Figure 4.7 shows the effect of varying feed concentration on permeate flux. The higher salt concentration decreased the water activity at the membrane interface and formed additional boundary layer which reduced the driving force across the membrane. These led to a small decrease in permeate flux similar to what has been reported before (Cath, et al., 2004,Martínez-Díez, et al., 2001,Wirth, et al., 2002,Schofield, et al., 1990). The overall water vapor flux decreased at 10000 ppm from 46.2 to 42.7 L/m^2.hr for the hydrophilized membrane and 31.7 to 28.3 L/m^2.hr for the unmodified membrane. The permeate conductivity did not change with feed salt concentration implying that there was no significant increase in salt leakage with concentration. The permeate conductivity measured was between 2 – 3 μS which was almost the equivalent to distilled water.

The rate of mass transfer across the membrane is given as:

$$Jw = k(P_f - P_p) \quad (4.6)$$

where J is the water vapor flux of the system, k mass transfer coefficient,P_f and P_p are partial vapor pressure of average feed and permeate temperatures. The mass transfer coefficients were found to be significantly higher for hydrophilized membrane as compared to unmodified membrane.

Table 4.1(A) Effect of Varying Feed Flowrate on Mass Transfer Coefficient at Constant Temperature; (B) Effect of Varying Permeate Flowrate on Mass Transfer Coefficient at Constant Temperature

A	k (kg/m^2.s. Pa) x 10^{-07}	
Feed flowrate (mL/min)	Hydrophilized Membrane	Unmodified Membrane
100	4.2	2.9
150	5.2	3.0
200	6.1	3.9
B	k (kg/m^2. s. Pa) x 10^{-07}	
Permeate flowrate (mL/min)	Hydrophilized Membrane	Unmodified Membrane
100	5.5	3.3
150	5.7	3.7
200	6.1	3.9

Table 4.1 summarizes the effect of varying flow rate and permeate flow rate on mass transfer coefficient respectively. At lower flow rates, overall mass transfer was controlled by diffusion through the boundary layers. However, with increase in flow rates, turbulence increased, thereby reducing the boundary layer resistance and significantly increasing the mass transfer coefficients. Both membranes exhibited similar phenomena with increase in flow rate. Overall mass transfer coefficients in the hydrophilized membrane increased from 4.1 x 10^{-07} to 6.1x 10^{-07} with increase in feed flow rate, and 5.5 x 10^{-07} to 6.1 x 10^{-07} with increase in permeate flow rate. The enhancements attained were as high as 58% over the unmodified membrane.

4.3.3 Proposed Mechanism

Permeation in DCMD depends upon vapor pressure gradient across the membrane which acts as driving force for water vapor diffusion. A boundary layer is formed on the feed side comprising probably of both liquid and vapor phases. This layer is unaffected by hydrophilization of the permeate side (shown in Figure 4.8(a)) (Dumée, et al., 2013,Nejati et al., 2015,Sheng et al., 2011,Li et al., 2010). A similar boundary layer comprising of the vapor layer is also formed on the permeate side. As shown in the Figure 4.8(b), the hydrophilization on permeate side allowed rapid condensation, destabilized the vapor-gap and reduced the mass transfer barrier between the membrane surface and bulk permeate (Dumée, et al., 2013,Khayet et al., 2005). This is the equivalent of shrinking the boundary layer on the permeate side as shown in Figure 4.7(b). Together these led to an increased temperature gradient across the membrane thus increasing the overall flux .

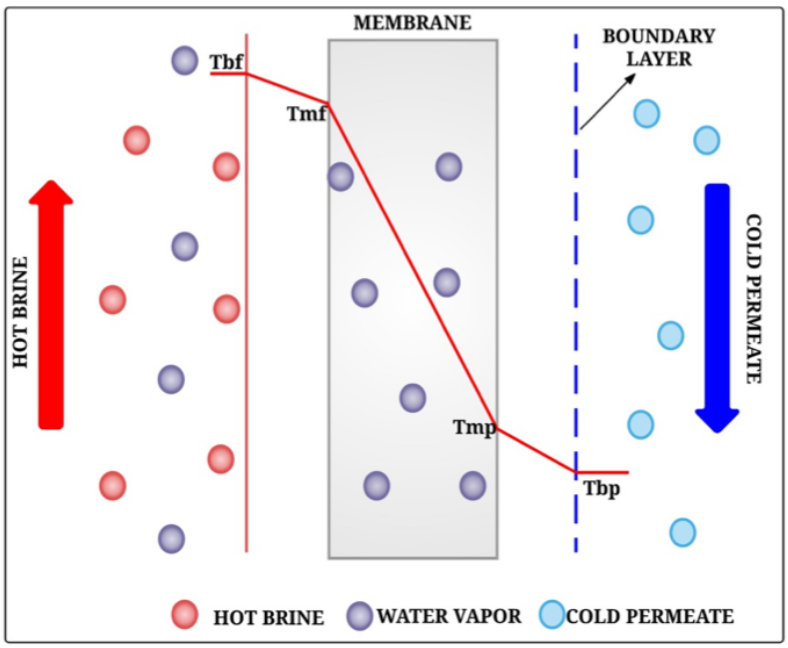

(a)

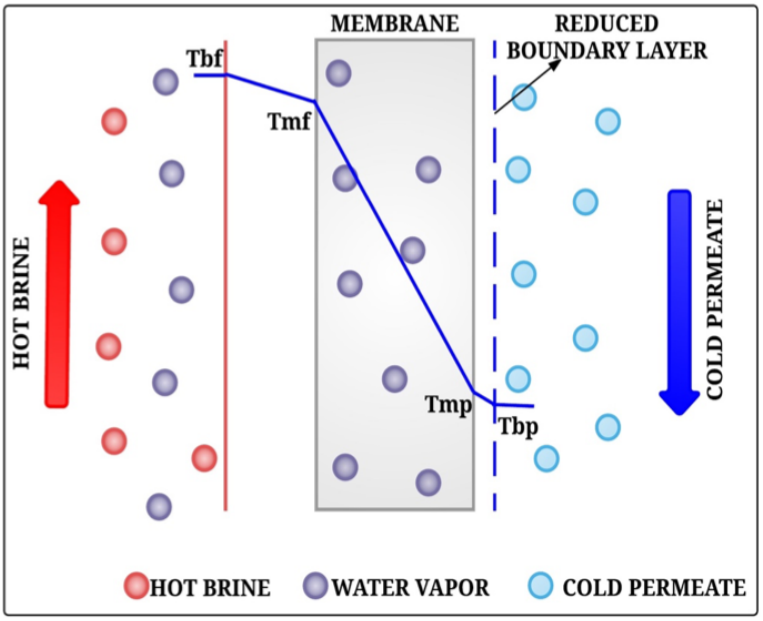

(b)

Figure 4.8 Proposed mechanism for (a) Unmodified Membrane (b) Hydrophilized membrane MD system.

4.4 Conclusion

Enhanced flux in DCMD using a hydrophilized membrane is reported. It was evident that hydrophilization was effective in rapid permeate removal thus enhancing mass transfer coefficients. The membrane distillation performance was consistently higher in case of hydrophilized membranes at all flow rates, temperature and salt concentrations. Flux enhancement reached as high as 73%.

CHAPTER 5

BACTERIAL DISINFECTION OF WATER USING DIRECT CONTACT MEMBRANE DISTILLATION

5.1 Introduction

Endotoxins are lipopolysaccharides (LPS) are essential components of cell membranes of gram-negative and cyanobacterial species and comprise of polysaccharides, oligosaccharide and acylated glycolipids (Shands Jr et al., 1967,Anderson et al., 2002,Stewart et al., 2006,Raetz, 1990,Prescott et al., 2002). The hydrophilic polysaccharides, hydrophobic lipids, and the long O-antigen in endotoxins forms different structural aggregates that are 100 nm to 3μm in size (Richter et al., 2011). Since bacteria growth is rampant under normal ambient conditions, LPS are a common water contaminant that are stable at high temperatures over 100°C and most pH (Almeida et al., 2016,Berthold et al., 1994). Excessive or systematic exposure to endotoxins, can result in inflammatory reactions in human (Rylander et al., 1978,Muittari et al., 1980,Wolff, 1973,Zhang et al., 2016,Morrison et al., 1978) and its contamination is a major concern in high purity water needed for pharmaceutical, biologicals and medical device industries because they show pathophysiological effects associated with both bacterial growth and lysis(Rietschel et al., 1992). The maximum allowable endotoxin limit for in pharmaceutical products used in intravenous injections is set at 5 EU/kg body weight per hour (Daneshian et al., 2006) while United States Pharmacopeia's endotoxin limit for sterile water for injection are 0.25 and 0.5 EU/mL(Williams, 2007). Reported endotoxin concentrations in natural waters across

the world ranges anywhere from 10 to thousands of EU/mL (Mokhtar et al., 2012), for instance one such study on Finland measured as high as 38000 EU/mL (Anderson et al., 2002).

Conventional water treatment process such as UV and oxidative inactivation, use of carbon filters, ceramic membranes, chlorination, ultrafiltration (UF), microfiltration (MF), nanofiltration (NF), reverse osmosis (RO) are not effective in endotoxin removal and efficiency depends on the sample concentration and its composition. For example, chlorination works at lower concentration, but is ineffective at higher concentration and increases the endotoxin levels in presences of bacterial cells (Huang et al., 2011), and UV and ozonation show reduction in the range of 30 to 50%. radiation. Commercial approach for generating water for injection (WFI) includes distillation and reverse osmosis (RO), where distillation is considered to be the most reliable method for endotoxin removal but can be prone to subsequent contamination and effectiveness of RO depends on initial concentration of the sample(Osol, 1976). Therefore, generating endotoxin free water is a challenge and is especially of great interest to downstream processing in healthcare industries (Xue et al., 2016,Uribe, 2007).

MD is a membrane based relatively low temperature (60 - 90°C) thermal evaporative process where selective diffusion of water vapor occurs through a microporous hydrophobic membrane (Alkhudhiri, et al., 2012,Lawson, et al., 1997,Lei, et al., 2005). Typical MD membranes includes polypropylene (PP), polytetrafluoroethylene (PTFE), polyvinylidenefluoride (PVDF). The ability of MD to produce highly pure water at low

temperatures makes this an attractive alternative in many applications such as food processing, desalination, purifying volatile compounds etc. The objective of this research is to study the effectiveness of MD in the removal of both bacterial cell debris and endotoxins from water.

5.2. Experiment

5.2.1 Materials and Methods

Limulus Amebocyte Lysate (LAL), reagent water (LRW) free of endotoxins, depyrogenated borosilicate dilution tubes, depyrogenated soda lime glass for gel - clot assay, Pyrotell Gel - Clot formulation multi test vial of 0.25 EU/mL detection limit and LAL reagent buffer for pH adjustments were purchased from Associates of Cape Cod Inc., (MA, USA). Sterile Eppendorf tips (20 – 300 μL), automatic pipette (100 -1000μL), CP Vortex Mixer, VWR Digital heat block for water bath were purchased from Cole Parmer (IL, USA).

5.2.2 Preparation of Bacterial Culture

E.coli AG1 cells containing plasmid pCA24N with chloramphenicol antibiotic resistance was used for the following experiments. The frozen stock of the cells was streaked on an LB-Agar plate containing 50 g/ml chloramphenicol antibiotic and incubated overnight for

single colonies. A single colony was used to inoculate a 15ml bacterial culture containing the above *E.coli* cells grown in LB medium with 50 g/ml antibiotic shaken at 250 rpm, 37^{o}C. This culture was used to inoculate the M9 minimal medium.

5.2.3 Preparation of M9 Minimal Medium

M9 salt solution (5x) was first prepared in 1L, having the following components: Na_2HPO_4, $7H_2O$ (64g/L), KH_2PO_4 (15g/L), NaCl (2.5g/L), NH_4Cl (5 g/L). This solution was autoclaved and stored. 100ml of the M9 salt solution was used to prepare the final media. We made a 500ml media with additional supplements 2mM $MgSO_4$ and 0.1mM $CaCl_2$. These were added from pre-sterilized 1M stock solutions. The medium was prepared in a 2L flask with 50 g/ml Chloramphenicol. 15 ml of the overnight culture was used for inoculation. The bacterial culture was shaken at 250 rpm, 30^{o}C for 12hrs and used for the subsequent steps. This method was developed after optimizing the growth time and the medium of choice, for the maximum number of viable cells at the start of the experimentation.

5.2.4 Bacterial Cell Quantification

Samples were collected before the start and at different stages of the experimentation. To quantify the concentration of live cells in the samples, we prepared LB-agar plates containing 50 g/ml chloramphenicol. The method is to track the amount of *E.coli* cells that were able to survive the experimentation and this is effective reducing the chance of a contamination because the cells we used already have an antibiotic resistance in them. Different amount of the samples was plated and the plates were incubated overnight at 37^{o}C. The number of single colonies were counted the following day using a AlphaImager® EP gel dock and the AlphaImager software. The number of colony forming unit per microliter (CFU/μL) of samples gave us a direct measure of concentration or the number of cells that were alive.

5.2.5 LAL Assay and Endotoxin Quantification

Endotoxin quantification was carried out by LAL gel-clot method where the tubes containing the LAL reagent and sample were placed in a water bath at 37°C. After an hour of incubation, the tubes were flipped upside down to verify formation of firm gel which indicates a positive reaction. Endotoxin samples for analysis were prepared by spiking

pyrogen free water with control standard endotoxins (CSE) of *Escherichia coli* strains O113:H10 of 125μg/vial potency. CSE with potency of 0.5μg/vial was used for standards and positive control tests.

All test samples were optimized to an acceptable pH range of 5.5 – 7.5 using LAL reagent buffer for performing the assay. LAL tests were performed by adding 0.1 mL of untreated sample to depyrogenated gel – clot assay soda lime reaction tubes. Samples were subjected to two-fold serial dilution using LAL reagent water. To the reaction tubes 0.1 mL of reconstituted pyrotell gel-clot formulation with 0.25 EU/mL detection limit was added. Upon thoroughly mixing all reaction tubes were incubated at 37 $\pm$ 1° C for 60 $\pm$ 2 minutes. After incubation, formation of gel is considered as positive end point for formation of endotoxin. Each test assay was performed along with series of endotoxin standard dilutions, positive control and negative control. The amount of endotoxin in the sample specimen was quantified as

$$Concentration\left({}^{EU}/_{mL}\right) = (\lambda)\times(dilution\ factor) \tag{5.1}$$

where λ - Pyrotell sensitivity (0.25 EU/mL).

5.2.6 Experimental Setup

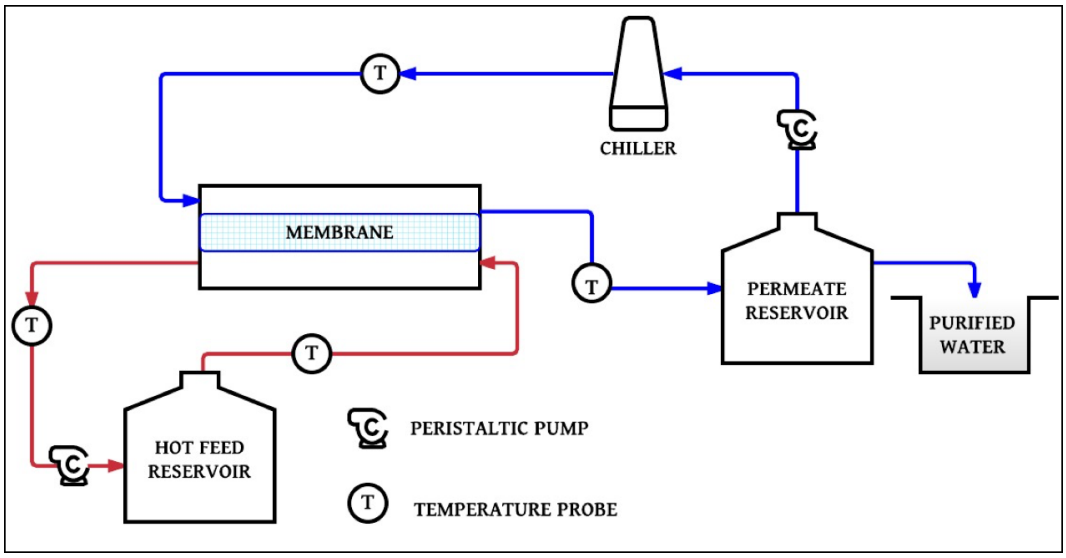

Figure 5.1 Schematic Experimental Setup for MD Process

Removal of endotoxin was studied using direct contact membrane distillation (DCMD) setup as shown in Figure 5.1. This has been described before(Ragunath, et al., 2016). Typical setup consisted of PTFE membrane cell having an effective membrane area of 14.5 cm^2, Viton O-rings, PTFE tubing (M-Flex C- Flex #17), PTFE connectors, feed and permeate flow pumps. Constant temperature heating water bath (Neslab Water Bath Model GP 200, NESLAB Instruments, Inc., Newington, NH, USA) was used to maintain constant feed temperature and a low temperature bench top chiller unit (Polyscience LS5, Cole-Parmer, USA) was used to maintain the permeate temperature between 15-20 °C. Feed and permeate solutions were circulated in a cross flow mode. Both feed and permeate flow passing through the membrane modules were recycled from their respective reservoirs

using peristaltic pumps (Cole-Parmer, USA). The inlet and outlet membrane temperatures were monitored using temperatures control probes (Four-channel Data Logging Thermometer, RS-232, Cole-Parmer, USA). Hydrophobic polytetrafluorethylene (PTFE) membranes with pore sizes of 0.2, 0.5, 1.0 μm purchased from Advantec Mfc Inc., (CA, USA) was chosen for out study.

All experiments were performed using Milli – Q water (pH ~ 6.8) generated by Millipore Direct Q3 water purification system. The Milli-Q water was spiked with known concentration of endotoxins for experimental purpose. Glassware was depyrogenated at 250°C for 30 mins. Samples collected after each experiment was duly preserved at lower temperatures (~ 4°C) before analysis and tested within 24 hours. All experiments were repeated three times and average results are reported.

5.3 Results and Discussion

The MD experiments were performed for a duration of 3 hours upon attaining equilibrium. The flux was monitored every 30 minutes and average was reported. All experiments were repeated three times and the relative standard deviation for the experiments was estimated to be within 1%. The water vapor flux J_w, across the membrane was expressed as (Lawson, et al., 1997):

$$J_w = \frac{W_p}{t \,.\, A} \tag{5.2}$$

where, w_p is the total mass of permeate, t is the permeate collection time and A is the membrane surface area. The removal of endotoxins from feed water was estimated as

$$\text{Rejection } (\%) = \frac{F_c - P_c}{F_c} \times 100 \qquad (5.3)$$

where F_c and Pc were the initial feed and the final permeate concentrations, respectively.

5.3.1 MD Performance for Endotoxin Removal

Figure 5.2 shows the effect of varying membrane pore size on distillate endotoxin concentration. Nominal pore size of membrane was varied between 0.2 to 1.0 μm, and MD experiments were performed at a temperature of 70°C, sample velocity of 100 mL/min and feed concentration of 1024 EU/mL. MD flux increased from 28.5 kg/m^2. Hr. for the 0.2μm to 39.2 kg/m^2. hr for the 1.0 μm membrane; a nearly 38% increase in flux. The water vapor flux was directly proportional to pore size and this was in agreement with previously reported studies (Khayet et al., 2004). Typically, endotoxin aggregates in water suspension are in the size range of 0.1μm (Petsch et al., 2000), which was smaller than the nominal pore size of the membranes under consideration. Since only the vapors permeate through, the endotoxin rejection in a 0.2 and 1 μm pore size were 99.5 and 96.9% respectively. At larger pore sizes, distillate endotoxins levels increased due to reduced liquid entry pressure. The permeate endotoxin levels in Figure 5.2 increased from 5.2 to 31.4 EU/mL or 83%.

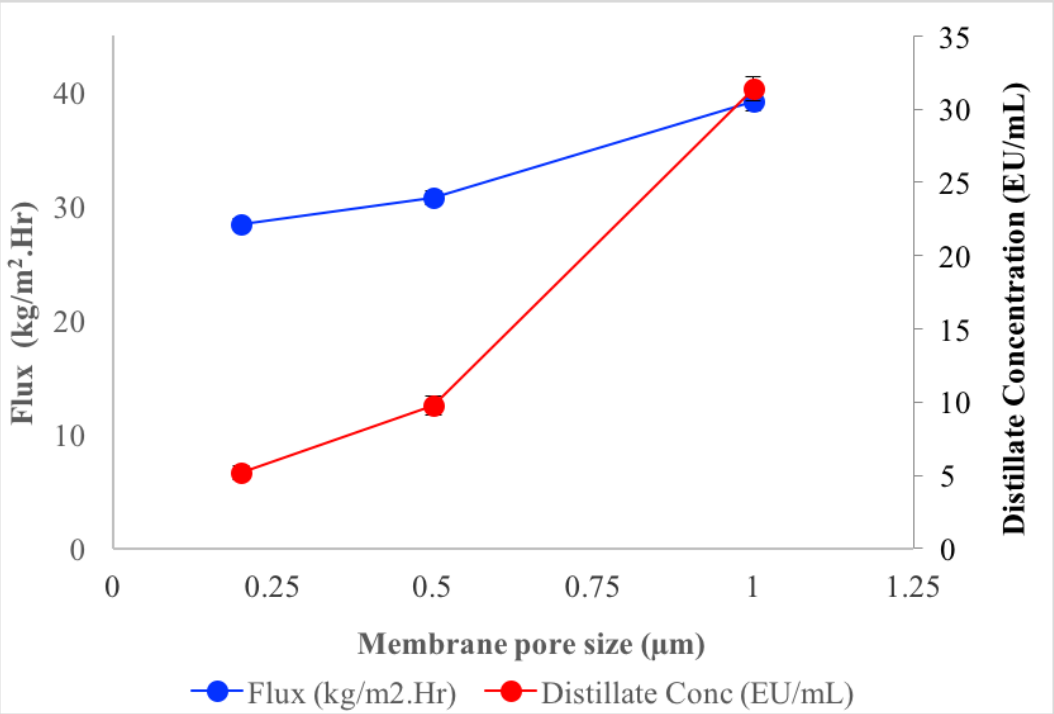

Figure 5.2 Effect of varying membrane pore size.

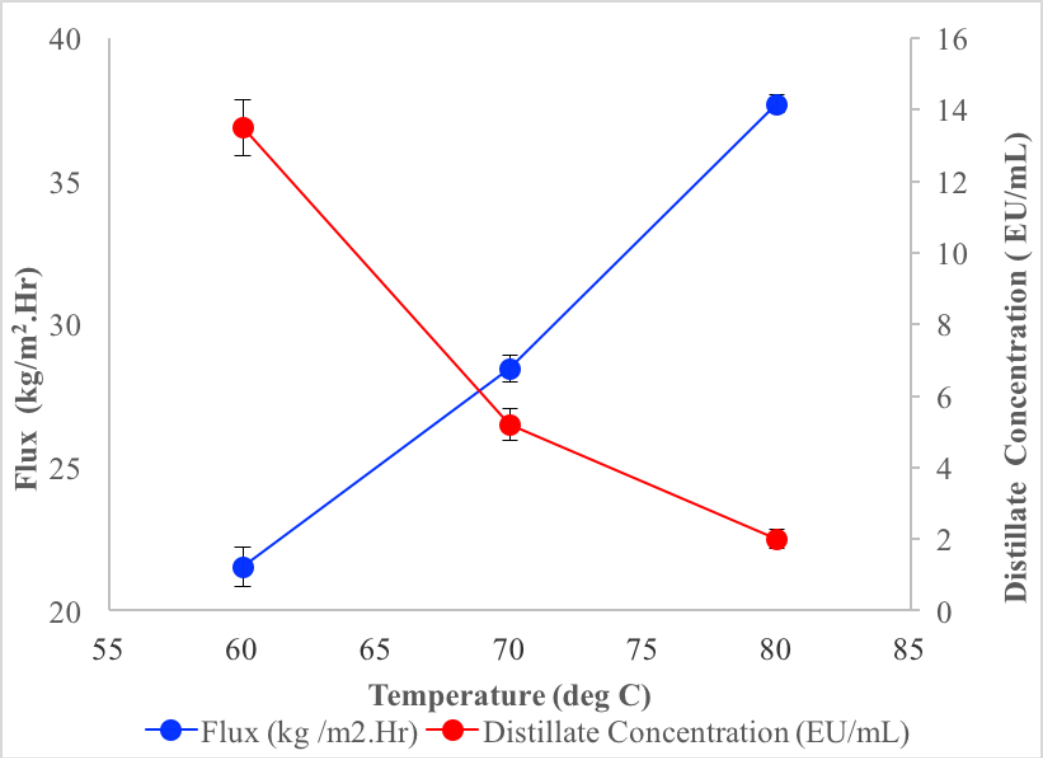

Figure 5.3 Effect of temperature at constant feed concentration of 1024EU/mL and flowrate of 50mL/min on MD performance.

Based on the results obtained, PTFE membrane with 0.2 µm was used for further MD experiments. Figure 5.3 presents permeate flux and endotoxin concentration in the permeate as a function of temperature at constant flow rate of 50 mL/min and feed concentration of 1024 EU/mL. As expected, the permeate flux increased with temperature because of the vapor pressure gradient (Phattaranawik et al., 2003). The flux increased from 21.5 Kg/m^2. hr at 60 ° C to 37.7 kg/m^2. hr at 90° C. The increase in temperatures also reduced the permeate endotoxin concentration from 13.5 EU/mL at 60 ° C to 2.0 EU/mL 80° C. Nearly 99.8 % rejection in endotoxin levels were observed at feed temperature of

80° C. This is because at high temperatures the hydration layer around the endotoxins are weakened leading to the formation of larger aggregates (Li et al., 2013). Additionally, the higher flux results in larger permeate volumes that dilute the endotoxins in the permeate.

The effect of sample flowrate on removal of endotoxins at constant temperature and feed concentration is presented in Figure 5.4. Sample flow velocity was varied between 50 to 100 mL/min at constant operating temperature of 70°C and feed concentration of 1024 EU/mL. As expected, the permeate flux increased as a function of flow rate which was attributed to the reduced boundary layer effect at higher flowrates (Banat et al., 1994). With increase in flowrate the permeate endotoxin concentration decreased from 10.2 EU/ml at 50 mL/min to 2.3 EU/mL at 100 mL/min. Reduced endotoxin levels at higher flow rates was attributed to decreased in contact time that restricted the diffusion of endotoxins through the membrane.

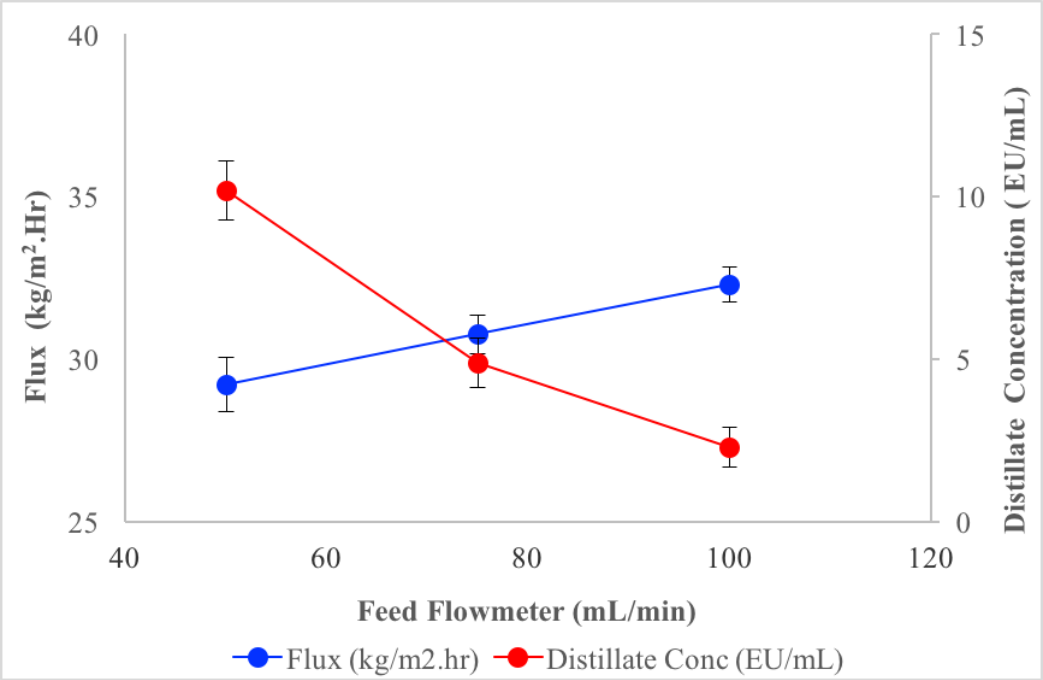

Figure 5.4 Effect of feed flowrate at constant feed concentration of 1024EU/mL and temperature of 70°C, on MD performance and permeate endotoxin concentration

Figure 5.5 shows the effect of varying endotoxin concentration from different water samples with varying endotoxin concentrations. Different water samples such as tap water, minimal media bacterial culture, water spiked with known endotoxin concentration were used, and the concentration of the samples ranged between 32 to 4096 EU/mL. MD experiments were performed at constant feed temperature of 70°C and sample flow rate of 100 mL/min. Overall flux decreased as a function of feed concentration; from 35.4 kg/m^2. hr for water with 32 EU/mL to 20 kg/m^2. hr. for water spiked with 4096 EU/mL. The 43% reduction in MD flux was attributed to the increased concentration polarization and the formation of larger vesicles (Petsch, et al., 2000,DePamphilis, 1971). At higher feed

concentrations, the endotoxins formed larger aggregates that adhered to the membrane surface increasing the mass transfer resistance (Czermak et al., 2010).

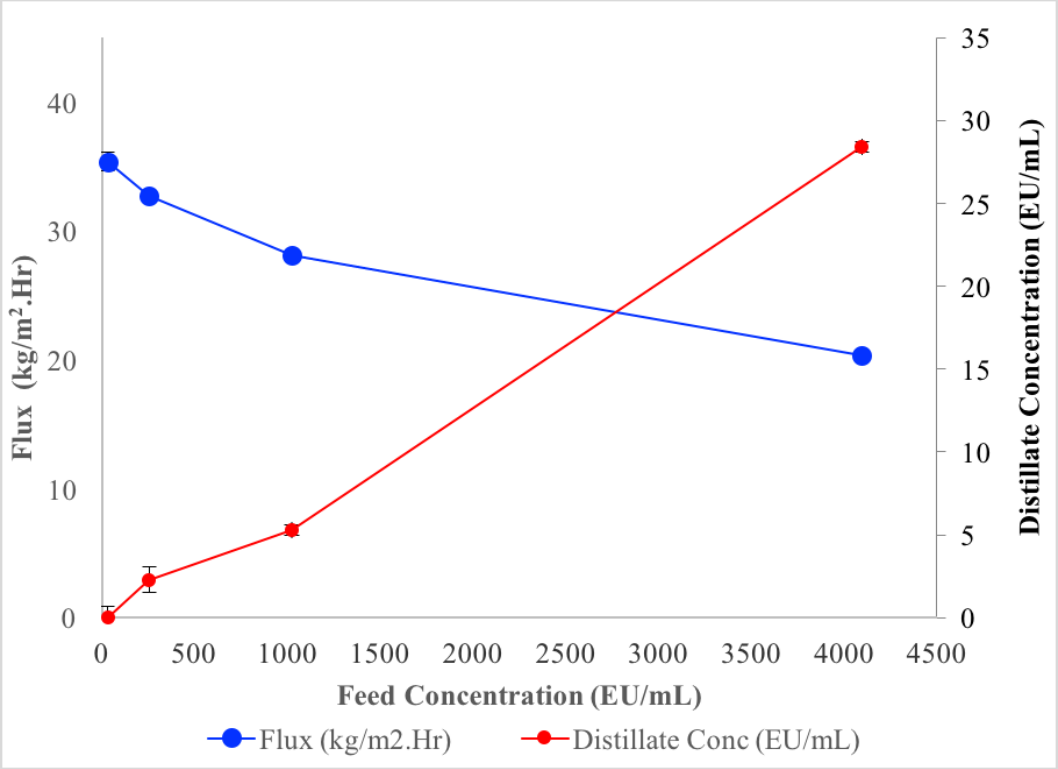

Figure 5.5 Effect of Sample Concentration on MD Performance and Permeate Endotoxin Concentrations at Constant Temperature of 70°C and Flowrate of 100 mL/min.

The endotoxin levels in the final distillated increased as a function of feed concentration. Overall, permeate concentration increased from 2.3 EU/mL at a feed concentration of 256 EU/mL to 28.4 EU/mL at a concentration of 4096 EU/mL. Increase in feed concentration brought more endotoxins to the membrane surface leading to permeation across the membrane. However, the endotoxin rejection rate was consistently above 99.0 % for all samples studied including those at high levels. The tap water studied

here had an initial endotoxin concentration of about 32 EU/mL, but there were no detectable endotoxins at final distillate. No detectable amount of endotoxin was observed with experiments performed with Milli-Q water was considered as blank.

5.3.1 MD Performance for Bacterial Cell Removal

The effect of membrane distillation in presence of both unmodified and CNT modified membrane was studied for both rejection in permeate side and reduction of bacterial cells on the feed side at constant flow and feed temperature of 50°C is shown in Figure 5.7 The bacterial cell rejection estimated were 100% for both modified and unmodified membrane indicating presence of no viable cells on distillate stream as an effect of the membrane distillation technique. Similarly, quantification of feed stream after the treatment process indicated significant difference. Percentage reduction of viable cells was comparatively higher for CNIM membrane with 98.6% and 65.9 % for unmodified membrane. Significant decrease in viable cells with CNIM membrane can be attributed to its antibacterial effect where the cell wall of bacterial cells is damaged in presence of CNTs, making this membrane a potential anti-bacterial membrane for disinfection(Kang et al., 2008). This was further confirmed by the SEM analysis conducted on the membranes after the process, presented in Figure 5.6. From the SEM images, it is evident that bacterial cells tend to adhere to the membrane surface, whereas with CNIM significant damage in bacterial cells are evident and presence of agglomerates of bacterial cell debris indicates the anti-bacterial property of CNTs.

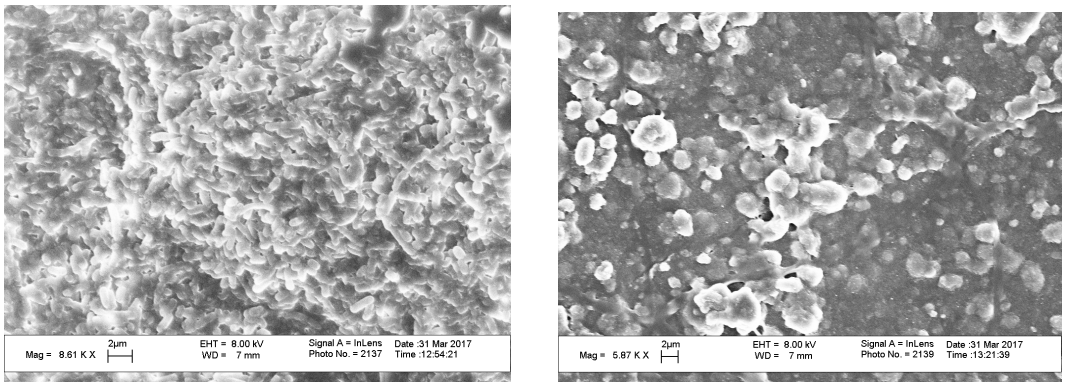

(a) (b)

Figure 5.6 Membrane characterization after MD process (a) Unmodified (b) CNIM

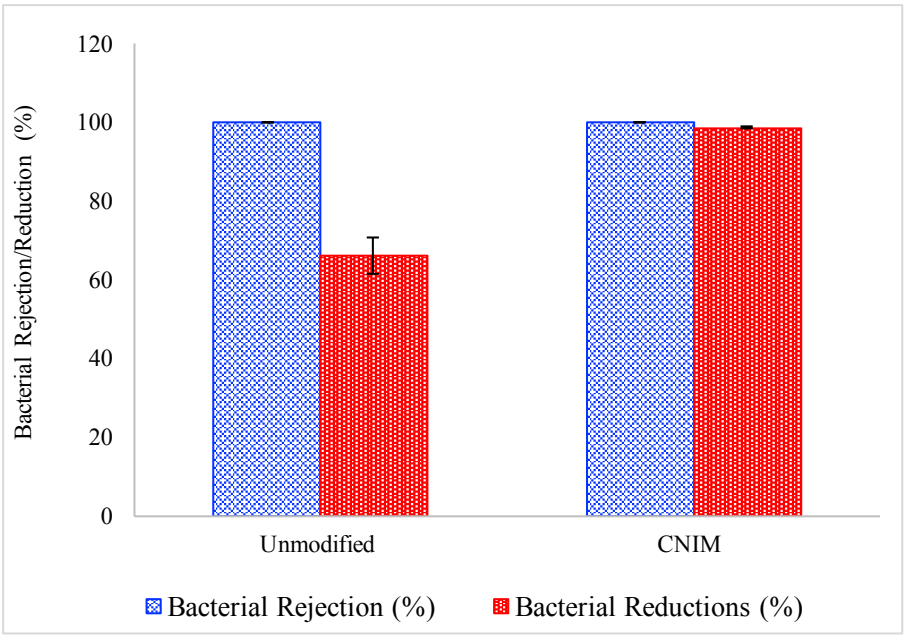

Figure 5.7 Effect of MD on bacterial cell rejection and reductions in feed & distillate respectively at 50°C.

5.4 Conclusion

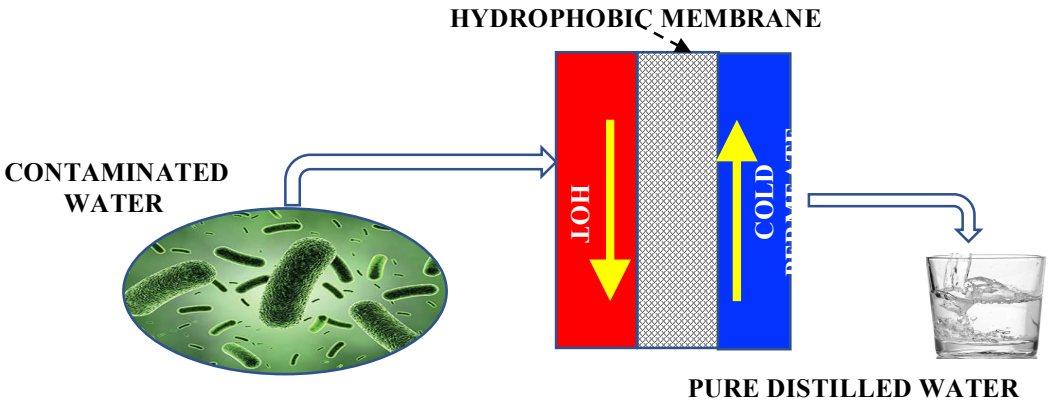

Figure 5.8 Schematic Representation of the Purification Process of Endotoxin Water

We demonstrate successful removal of endotoxins via membrane distillation. Via DCMD, using PTFE membranes as shown in Figure 5.8. Various operating parameters such as temperature, sample flowrate, feed concentration and membrane pore size were studied. The permeate flux attained showed a trend that is similar to what was obtained in conventional DCMD, implying that the endotoxins did not alter permeation characteristics. Larger pore size lead to reduced liquid entry pressure leading to higher permeation of endotoxins. Endotoxin levels in the permeate water depended on the feed concentration but removal efficiency was over 99% even at low temperatures as low as 60^{o}C. Average endotoxin rejection of about 99.4% was recorded by MD process. Due to the low energy requirement of the process, this approach can be potentially applied for purification of different water samples containing endotoxins and can be potentially used for depyrogenation technique.

CHAPTER 6

SUMMARY

In summary, this research presents novel membranes and membrane based approaches for air and water treatment applications. Carbon nanotube immobilized membranes were successful in extracting VOCs and in desalination via membrane distillation technique. CNT immobilized membrane was efficient in extracting VOCs from air and had enhanced performance in particular for toluene sample due to its non-polar interactions. With due functionalization of CNTs, the membranes can be used for selective extraction of other volatile organics with different polarities. In case of membrane distillation for desalination applications, CNT immobilized membrane had enhanced flux in comparison to unmodified membrane. Fabrication of CNIM by phase inversion provided a controlled approach for CNIM fabrication which can alter the water vapor interaction with the membrane interface, and resulting in higher flux.

Likewise, permeate surface modification by hydrophilization reduced the resistance imposed by boundary layer effect on membrane interface, in turn addressing polarization impact on MD process and allowing rapid condensation of diffused vapor which resulted in enhanced MD flux for desalination. The final part of this research focuses on extrapolating the advantages of membrane distillation to other application where the process simultaneously eliminates contaminants and generate pure water in microbial disinfection application. Overall, membrane based techniques with due advancement in novel membrane fabrication can be a possible solution for various air and water treatments.

REFERENCES

Baker RW. 2000. Membrane technology: Wiley Online Library.

Patnaik P. 2010. Handbook of environmental analysis: chemical pollutants in air, water, soil, and solid wastes: CRC Press.

Davarani SSH, Pourahadi A, Nojavan S, Banitaba MH, Nasiri-Aghdam M. 2012. Electro membrane extraction of sodium diclofenac as an acidic compound from wastewater, urine, bovine milk, and plasma samples and quantification by high-performance liquid chromatography. Analytica Chimica Acta 722:55-62.

Pálmarsdóttir S, Mathiasson L, Jönsson JÅ, Edholm LE. 1997. Determination of a basic drug, bambuterol, in human plasma by capillary electrophoresis using double stacking for large volume injection and supported liquid membranes for sample pretreatment. Journal of Chromatography B: Biomedical Sciences and Applications 688:127-134.

Ndungù K, Djane N-K, Mathiasson L. 1998. Determination of trace metal ions by ion-pair chromatography after enrichment using supported liquid membrane. Journal of Chromatography A 826:103-108.

Berhanu T, Liu J-f, Romero R, Megersa N, Jönsson JÅ. 2006. Determination of trace levels of dinitrophenolic compounds in environmental water samples using hollow fiber supported liquid membrane extraction and high performance liquid chromatography. Journal of Chromatography A 1103:1-8.

Halvorsen TG, Pedersen-Bjergaard S, Reubsaet JLE, Rasmussen KE. 2001. Liquid-phase microextraction combined with flow-injection tandem mass spectrometry: Rapid screening of amphetamines from biological matrices. Journal of Separation Science 24:615-622.

Andersen S, Halvorsen TG, Pedersen-Bjergaard S, Rasmussen KE, Tanum L, Refsum H. 2003. Stereospecific determination of citalopram and desmethylcitalopram by capillary electrophoresis and liquid-phase microextraction. Journal of Pharmaceutical and Biomedical Analysis 33:263-273.

Chimuka L, Cukrowska E, Jönsson JÅ. 2004. Why liquid membrane extraction is an attractive alternative in sample preparation. Pure and Applied Chemistry 76:707-722.

Hylton K, Mitra S. 2007. Automated, on-line membrane extraction. Journal of Chromatography A 1152:199-214.

Kathios DJ, Jarvinen GD, Yarbro SL, Smith BF. 1994. A preliminary evaluation of microporous hollow fiber membrane modules for the liquid-liquid extraction of actinides. Journal of Membrane Science 97:251-261.

Hussain CM, Mitra S. 2012. 2.20 - Nanomaterials for Sample Preparation A2 - Pawliszyn, JanuszComprehensive Sampling and Sample Preparation. Oxford: Academic Press. p 389-418.

Wang X, Kou D, Mitra S. 2005. Continuous, on-line monitoring of haloacetic acids via membrane extraction. Journal of Chromatography A 1089:39-44.

Loeb S, Sourirajan S. 1962. Sea water demineralization by means of an osmotic membrane. ACS Publications.

Sholl DS, Johnson JK. 2006. Making high-flux membranes with carbon nanotubes. Science 312:1003-1004.

Hinds BJ, Chopra N, Rantell T, Andrews R, Gavalas V, Bachas LG. 2004. Aligned Multiwalled Carbon Nanotube Membranes. Science 303:62-65.

Gethard K, Sae-Khow O, Mitra S. 2011. Water desalination using carbon-nanotube-enhanced membrane distillation. ACS Applied Materials and Interfaces 3:110-114.

Arora G, Sandler SI. 2007. Molecular sieving using single wall carbon nanotubes. Nano Letters 7:565-569.

Sanip SM, Ismail AF, Goh PS, Soga T, Tanemura M, Yasuhiko H. 2011. Gas separation properties of functionalized carbon nanotubes mixed matrix membranes. Separation and Purification Technology 78:208-213.

Kim S, Chen L, Johnson JK, Marand E. 2007. Polysulfone and functionalized carbon nanotube mixed matrix membranes for gas separation: Theory and experiment. Journal of Membrane Science 294:147-158.

Hylton K, Chen Y, Mitra S. 2008. Carbon nanotube mediated microscale membrane extraction. Journal of Chromatography A 1211:43-48.

Peng F, Hu C, Jiang Z. 2007. Novel ploy(vinyl alcohol)/carbon nanotube hybrid membranes for pervaporation separation of benzene/cyclohexane mixtures. Journal of Membrane Science 297:236-242.

Lee K. 2011. Guest editorial. Solar Energy Materials and Solar Cells 95:1.

Hylton K, Chen Y, Mitra S. 2008. Carbon nanotube mediated microscale membrane extraction. Journal of Chromatography A 1211:43-48.

Huang D, Fu C, Li Z, Deng C. 2012. Development of magnetic multiwalled carbon nanotubes as solid-phase extraction technique for the determination of p-hydroxybenzoates in beverage. Journal of Separation Science 35:1667-1674.

Fang G-Z, He J-X, Wang S. 2006. Multiwalled carbon nanotubes as sorbent for on-line coupling of solid-phase extraction to high-performance liquid chromatography for simultaneous determination of 10 sulfonamides in eggs and pork. Journal of Chromatography A 1127:12-17.

Hussain CM, Saridara C, Mitra S. 2008. Microtrapping characteristics of single and multi-walled carbon nanotubes. Journal of Chromatography A 1185:161-166.

Saridara C, Ragunath S, Pu Y, Mitra S. 2010. Methane preconcentration in a microtrap using multiwalled carbon nanotubes as sorbents. Analytica Chimica Acta 677:50-54.

Ellison MD, Good AP, Kinnaman CS, Padgett NE. 2005. Interaction of water with single-walled carbon nanotubes: Reaction and adsorption. Journal of Physical Chemistry B 109:10640-10646.

Fujiwara A, Ishii K, Suematsu H, Kataura H, Maniwa Y, Suzuki S, Achiba Y. 2001. Gas adsorption in the inside and outside of single-walled carbon nanotubes. Chemical Physics Letters 336:205-211.

Bhadra M, Sae-Khow O, Mitra S. 2012. Effect of carbon nanotube functionalization in micro-solid-phase extraction (μ-SPE) integrated into the needle of a syringe. Analytical and Bioanalytical Chemistry 402:1029-1039.

Hussain CM, Mitra S. 2011. Micropreconcentration units based on carbon nanotubes (CNT). Analytical and Bioanalytical Chemistry 399:75-89.

Peng F, Pan F, Sun H, Lu L, Jiang Z. 2007. Novel nanocomposite pervaporation membranes composed of poly(vinyl alcohol) and chitosan-wrapped carbon nanotube. Journal of Membrane Science 300:13-19.

Bhadra M, Mitra S. 2013. Nanostructured membranes in analytical chemistry. TrAC Trends in Analytical Chemistry 45:248-263.

Sae-Khow O, Mitra S. 2009. Fabrication and characterization of carbon nanotubes immobilized in porous polymeric membranes. Journal of Materials Chemistry 19:3713-3718.

Sae-Khow O, Mitra S. 2010. Simultaneous extraction and concentration in carbon nanotube immobilized hollow fiber membranes. Analytical Chemistry 82:5561-5567.

Sae-Khow O, Mitra S. 2010. Carbon nanotube immobilized composite hollow fiber membranes for pervaporative removal of volatile organics from water. Journal of Physical Chemistry C 114:16351-16356.

Gethard K, Mitra S. 2011. Membrane distillation as an online concentration technique: Application to the determination of pharmaceutical residues in natural waters. Analytical and Bioanalytical Chemistry 400:571-575.

Gethard K, Mitra S. 2011. Carbon nanotube enhanced membrane distillation for online preconcentration of trace pharmaceuticals in polar solvents. Analyst 136:2643-2648.

Choi JH, Jegal J, Kim WN. 2007. Modification of performances of various membranes using MWNTs as a modifier. Macromolecular Symposia 249-250:610-617.

Mondal S, Hu JL. 2008. Microstructure and water vapor transport properties of functionalized carbon nanotube-reinforced dense-segmented polyurethane composite membranes. Polymer Engineering & Science 48:1718-1724.

Es'haghi Z, Golsefidi MA, Saify A, Tanha AA, Rezaeifar Z, Alian-Nezhadi Z. 2010. Carbon nanotube reinforced hollow fiber solid/liquid phase microextraction: A novel extraction technique for the measurement of caffeic acid in Echinacea purpurea herbal extracts combined with high-performance liquid chromatography. Journal of Chromatography A 1217:2768-2775.

Bhadra M, Mitra S. 2012. Carbon nanotube immobilized polar membranes for enhanced extraction of polar analytes. Analyst 137:4464-4468.

Król S, Zabiegała B, Namieśnik J. 2010. Monitoring VOCs in Atmospheric Air I. On-line Gas Analyzers. TrAC Trends in Analytical Chemistry 29:1092-1100.

Król S, Zabiegała B, Namieśnik J. 2010. Monitoring VOCs in Atmospheric Air II. Sample Collection and Preparation. TrAC Trends in Analytical Chemistry 29:1101-1112.

Dewulf J, Van Langenhove H. 1999. Anthropogenic Volatile Organic Compounds in Ambient Air and Natural Waters: A Review on Recent Developments of Analytical Methodology,

Performance and Interpretation of Field Measurements. Journal of Chromatography A 843:163-177.

Khan FI, Kr. Ghoshal A. 2000. Removal of Volatile Organic Compounds from Polluted Air. Journal of Loss Prevention in the Process Industries 13:527-545.

Ruddy EN, Carroll LA. 1993. Select the Best VOC Control Strategy. Chemical Engineering Progress 89:28-35.

Barro R, Regueiro J, Llompart M, Garcia-Jares C. 2009. Analysis of Industrial Contaminants in Indoor Air: Part 1. Volatile Organic Compounds, Carbonyl Compounds, Polycyclic Aromatic hydrocarbons and Polychlorinated Biphenyls. Journal of Chromatography A 1216:540-566.

Harper M. 2000. Sorbent Trapping of Volatile Organic Compounds from Air. Journal of Chromatography A 885:129-151.

Urashima K, Chang J, x, Shih. 2000. Removal of Volatile Organic Compounds from Air Streams and Industrial Flue Gases by Non-Thermal Plasma Technology. Dielectrics and Electrical Insulation, IEEE Transactions on 7:602-614.

Ghoshal AK, Manjare SD. 2002. Selection of Appropriate Adsorption Technique for Recovery of VOCs: An Analysis. Journal of Loss Prevention in the Process Industries 15:413-421.

Ras MR, Borrull F, Marcé RM. 2009. Sampling and Preconcentration Techniques for Determination of Volatile Organic Compounds in Air Samples. TrAC Trends in Analytical Chemistry 28:347-361.

Kimmerle K, Bell CM, Gudernatsch W, Chmiel H. 1988. Solvent Recovery from Air. Journal of Membrane Science 36:477-488.

W. Baker R, Yoshioka N, M. Mohr J, J. Khan A. 1987. Separation of Organic Vapors from Air. Journal of Membrane Science 31:259-271.

Sohn W-I, Ryu D-H, Oh S-J, Koo J-K. 2000. A Study on the Development of Composite Membranes for the Separation of Organic Vapors. Journal of Membrane Science 175:163-170.

Paul H, Philipsen C, Gerner FJ, Strathmann H. 1988. Removal of Organic Vapors from Air by Selective Membrane Permeation. Journal of Membrane Science 36:363-372.

Baker RW, Simmons VL, Kaschemekat J, Wijmans JG. 1994. Membrane Systems for VOC Recovery from Air Streams. Filtration & Separation 31:231-235.

Ho WW, Sirkar KK. 1992. Membrane handbook: Springer.

Badjagbo K, Sauvé S, Moore S. 2007. Real-time Continuous Monitoring Methods for Airborne VOCs. TrAC Trends in Analytical Chemistry 26:931-940.

Panek D, Konieczny K. 2009. Pervaporative Separation of Toluene from Wastewaters by Use of Filled and Unfilled Poly(dimethylosiloxane) (PDMS) Membranes. Desalination 241:197-200.

Ketola RA, Kotiaho T, Cisper ME, Allen TM. 2002. Environmental Applications of Membrane Introduction Mass Spectrometry. Journal of Mass Spectrometry 37:457-476.

Noble RD, Stern SA. 1995. Membrane Separations Technology: Principles and Applications: Elsevier.

Koops GH, Nolten JAM, Mulder MHV, Smolders CA. 1993. Poly(vinyl chloride) Polyacrylonitrile Composite Membranes for the Dehydration of Acetic Acid. Journal of Membrane Science 81:57-70.

Smitha B, Suhanya D, Sridhar S, Ramakrishna M. 2004. Separation of Organic–Organic Mixtures by Pervaporation—A Review. Journal of Membrane Science 241:1-21.

Jiang LY, Chung TS, Rajagopalan R. 2007. Matrimid®/MgO Mixed Matrix Membranes for Pervaporation. AIChE Journal 53:1745-1757.

Kittur AA, Kulkarni SS, Aralaguppi MI, Kariduraganavar MY. 2005. Preparation and Characterization of Novel Pervaporation Membranes for the Separation of Water–Isopropanol Mixtures using Chitosan and NaY Zeolite. Journal of Membrane Science 247:75-86.

Hussain CM, Saridara C, Mitra S. 2008. Carbon nanotubes as sorbents for the gas phase preconcentration of semivolatile organics in a microtrap. Analyst 133:1076-1082.

Hummer G, Rasaiah JC, Noworyta JP. 2001. Water Conduction Through the Hydrophobic Channel of a Carbon Nanotube. Nature 414:188-190.

Noy A, Park HG, Fornasiero F, Holt JK, Grigoropoulos CP, Bakajin O. 2007. Nanofluidics in Carbon Nanotubes. Nano Today 2:22-29.

Holt JK, Park HG, Wang Y, Stadermann M, Artyukhin AB, Grigoropoulos CP, Noy A, Bakajin O. 2006. Fast Mass Transport Through Sub-2-Nanometer Carbon Nanotubes. Science 312:1034-1037.

Chen H, Sholl DS. 2006. Predictions of Selectivity and Flux for CH4/H2 Separations using Single walled Carbon Nanotubes as Membranes. Journal of Membrane Science 269:152-160.

Sae-Khow O, Mitra S. 2010. Carbon nanotube immobilized composite hollow fiber membranes for pervaporative removal of volatile organics from water. The Journal of Physical Chemistry C 114:16351-16356.

Sae-Khow O, Mitra S. 2010. Pervaporation in Chemical Analysis. Journal of Chromatography A 1217:2736-2746.

Gethard K, Sae-Khow O, Mitra S. 2010. Water Desalination using Carbon-nanotube Enhanced Membrane Distillation. ACS applied materials & interfaces 3:110-114.

Gethard K, Sae-Khow O, Mitra S. 2012. Carbon nanotube enhanced membrane distillation for simultaneous generation of pure water and concentrating pharmaceutical waste. Separation and purification technology 90:239-245.

Chen Y, Mitra S. 2008. Fast Microwave-assisted Purification, Functionalization and Dispersion of Multi-walled Carbon Nanotubes. Journal of nanoscience and nanotechnology 8:5770-5775.

Chen Y, Iqbal Z, Mitra S. 2007. Microwave-Induced Controlled Purification of Single-Walled Carbon Nanotubes without Sidewall Functionalization. Advanced Functional Materials 17:3946-3951.

Vane LM, Alvarez FR, Giroux EL. 1999. Reduction of Concentration Polarization in Pervaporation using Vibrating Membrane Module. Journal of Membrane Science 153:233-241.

Service RF. 2006. Desalination Freshens Up. Science 313:1088-1090.

Shannon MA, Bohn PW, Elimelech M, Georgiadis JG, Marinas BJ, Mayes AM. 2008. Science and technology for water purification in the coming decades. Nature 452:301-310.

Wade NM. 2001. Distillation plant development and cost update. Desalination 136:3-12.

Alkhudhiri A, Darwish N, Hilal N. 2012. Membrane distillation: A comprehensive review. Desalination 287:2-18.

Lawson KW, Lloyd DR. 1997. Membrane distillation. Journal of Membrane Science 124:1-25.

Lei Z, Chen B, Ding Z. 2005. Special distillation processes: Elsevier.

Banat F, Jumah R, Garaibeh M. 2002. Exploitation of solar energy collected by solar stills for desalination by membrane distillation. Renewable Energy 25:293-305.

Ding Z, Liu L, El-Bourawi MS, Ma R. 2005. Analysis of a solar-powered membrane distillation system. Desalination 172:27-40.

Koschikowski J, Wieghaus M, Rommel M. 2003. Solar thermal-driven desalination plants based on membrane distillation. Desalination 156:295-304.

Dow N, García JV, Niadoo L, Milne N, Zhang J, Gray S, Duke M. 2017. Demonstration of membrane distillation on textile waste water: assessment of long term performance, membrane cleaning and waste heat integration. Environmental Science: Water Research & Technology.

Alklaibi A, Lior N. 2005. Membrane-distillation desalination: status and potential. Desalination 171:111-131.

Kong Y, Lin X, Wu Y, Chen J, Xu J. 1992. Plasma polymerization of octafluorocyclobutane and hydrophobic microporous composite membranes for membrane distillation. Journal of Applied Polymer Science 46:191-199.

Ulbricht M. 2006. Advanced functional polymer membranes. Polymer 47:2217-2262.

Khayet M, Suk D, Narbaitz R, Santerre J, Matsuura T. 2003. Study on surface modification by surface-modifying macromolecules and its applications in membrane-separation processes. Journal of applied polymer science 89:2902-2916.

Qtaishat M, Khayet M, Matsuura T. 2009. Novel porous composite hydrophobic/hydrophilic polysulfone membranes for desalination by direct contact membrane distillation. Journal of Membrane science 341:139-148.

Khayet M, Feng C, Matsuura T. 2003. Morphological study of fluorinated asymmetric polyetherimide ultrafiltration membranes by surface modifying macromolecules. Journal of membrane science 213:159-180.

Das R, Ali ME, Hamid SBA, Ramakrishna S, Chowdhury ZZ. 2014. Carbon nanotube membranes for water purification: a bright future in water desalination. Desalination 336:97-109.

Kim J, Van der Bruggen B. 2010. The use of nanoparticles in polymeric and ceramic membrane structures: Review of manufacturing procedures and performance improvement for water treatment. Environmental Pollution 158:2335-2349.

Zhou S, Fan Y, He Y, Xu N. 2008. Preparation of titania microfiltration membranes supported on porous Ti–Al alloys. Journal of Membrane Science 325:546-552.

Musico YLF, Santos CM, Dalida MLP, Rodrigues DF. 2014. Surface modification of membrane filters using graphene and graphene oxide-based nanomaterials for bacterial inactivation and removal. ACS Sustainable Chemistry and Engineering 2:1559-1565.

Ragunath S, Roy S, Mitra S. 2016. Selective hydrophilization of the permeate surface to enhance flux in membrane distillation. Separation and Purification Technology 170:427-433.

Bhadra M, Roy S, Mitra S. 2016. Flux enhancement in direct contact membrane distillation by implementing carbon nanotube immobilized PTFE membrane. Separation and Purification Technology 161:136-143.

Dumée LF, Sears K, Schütz J, Finn N, Huynh C, Hawkins S, Duke M, Gray S. 2010. Characterization and evaluation of carbon nanotube Bucky-Paper membranes for direct contact membrane distillation. Journal of Membrane Science 351:36-43.

Dumée L, Campbell JL, Sears K, Schütz J, Finn N, Duke M, Gray S. 2011. The impact of hydrophobic coating on the performance of carbon nanotube bucky-paper membranes in membrane distillation. Desalination 283:64-67.

Drioli E, Ali A, Macedonio F. 2015. Membrane distillation: Recent developments and perspectives. Desalination 356:56-84.

Bhadra M, Roy S, Mitra S. 2013. Enhanced desalination using carboxylated carbon nanotube immobilized membranes. Separation and Purification Technology 120:373-377.

Roy S, Bhadra M, Mitra S. 2014. Enhanced desalination via functionalized carbon nanotube immobilized membrane in direct contact membrane distillation. Separation and Purification Technology 136:58-65.

Bhadra M, Roy S, Mitra S. 2014. Nanodiamond immobilized membranes for enhanced desalination via membrane distillation. Desalination 341:115-119.

Ragunath S, Mitra S. 2015. Carbon Nanotube Immobilized Composite Hollow Fiber Membranes for Extraction of Volatile Organics from Air. The Journal of Physical Chemistry C 119:13231-13237.

Roy S, Hussain CM, Mitra S. 2013. Poly (acrylamide-co-acrylic acid) hydrophilization of porous polypropylene membrane for dehumidification. Separation and Purification Technology 107:54-60.

Van de Witte P, Dijkstra PJ, van den Berg JWA, Feijen J. 1996. Phase separation processes in polymer solutions in relation to membrane formation. Journal of Membrane Science 117:1-31.

Zhao Y-H, Qian Y-L, Zhu B-K, Xu Y-Y. 2008. Modification of porous poly (vinylidene fluoride) membrane using amphiphilic polymers with different structures in phase inversion process. Journal of Membrane Science 310:567-576.

Qian Y, Wang J, Zhu B, Zhang M, Du C, Xu Y. 2008. Modification effects of amphiphilic comb-like polysiloxane containing polyether side chains on the PVDF membranes prepared via phase inversion process. Frontiers of Chemistry in China 3:432-439.

Van de Witte P, Dijkstra P, Van den Berg J, Feijen J. 1996. Phase separation processes in polymer solutions in relation to membrane formation. Journal of Membrane Science 117:1-31.

Wang D, Li K, Teo WK. 1999. Preparation and characterization of polyvinylidene fluoride (PVDF) hollow fiber membranes. Journal of Membrane Science 163:211-220.

Edwie F, Teoh MM, Chung T-S. 2012. Effects of additives on dual-layer hydrophobic–hydrophilic PVDF hollow fiber membranes for membrane distillation and continuous performance. Chemical Engineering Science 68:567-578.

Schofield R, Fane A, Fell C. 1987. Heat and mass transfer in membrane distillation. Journal of membrane Science 33:299-313.

Qtaishat M, Matsuura T, Kruczek B, Khayet M. 2008. Heat and mass transfer analysis in direct contact membrane distillation. Desalination 219:272-292.

Phattaranawik J, Jiraratananon R. 2001. Direct contact membrane distillation: effect of mass transfer on heat transfer. Journal of Membrane Science 188:137-143.

Mengual JI, Khayet M, Godino MP. 2004. Heat and mass transfer in vacuum membrane distillation. International Journal of Heat and Mass Transfer 47:865-875.

Gethard K, Sae-Khow O, Mitra S. 2011. Water Desalination Using Carbon-Nanotube-Enhanced Membrane Distillation. ACS Applied Materials & Interfaces 3:110-114.

Gryta M. 2002. Concentration of NaCl solution by membrane distillation integrated with crystallization. Separation science and technology 37:3535-3558.

Cath TY, Adams VD, Childress AE. 2004. Experimental study of desalination using direct contact membrane distillation: a new approach to flux enhancement. Journal of Membrane Science 228:5-16.

Martínez-Díez L, Florido-Díaz FJ. 2001. Desalination of brines by membrane distillation. Desalination 137:267-273.

Wirth D, Cabassud C. 2002. Water desalination using membrane distillation: comparison between inside/out and outside/in permeation. Desalination 147:139-145.

Schofield RW, Fane AG, Fell CJD, Macoun R. 1990. Proceedings of the Symposium on Membrane TechnologyFactors affecting flux in membrane distillation. Desalination 77:279-294.

Dumée LF, Gray S, Duke M, Sears K, Schütz J, Finn N. 2013. The role of membrane surface energy on direct contact membrane distillation performance. Desalination 323:22-30.

Wade NM. 2001. Distillation plant development and cost update. Desalination 136:3-12.

Goh PS, Matsuura T, Ismail AF, Hilal N. Recent trends in membranes and membrane processes for desalination. Desalination.

Lei Z, Chen B, Ding Z. 2005. Membrane distillation. Special Distillation Processes, Elsevier Science, Amsterdam:241-319.

Calabrò V, Drioli E, Matera F. 1991. Membrane distillation in the textile wastewater treatment. Desalination 83:209-224.

El-Bourawi M, Ding Z, Ma R, Khayet M. 2006. A framework for better understanding membrane distillation separation process. Journal of Membrane Science 285:4-29.

Calabro V, Jiao BL, Drioli E. 1994. Theoretical and experimental study on membrane distillation in the concentration of orange juice. Industrial & engineering chemistry research 33:1803-1808.

Cassano A, Conidi C, Tasselli F. 2015. Clarification of pomegranate juice (Punica Granatum L.) by hollow fibre membranes: analyses of membrane fouling and performance. Journal of Chemical Technology & Biotechnology 90:859-866.

Fujii Y, Kigoshi S, Iwatani H, Aoyama M, Fusaoka Y. 1992. Selectivity and characteristics of direct contact membrane distillation type experiment. II. Membrane treatment and selectivity increase. Journal of Membrane Science 72:73-89.

Kesting RE. 1985. Synthetic polymeric membranes: a structural perspective: Wiley NY etc.

Kim JF, Kim JH, Lee YM, Drioli E. 2016. Thermally induced phase separation and electrospinning methods for emerging membrane applications: A review. AIChE Journal 62:461-490.

Lloyd DR, Kim SS, Kinzer KE. 1991. Microporous membrane formation via thermally-induced phase separation. II. Liquid—liquid phase separation. Journal of Membrane Science 64:1-11.

Lloyd DR, Kinzer KE, Tseng H. 1990. Microporous membrane formation via thermally induced phase separation. I. Solid-liquid phase separation. Journal of Membrane Science 52:239-261.

Kim SS, Lim GBA, Alwattari AA, Wang YF, Lloyd DR. 1991. Microporous membrane formation via thermally-induced phase separation. V. Effect of diluent mobility and crystallization on the structure of isotactic polypropylene membranes. Journal of Membrane Science 64:41-53.

McGuire Ks, Lloyd DR, Lim GBA. 1993. Microporous membrane formation via thermally-induced phase separation. VII. Effect of dilution, cooling rate, and nucleating agent addition on morphology. Journal of Membrane Science 79:27-34.

Wu Y, Kong Y, Lin X, Liu W, Xu J. 1992. Surface-modified hydrophilic membranes in membrane distillation. Journal of Membrane Science 72:189-196.

Lim GBA, Kim SS, Ye Q, Wang YF, Lloyd DR. 1991. Microporous membrane formation via thermally-induced phase separation. IV. Effect of isotactic polypropylene crystallization kinetics on membrane structure. Journal of Membrane Science 64:31-40.

Martínez L, Rodríguez-Maroto JM. 2007. Effects of membrane and module design improvements on flux in direct contact membrane distillation. Desalination 205:97-103.

Martínez-Díez L, Vazquez-Gonzalez MI. 1999. Temperature and concentration polarization in membrane distillation of aqueous salt solutions. Journal of Membrane Science 156:265-273.

Vatanpour V, Esmaeili M, Farahani MHDA. 2014. Fouling reduction and retention increment of polyethersulfone nanofiltration membranes embedded by amine-functionalized multi-walled carbon nanotubes. Journal of Membrane Science 466:70-81.

Bet-moushoul E, Mansourpanah Y, Farhadi K, Tabatabaei M. 2016. TiO2 nanocomposite based polymeric membranes: A review on performance improvement for various applications in chemical engineering processes. Chemical Engineering Journal 283:29-46.

Bonyadi S, Chung TS. 2007. Flux enhancement in membrane distillation by fabrication of dual layer hydrophilic–hydrophobic hollow fiber membranes. Journal of Membrane Science 306:134-146.

Cho CH, Oh KY, Kim SK, Yeo JG, Sharma P. 2011. Pervaporative seawater desalination using NaA zeolite membrane: Mechanisms of high water flux and high salt rejection. Journal of Membrane Science 371:226-238.

Prince JA, Singh G, Rana D, Matsuura T, Anbharasi V, Shanmugasundaram TS. 2012. Preparation and characterization of highly hydrophobic poly(vinylidene fluoride) – Clay nanocomposite nanofiber membranes (PVDF–clay NNMs) for desalination using direct contact membrane distillation. Journal of Membrane Science 397–398:80-86.

Bhadra M, Roy S, Mitra S. Flux Enhancement in Direct Contact Membrane Distillation by Implementing Carbon Nanotube Immobilized PTFE Membrane. Separation and Purification Technology.

Xu Z-K, Huang X-J, Wan L-S. 2009. Surface engineering of polymer membranes: Springer Science & Business Media.

Tylkowski B, Tsibranska I. 2015. Overview of main techniques used for membrane characterization. Journal of Chemical Technology and Metallurgy 50:3-12.

De los Rios A, Hernández-Fernández F, Tomás-Alonso F, Palacios J, Gómez D, Rubio M, Villora G. 2007. A SEM–EDX study of highly stable supported liquid membranes based on ionic liquids. Journal of Membrane Science 300:88-94.

Criscuoli A, Carnevale MC, Drioli E. 2013. Modeling the performance of flat and capillary membrane modules in vacuum membrane distillation. Journal of Membrane Science 447:369-375.

Nejati S, Boo C, Osuji CO, Elimelech M. 2015. Engineering flat sheet microporous PVDF films for membrane distillation. Journal of Membrane Science 492:355-363.

Sheng X, Zhang J. 2011. Air layer on superhydrophobic surface underwater. Colloids and Surfaces A: Physicochemical and Engineering Aspects 377:374-378.

Li J, Wang L, Jiang W. 2010. Super-hydrophobic surface of bulk carbon nanotubes compacted by spark plasma sintering followed by modification with polytetrofluorethylene. Carbon 48:2668-2671.

Khayet M, Mengual JI, Matsuura T. 2005. Porous hydrophobic/hydrophilic composite membranes: Application in desalination using direct contact membrane distillation. Journal of Membrane Science 252:101-113.

Shands Jr JW, Graham JA, Nath K. 1967. The morphologic structure of isolated bacterial lipopolysaccharide. Journal of Molecular Biology 25:15-21.

Anderson WB, Slawson RM, Mayfield CI. 2002. Review/Synthèse A review of drinking-water-associated endotoxin, including potential routes of human exposure. Canadian journal of microbiology 48:567-587.

Stewart I, Schluter PJ, Shaw GR. 2006. Cyanobacterial lipopolysaccharides and human health–a review. Environmental Health 5:7.

Raetz CR. 1990. Biochemistry of endotoxins. Annual review of biochemistry 59:129-170.

Prescott LM, Harley JP, Klein DA. 2002. Microbiology. New York, NY: McGraw-Hill Companies Inc

Richter W, Vogel V, Howe J, Steiniger F, Brauser A, Koch MH, Roessle M, Gutsmann T, Garidel P, Mäntele W. 2011. Morphology, size distribution, and aggregate structure of lipopolysaccharide and lipid A dispersions from enterobacterial origin. Innate immunity 17:427-438.

Almeida KMd, Almeida MM, Fingola FF, Ferraz HC. 2016. Membrane adsorber for endotoxin removal. Brazilian Journal of Pharmaceutical Sciences 52:171-178.

Berthold W, Walter J. 1994. Protein purification: aspects of processes for pharmaceutical products. Biologicals 22:135-150.

Rylander R, Haglind P, Lundholm M, Mattsby I, Stenqvist K. 1978. Humidifier fever and endotoxin exposure. Clinical & Experimental Allergy 8:511-516.

Muittari A, Kuusisto P, Virtanen P, Sovijärvi A, Grönroos P, Harmoinen A, Antila P, Kellomäki L. 1980. An epidemic of extrinsic allergic alveolitis caused by tap water. Clinical Allergy 10:77-90.

Wolff SM. 1973. Biological effects of bacterial endotoxins in man. Journal of Infectious diseases 128:S259-S264.

Zhang J, Xue J, Xu B, Xie J, Qiao J, Lu Y. 2016. Inhibition of lipopolysaccharide induced acute inflammation in lung by chlorination. Journal of Hazardous Materials 303:131-136.

Morrison D, Ulevitch R. 1978. A review-the interaction of bacterial endotoxins with cellular and humoral mediation systems. Am. J. Pathol 92:527-618.

Rietschel ET, Brade H. 1992. Bacterial endotoxins. Scientific american 267:54.

Daneshian M, Guenther A, Wendel A, Hartung T, von Aulock S. 2006. In vitro pyrogen test for toxic or immunomodulatory drugs. Journal of immunological methods 313:169-175.

Williams KL. 2007. Endotoxins: pyrogens, LAL testing and depyrogenation: CRC Press.

Mokhtar G, Naoyuki F. 2012. Overview on the lipo-polysaccharide endotoxin as emergent contaminant in reclaimed wastewater Environmental Research Journal 6.

Anderson WB, Slawson RM, Mayfield CI. 2002. A review of drinking-water-associated endotoxin, including potential routes of human exposure. Canadian Journal of Microbiology 48:567-587.

Huang H, Wu Q-Y, Yang Y, Hu H-Y. 2011. Effect of chlorination on endotoxin activities in secondary sewage effluent and typical Gram-negative bacteria. Water Research 45:4751-4757.

Osol A. 1976. Remington's pharmaceutical sciences. Journal of Pharmaceutical Sciences 65:933.

Xue J, Zhang J, Xu B, Xie J, Wu W, Lu Y. 2016. Endotoxins: The Critical Risk Factor in Reclaimed Water via Inhalation Exposure. Environmental Science & Technology 50:11957-11964.

Uribe SP. 2007. Endotoxins detection and control in drinking water systems.

Khayet M, Khulbe K, Matsuura T. 2004. Characterization of membranes for membrane distillation by atomic force microscopy and estimation of their water vapor transfer coefficients in vacuum membrane distillation process. Journal of membrane science 238:199-211.

Petsch D, Anspach FB. 2000. Endotoxin removal from protein solutions. Journal of Biotechnology 76:97-119.

Phattaranawik J, Jiraratananon R, Fane AG. 2003. Heat transport and membrane distillation coefficients in direct contact membrane distillation. Journal of Membrane Science 212:177-193.

Li H, Li C, Zheng Y, Zhi X, Peng G, Li H, Lu H. 2013. Effect of solution factors on endotoxin coagulation state. Asian Journal of Chemistry 25:6915.

Banat FA, Simandl J. 1994. Theoretical and experimental study in membrane distillation. Desalination 95:39-52.

DePamphilis M. 1971. Dissociation and reassembly of Escherichia coli outer membrane and of lipopolysaccharide, and their reassembly onto flagellar basal bodies. Journal of bacteriology 105:1184-1199.

Czermak P, Ebrahimi M, Catapano G. 2010. New generation ceramic membranes have the potential of removing endotoxins from dialysis water and dialysate. International journal of artificial organs 28:694-700.

Kang S, Herzberg M, Rodrigues DF, Elimelech M. 2008. Antibacterial Effects of Carbon Nanotubes: Size Does Matter! Langmuir 24:6409-6413.